Maria Rubega

Quantitative Assessment of Hypoglycaemia-Induced EEG changes in Type 1 Diabetes Subjects

Tesi di laurea magistrale

Relatore: Prof. Giovanni Sparacino
Correlatrice: D.ssa Chiara Fabris

Università degli Studi di Padova
Facoltà di Ingegneria
Dipartimento di Ingegneria dell'Informazione
Ottobre 2013

Ai miei genitori.

Abstract

Type 1 diabetes (T1D) is a chronic disease that causes a complete insulin deficiency. Thus, patients affected by T1D have to undergo a suitable therapy (comprising exogenous insulin administration) and to monitor, as tight as possible, their blood glucose concentration (BG) levels, in order to avoid dangerous hyper- (BG $>$ 180 mg/dl) and hypoglycaemic (BG $<$ 70 mg/dl) events. In particular, while hyperglycaemia is related with the development of long term complications, hypoglycaemia is an even more severe condition, since it may rapidly progress into come, also without subject awareness, especially at night.
Excursions of glycaemia outside the normal 70-180 mg/dl range influence several vital functions and signs. In particular, in the last years, the occurrence of the electroencephalogram (EEG) changes related to hypoglycaemia has been investigated by many researchers, highlighting an increase in the low frequency EEG bands during the transition to this condition. This suggested the possibility of using the brain as a biosensor to detect hypoglycaemia in real-time from suitable EEG signal processing.
The aim of the present thesis is to quantitatively assess how hypoglycaemia influences EEG features by analizing 19 EEG recordings and sparse BG data collected in parallel in T1D subjects during an insulin-induced hypoglycaemia experiment (data were kindly provided by Hypo-Safe A/S, Odense University Hospital, Sydvestjysk Sygehus Esbjerg, Denmark). Three 1-hour time-intervals corresponding to hyper-, eu- and hypo-glycaemia, respectively, were then selected from BG data, and the P3-C3 EEG channel was processed through several techniques based on spectral analysis, to investigate if specific EEG features change during the transition from eu- to hypo-glycaemia. In particular, lots of different methods found in literature have been considered, from well-established classic methods (such as the power spectral density computation) to more recent ones (such as the use of a reactivity index), in order to assess the different trend of the EEG time-series in hypo- and in eu-glycaemia. Promising results have been obtained with all considered methods, proving the possibility to properly characterize the hypoglycaemic condition from retrospective analysis of the EEG signal and encouraging the development of systems to detect or prevent hypoglycaemic events from the on-line EEG signal processing.

As far as the thesis structure is concerned, Chapter 1 first introduces the diabetes pathology and its implication on the EEG signal, with a detailed description of methods and results of literature works dealing with hypoglycaemia-related EEG changes. In Chapter 2, the data base considered in the study is presented. In

Chapter 3 we analyse the EEG in eu- and hypo-glycaemia, by indicators computation in the frequency domain. Chapter 4 focuses on a possible improvement of the methods presented in Chapter 3, based on the individualization of the EEG bands. In Chapter 5 we discuss the use of a new reactivity index measure to detect hypoglycaemia in real time. In Chapter 6, conclusions that can be drawn from the study are summarized, with some indications for further margins of investigation.

Sommario

Il diabete di tipo 1 (T1D) è una malattia cronica che provoca mancanza completa di insulina.
Per questo, i pazienti che soffrono di T1D devono seguire una terapia mirata (che consiste di dosi esogene di insulina) e devono monitorare, più spesso possibile, il loro livello di concentrazione di glucosio nel sangue per evitare pericolosi eventi iper- (BG $>$ 180 mg/dl) e ipo-glicemici (BG $<$ 70 mg/dl). In particolare, mentre l'iperglicemia è legata allo sviluppo di complicazioni a lungo termine, l'ipoglicemia è addirittura una condizione peggiore, perchè può presentarsi improvvisamente senza che il paziente ne sia cosciente, soprattutto di notte.
Valori di glicemia fuori dall'intervallo normale di 70-180 mg/dl influenzano alquanto le funzioni vitali. In particolare, negli ultimi anni, è stato studiato da molti ricercatori come il segnale elettroencefalografico cambia con l'ipoglicemia, evidenziando un aumento nelle bande EEG alla basse frequenze durante il passaggio a questa condizione. Ciò ha suggerito di usare il cervello come biosensore per individuare episodi ipoglicemici in real-time con i metodi disponibili di elaborazione del segnale EEG.
Lo scopo di questa tesi è di valutare quantitativamente come l'ipoglicemia influenza le caratteristiche dell'EEG, analizzando 19 tracciati EEG e i corrispettivi dati BG registrati in parallelo in soggetti T1D durante un esperimento di ipoglicemia indotta (i dati sono stati gentilmente messi a disposizione da HypoSafe A/S, Odense University Hospital, Sydvestjysk Sygehus Esbjerg, Denmark). Tre periodi di un'ora, corrispondenti rispettivamente a iper- eu- e ipo-glicemia, sono stati selezionati dai dati BG, e il canale P3-C3 è stato elaborato con diverse tecniche basate sull'analisi spettrale per scoprire se specifiche caratteristiche del segnale EEG cambiano durante il passaggio da eu- a ipo-glicemia. In particolare, sono stati considerati molti metodi differenti trovati in letteratura, da metodi classici ben consolidati (come il calcolo della potenza spettrale) ai più recenti (come l'uso del reactivity index), per individuare i diversi andamenti del segnale EEG in ipo- iper- ed eu-glicemia. Sono stati ottenuti risultati promettenti con i metodi considerati, dimostrando la possibilità di caratterizzare efficacemente la condizione di ipoglicemia attraverso l'analisi retrospettiva del segnale EEG e incoraggiando lo sviluppo di sistemi per individuare o prevenire eventi ipoglicemici dall'elaborazione del segnale EEG in tempo reale.

Per quanto riguarda la struttura della tesi, il Capitolo 1 introduce la patologia del diabete e le sue implicazioni sul segnale EEG, con una descrizione dettagliata dei metodi e dei risultati presenti in letteratura. Nel Capitolo 2, sono presentati i dati

reali di pazienti diabetici elaborati in questo studio. Nel Capitolo 3 si analizza il segnale EEG in eu- e ipo-gicemia tramite l'applicazione di indicatori ipoglicemici nel dominio della frequenza. Il Capitolo 4 si concentra su un possibile miglioramento dei metodi presentati nel Capitolo 3, metodi basati sulla personalizzazione delle bande EEG. Nel Capitolo 5 si tratta del reactivity index per individuare l'ipoglicemia in tempo reale. Nel Capitolo 6, sono sintetizzate le conclusioni derivanti da questo studio con alcune indicazioni per futuri miglioramenti.

Acknowledgements

My gratitude goes to all the people who have contributed to this work. I would like to deeply thank my Professor Giovanni Sparacino, as well as my supervisor Ing. Chiara Fabris.

M. R.

Contents

List of Figures

List of Tables

Chapter 1

The diabetes pathology and its influence on the EEG signal

1.1 Diabetes, socio-economical impact and therapy

Diabetes is one of the most important and diffused chronic diseases [1]. About 366 million people worldwide were estimated to have diabetes in 2011 and if these trends goes on, 522 million people will have diabetes in 2030 [2]. The largest increase will take place in the developing economies, because diabetes has grown together with rapid cultural and social changes, ageing populations, increasing urbanisation, dietary changes, reduced physical activity and others unhealthy behaviours [2].
In Figure1.1, the prevalence of diabetes in 2011 and its estimation in 2030 by the different world regions are shown in Figure1.1a, while Figure1.1b represents the prevalence of people with diabetes by age and sex in 2011[3].

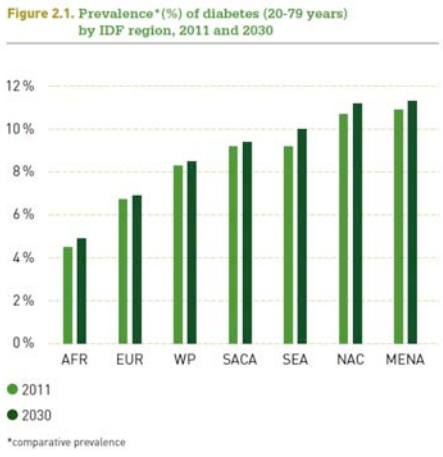

(a) Comparison of prevalence of diabetes by IDF region

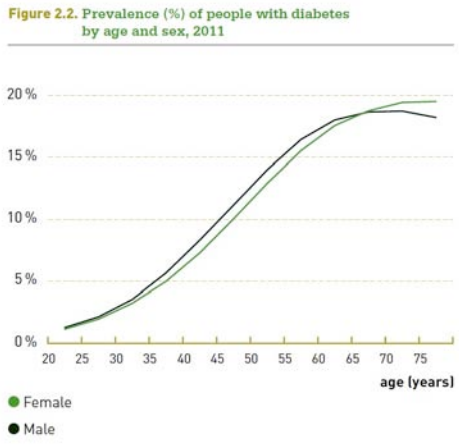

(b) Prevalence of people with diabetes by age and sex

Figure 1.1: 2011 Diabetes diffusion [3]

The pathology of diabetes appears when the body is not able to produce enough

or efficacious insulin[1] [4]. In particular, there are two principal types of diabetes:

- type 1 diabetes (T1D);
- type 2 diabetes (T2D);

Starting from the second pathology, T2D, also called insulin-independent diabetes, is mostly due to a poor diet, increasing age, physical inactivity or family history of diabetes, and causes a resistance to insulin developed by body tissues. This pathology mainly occurs in obese adults and, at the present time, affects about the 90-95% of diabetic people [2]; however, the number of T2D subjects will rapidly increase next years. T2D patients don't usually need daily doses of insulin to survive but they typically require to improve their diet and to increase their physical activity, in order to enhance their conditions. T1D, on the other hand, is due to an insulin production deficiency, and it's caused by a progressive autoimmune destruction of the pancreatic beta-cells that make the hormone insulin. Normally, the body immune system fights off foreign invaders such as bacteria or viruses, but for unknown reasons, the immune system attacks various cells in the body, causing a complete deficiency of the insulin hormone. [5]. The hormone insulin has an anabolic function, it helps sugar to enter the body cells that exploit it as energy source [6]. So thanks to insulin, the amount of sugar in the blood decreases. But too much insulin causes hypoglycaemia (low blood sugar level), otherwise its (complete or partial) deficiency leads to diabetes [7].
Type 1 diabetes is also called insulin-dependent diabetes and it usually occurs in children or young adults. It currently affects about 5-10% of the whole diabetic population [7], but, the number of people developing T1D is increasing each year, probably because of changes in environmental risk factors, early events in the womb, diet early in life or viral infections[3]. Since T1D progresses into a complete insulin deficiency, people affected by this pathology need an insulin therapy (insulin shots to use glucose from meals[1]) to control their blood glucose concentration levels. Despite the increased use of insulin analogues and pumps for continuous insulin infusion, however, it is very difficult to replace the insulin need exactly and, as a result, blood glucose concentration often exceeds the normality range towards hypo- ($<$70 mg/dl) or hyper- ($>$180 mg/dl) glycaemia. Both these conditions are related to the development of complications from diabetes, but, while hyperglycaemia causes long-term complications, such as nephropathy, retinopathy and cardiovascular diseases, hypoglycaemia may rapidly progress into coma, also without subject awareness, especially at night. For this reason, T1D subjects should be monitored in real-time, in order to prevent the occurrence of dangerous hypo events. In this context, the introduction of minimally-invasive, if not non-invasive, sensors proposed in the 2000's to continuously monitor glycaemia can be of significant help in the timely detection, and even prevention, of dangerous hyper-/hypo-glycaemic events [8].

[1]The insulin is the most important energy body regulator. It is injected into the blood because of an increase in blood glucose. It allows the glucose absorption and storage in the liver, muscle and adipose tissue.

1.2 The EEG signal

The EEG is the recording of brain electrical activity made along the scalp in standard locations (according, for example, with the 10/20, 10/10 or 10/5 international system) [9]. Despite the high temporal resolution, EEG systems are characterized by a poor spatial resolution, and artefacts and noise typically affect the EEG recordings.
The main features of EEG time-series are:

- frequency band 1-70 Hz;
- amplitude tens of microV;
- it's a stationary signal[2] at times;
- it's not periodic but often has a dominant rhythm.

In the frequency domain the EEG signal can be divided in different frequency ranges (bands), as described in the following:

- Delta is from 1 to 4 Hz. This frequency range is characterized by high-amplitude waves. It's recorded frontally in adults and posteriorly in babies.
- Theta is from 4 to 8 Hz. This band is usually found in children and it represents a meditative and relaxed state in adults.
- Alpha is from 8 to 13 Hz. This waveform is seen in both posterior regions of the brain and it appears with closing eyes and it decreases during mental efforts and opening eyes.
- Beta is from 13 to 30 Hz. This frequency range is seen in both sides of the brain and it's characterized by low-amplitude waves. It represents thinking, active concentration and movements.
- Gamma is from 30 to 100 Hz. It illustrates the linking between neurons, in fact it's probably responsible of motor and cognitive functions.

In the clinic practice, EEG time-series are used to identify and quantify deficit of the brain activity, detect epilepsy, monitor the patient during anesthesia, study sleep stages and study the effect of medication/drugs/meditation.

Since glucose represents an essential substrate for brain functioning, hypoglycaemia and the consequent neuroglycopenia may result in an altered cerebral activity. In fact, while some tissues, such as muscle, liver and kidneys, can store a certain amount of glycogen [3] as a reserve to draw upon if blood sugar drops too low, the brain has no reserves and it entirely depends on the blood for the glucose supply[4]. Therefore, the brain is the first organ to be affected by hypoglycaemia and the decrease of cerebral functioning consequent to this condition can be investigated through suitable analysis of the electroencephalogram signal (EEG).

[2] A signal is stationary if its statistical behavior is invariant after a translation of the time axis.
[3] Glucose is converted in glycogen to become a form of energy storage in humans.
[4] Glucose arrives to neurons and other nerve cells by diffusion thanks to capillaries.

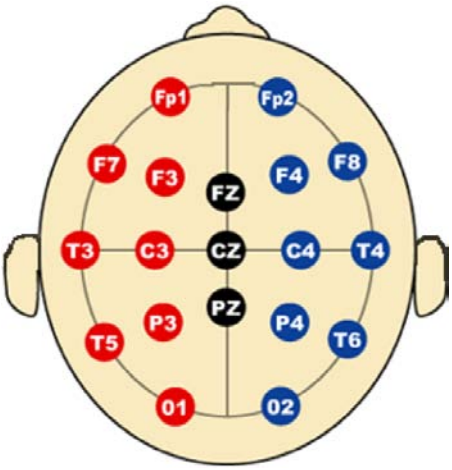

Figure 1.2: EEG 10–20 Electrode/Channel Placement. The channels correspond to the number from 1 to 19 starting from the left to right and top to bottom. Abbreviations: F = frontal, C = central, P = parietal, T = temporal, O = occipital, Fp = frontopolar. [10]

1.3 Hypoglycaemia-related EEG changes evidence in the literature

The first studies investigating the relationship between hypoglycaemia and the EEG signal date back to the 1950 [11]. Since then, several works, e.g.[12] [13] [14], have proved that a power increase in the low frequency EEG bands takes place during hypoglycaemia. In [12], Ross and Loeser proved that many patients with essential hypoglycemia develop disturbances of their cerebral electroactivity during five hour glucose tolerance tests and that higher blood sugar concentrations are necessary to prevent cerebral electrical irregularities in younger individuals. In [14], authors showed that biochemical hypoglycaemia in conscious patients with diabetes is accompanied by changes in the electroencephalogram: a combined decrease in alpha activity and increase in theta activity. Eventually, in [13], researchers found in an unselected group of adolescents with type 1 diabetes EEG abnormalities. In the frontal regions, the slower frequencies (theta and delta) had an increased power, in particular the increase in theta activity was most strongly correlated with a history of severe hypoglycaemia.
These findings stimulated the development of specific algorithms for the prediction and detection of severe hypoglycaemia events from the analysis of EEG time-series [16]. In particular, the possibility of using the brain as a biosensor to detect hypoglycaemia in real-time from suitable processing of EEG signals was largely investigated within the Hyposafe experience, exhaustively described in [15]. In such a context, a specific device made of subcutaneous electrodes placed a few millimetres below the skin and represented in Figure1.4, was used to acquire EEG time-series, allowing to provide remarkable high quality EEG recordings continuously over long periods of time [17]. Figure1.3 shows an example of a single channel EEG recorded during eu- and hypo-glycaemia during daytime, it is evident that the hypoglycaemic

EEG originates from a process of lower frequency, which is more synchronized, leading to EEG of higher amplitude [15].

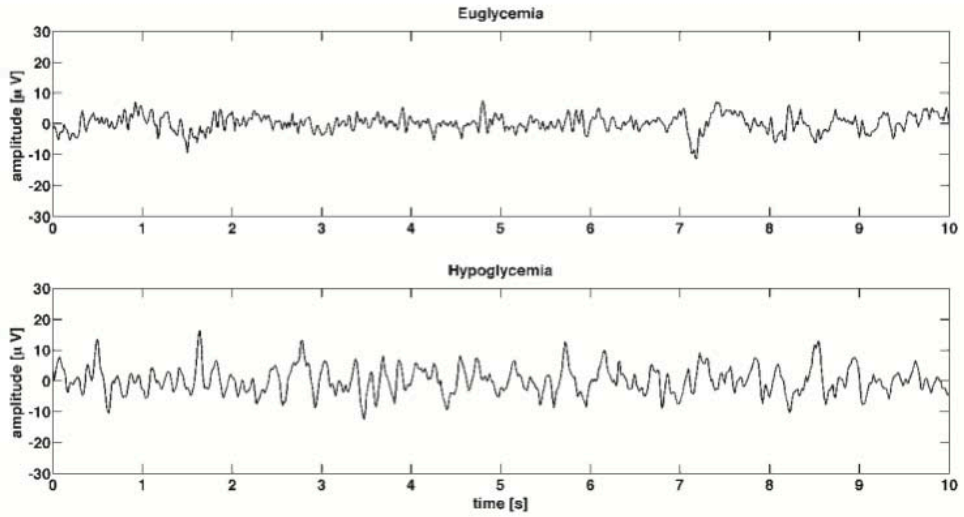

Figure 1.3: Representative examples of single channel EEG recorded during euglycaemia and hypoglycaemia in the same person [15].

1.4 The Hyposafe device

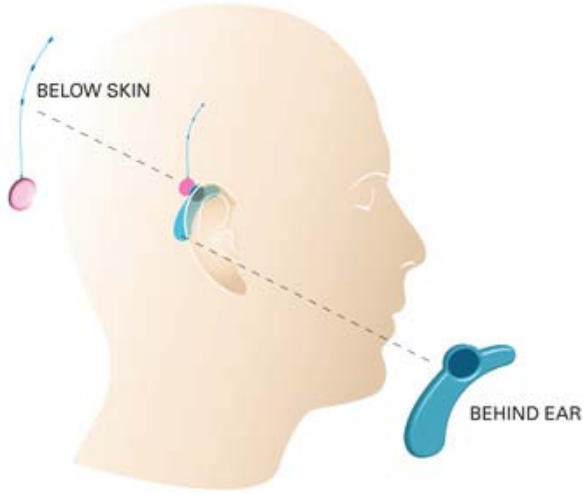

Figure 1.4: The hyposafe device is implanted under the diabetic's skin on the side of the head [17].

The HypoSafe device is the first EEG device made for subcutaneous implantation [17]. In particular, it is implanted under the diabetic's skin on the side of the head,

in the sub cutis layer, only a few millimeters below the skin, making the implant procedure rather simple. The device can remain implanted for more than 10 years (depending on regulatory approval). The implanted part is soft and small and does not create inconvenience to the user. When implanted, there are no physical elements passing through the skin and the use of bandage/plaster is not required. Thus, there is no risk of infection or allergic reactions. Furthermore, as the device is hidden under the skin, it has low implications for the users chosen lifestyle. [17]. The Hyposafe device was developed to real-time process the EEG recordings obtained through the subcutaneous electrode, in order to individuate when a T1D patient is approaching the hypoglycaemic condition and to avoid it by providing an alarm. The Hyposafe team proposed to detect specific changes in the EEG time-series, by processing the signals through a general mathematical algorithm based on power estimations and noise indicators, with the aim of detect hypoglycaemia before the development of cognitive failure [18]. In particular, in [18], hypoglycaemia was induced in 15 T1D patients not allowed to sleep. EEG was recorded within a pilot-experiment, to assess if EEG epochs are consistent or not consistent with hypoglycaemia. Frequency, amplitude and power of the EEG signal recorded were extracted as features from the pilot experiment to realize the final model. The final model consists of a curve of integrated events: a window in time domain weights past hypoglycaemia epochs by integrating events weighted by a kernel. The threshold value to detect hypoglycaemia is a steep increase above 20 as you can see in Figure1.5.

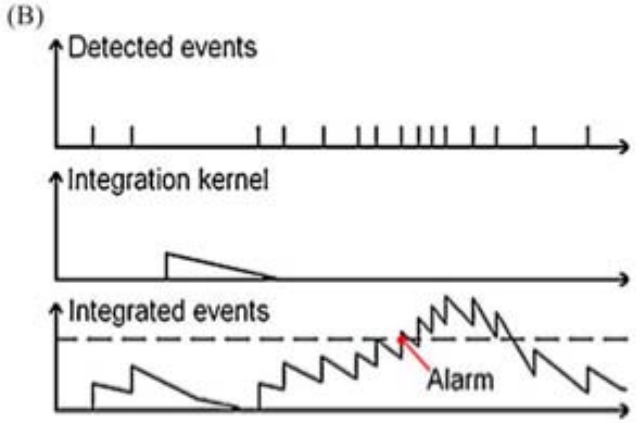

Figure 1.5: Integrated events algorithm [18]. You can see the detected events in the first chart. These events were integrated applying the integration kernel (in the second chart) and obtaining the integration curve (in the third chart). You can notice that the integration curve overcames the threshold, thus it's generated a warning to the patient.

In [19], the same authors also studied if severe hypoglycaemia is preceded by changes in both ECG (electrocardiography[5]) and EEG features by extraction of

[5]Electrocardiography (ECG or EKG from Greek: kardia, meaning heart) is a transthoracic (across the thorax or chest) interpretation of the electrical activity of the heart over a period of time, as detected by electrodes attached to the surface of the skin and recorded by a device

delta, theta and alpha bands power and QT[6] interval features.
Then, they computed ECG and EEG features mean and standard deviation in a baseline period. If the moving average were greater than the mean plus two standard deviations, it was detected an hypoglycaemia event (Figure1.6).

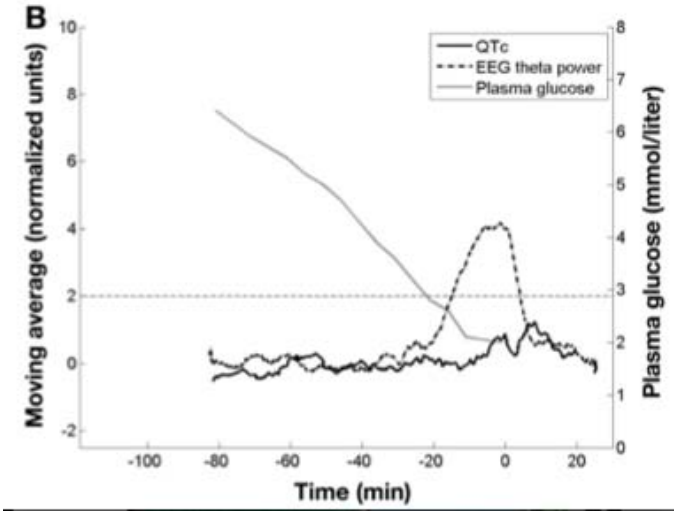

Figure 1.6: EEG and ECG features vs plasma glucose measure: you can notice that EEG theta power increases when the plasma glucose detects hypoglycaemia.

Results, obtained by these works, support the use of the brain as a biosensor for hypoglycaemia detection.

In [22], it was also tested if hypoglycaemia EEG changes would remain stable across age, group, gender, duration of diabetes and hypoglycaemia awareness status in order to establish a very general algorithm for hypoglycaemia detection.
Researchers did a quantitative EEG analysis, based on the the spectral content of the signal, to find possible group differences among patients classified by age, gender, duration of diabetes and hypoglycaemia awareness status. They discovered that their hypoglycaemia indicators were no influenced by these classifications.

Analysis of EEG changes, as a device to detect and predict hypoglycaemia events, was proposed in some other following papers.
The main results are very similar in all publications:

- the use of subcutaneous electrodes provides a good alternative to surface ones;
- the most sensitive measure of hypoglycemia seems to be a global increase in theta activity;

external to the body[20].

[6]In cardiology, the QT interval is a measure of the time between the start of the Q wave and the end of the T wave in the heart's electrical cycle. In general, the QT interval represents electrical depolarization and repolarization of the left and right ventricles.[21]

- gender and age have no effects.

Researchers also tried to focus their attention on different techniques for analysing EEG. For instance, they paid attention to the measure of chaos in the EEG signal in hypoglycaemia in frequency and time domain.
In [23], they utilized a recent index, called reactivity index, to measure its variability in the standard frequency bands. They found that the reactivity index variability was higher in hypoglycaemia than in euglycaemia in theta band in Type 1 Diabetes subjects.
In [24], hypoglycaemia-related EEG changes were investigated by Approximate Entropy (ApEn) at multiple temporal scales, to assess if EEG complexity changes during the transition to hypoglycaemia. ApEn is a rather famous entropy measure introduced by Pincus in 1991 [25] and widely used to study biological time-series, quantifying the degree of irregularity within a singe time-series: the higher the ApEn value, the more irregular/complex the signal. The authors showed that ApEn decreases passing from hyperglycaemia and euglycaemia to hypoglycaemia, highlighting a decrease of EEG complexity when the hypo condition occurs.

1.5 Aim of the thesis

The aim of this study is to deepen the EEG analysis proposed in the papers cited in section 1.4 and to investigate if other solid hypoglycaemia indicators can be defined. In particular, our first specific aim is to reproduce the results of [15]. Then, we will expand the EEG investigation in more than one channel. Hence, we will overlap a traditional analysis based on the signal spectral content by personalizing it, using new indexes and customizing frequency bands.
To facilitate the reading and the following of our line of reasoning, the chapters are presented in the same order in which they were temporally conceived. In particular, each chapter is structured as follows: theory behind the method employed, application to data, results and critical discussion.
The overall results of the thesis will be however summarized in the Conclusions (Chapter 7).

Chapter 2

Data Base

The data were collected in 19 type-1 diabetic subjects studied at Hillerød Hospital (Denmark).
An intravenous administration of Actrapid (Novo Nordisk, Bagsværd, Denmark) was administered to subjects to insulin-induce hypoglycaemia.
EEG and blood glucose concentration (BG) were simultaneously recorded during the insulin-induced hypoglycaemia experiment.
In particular, BG was frequently determined by a laboratory analyzer YSI (Yellow Springs In- strument Company, Ohio, USA), while 19 EEG channels were recorded by standard cap electrodes placed on the scalp according to the 10/20 international system. EEG was recorded by a digital EEG recorder (Cadwell Easy II, Kennewick, Washington, USA). EEG signals were analogically low-pass filtered in order to avoid aliasing, then digitally acquired and finally down-sampled at 64 Hz. The dynamic range of the EEG was $\pm 4620 \mu V$ with an amplitude resolution of 0.14 μV. The internal noise level in the analog data acquisition system was estimated to be 1.3 μV RMS. The protocol was approved by the local ethical committee [24].
Moreover, three 1-hour intervals referred to hyper- eu- and hypoglycaemic conditions were targeted for each subject thanks to the blood glucose concentration measure.

In Figure2.1, it's represented the P3-C3 EEG recording and the simultaneous BG data in a representative subject. The three 1-hour time intervals corresponding to hyper- eu- and hypo-glycaemia are highlighted by, respectively, red, green and blue lines. As described in [23], these intervals were determined by visual inspection of BG time-series. To facilitate the determination of the three intervals and reduce subjectivity in the analysis, hyper- and hypo-glycaemic thresholds (180 and 70 mg/dl) were compared with a smoothing spline previously fitted against the raw BG samples by using the method of [26].

The subjects and their time range of observation are summarized in Table2.1.

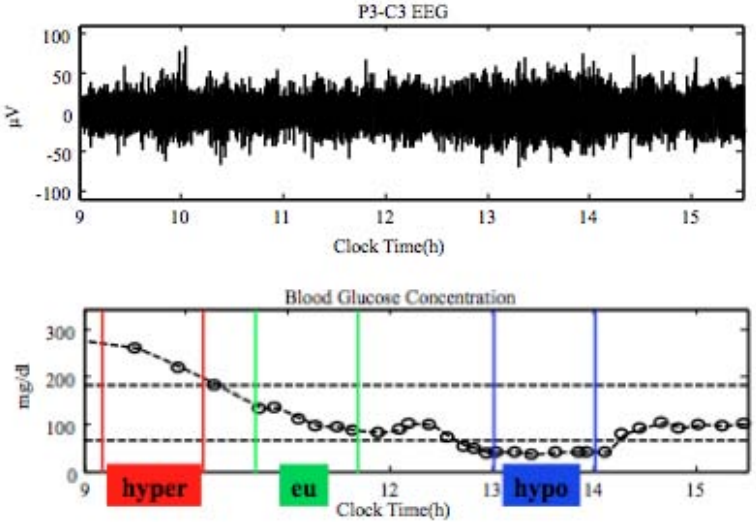

Figure 2.1: EEG recording (upper panel) and simulaneous BG measurement. Horizontal lines in the second panel identify hyperglycaemia (180 mg/dL) and hypoglycaemia (70 mg/dL) thresholds. Vertical red, green and blue lines refer to hyper-, eu- and hypo-glycaemia intervals, respectively.

Subject	From...To [h]	Insulin Shot [h]	Hyper [h]	Eu [h]	Hypo [h]
ERN02	8 a.m-5 p.m.	11.65 a.m.	9-10 a.m	11-12 a.m.	3-4 p.m.
LOH23	9 a.m-1 p.m.	9.91 a.m.	9.17-10.17 a.m	9.67-10.67 a.m.	11.33 a.m.-12.33 p.m.
PET03	9 a.m-5 p.m.	10.31 a.m.	9-10 a.m	11.50-12.50 a.m.	2.50-3.50 p.m.
LAB19	8 a.m-1 p.m.	9.55 a.m.	8.33-9.33 a.m	9.50-10.50 a.m.	11.16 a.m.-12.16 p.m.
SOP11	8 a.m-1 p.m.	10.08 a.m.	8.83-9.83 a.m	10-11 a.m.	11.50 a.m.-12.50 p.m.
ANB20	8 a.m-2 p.m.	8.78 a.m.	8.83-9.83 a.m	9-10 a.m.	11.67 a.m. -12.67 p.m.
CAJ06	8 a.m-2 p.m.	10.75 a.m.	8.67-9.67 a.m	10.17-11.17 a.m.	12.33-1.33 p.m.
GIM27	8 a.m-2 p.m.	10.20 a.m.	8.5-9.5 a.m	9.83-10.83 a.m.	12-1 p.m.
KIP12	8 a.m-2 p.m.	10.47 a.m.	9-10 a.m	10.50-11.50 a.m.	12-1 p.m.
MAA21	8 a.m-2 p.m.	9.75 a.m.	8.83-9.83 a.m	9.67-10.67 a.m.	11.17 a.m.-12.17 p.m.
PEH16	8 a.m-2 p.m.	10.38 a.m.	8.5-9.5 a.m	10-11 a.m.	12-1 p.m.
OLR08	8 a.m-3 p.m.	11.28 a.m.	9-10 a.m	11-12 a.m.	12.67-1.67 p.m.
KIH15	8 a.m-3 p.m.	11.35 a.m.	9-10 a.m	10.67-11.67 a.m.	1.17-2.17 p.m.
ANT09	8 a.m-4 p.m.	11.31 a.m.	8.83-9.83 a.m	10.50-11.50 a.m.	1.50-2.50 p.m.
BOE01	8 a.m-4 p.m.	12.57 a.m.	9.67-10.67 a.m	12-1 p.m.	2-3 p.m.
FLP10	8 a.m-4 p.m.	11.17 a.m.	9-10 a.m	10.50-11.50 a.m.	1-2 p.m.
ETW13	9 a.m-3 p.m.	11.28 a.m.	9.17-10.17 a.m	10.67-11.67 a.m.	1-2 p.m.
PEL26	9 a.m-3 p.m.	11.43 a.m.	9.17-10.17 a.m	11.17 a.m. -12.17 p.m.	1.17-2.17 p.m.
PEN24	9 a.m-3 p.m.	10.67 a.m.	9.17-10.17 a.m	10.50-11.50 a.m.	12.33-1.33 p.m.

Table 2.1: Data base. In the first column the list of subjects, in the second one the total observation period, in the third one the time of the insulin shot (to induce hypoglycaemia) and in the remaining columns the three 1-hour intervals referred to hyper- eu- and hypoglycaemic conditions.

Chapter 3

Spectral density analysis of EEG and relationships with hypoglycaemia

The aim of the following study is to clearly show the presence of changes in the EEG signal through spectral analysis.
A lot of papers, e.g.[18][27], have been written to emphasize these different behaviours during hypoglycaemia and euglycaemia.
The main studies are based on the EEG elaboration in the frequency domain. The EEG signal power or spectral density, in the Fourier domain, was estimated for every subject for the whole EEG signal. The results were then divided into the conventional EEG rhytmic activity frequency bands: delta (1-4 Hz), theta (4-8 Hz) and alpha (8-13 Hz) and into each known period of hypoglycaemia, hyperglycaemia and euglycaemia.
Our first goal was to reproduce the analysis above and to observe the EEG changes in each conventional band during the different periods.
The EEG signal was elaborated before the spectral density computation. It was divided into epochs of few seconds, with or without overlapping with near segments. In fact, the first problem we faced was how to choose the lenght of the EEG signal separation, since in the bibliography the choice wasn't either completely justified or unanimous:

- 1 second windows without overlapping in [18];
- 4 second windows with a 75% overlapping in [19];
- 4 second windows with a 50% overlapping in [22];
- 4 second windows without overlapping in [13].

For this reason we have chosen to test different durations with different overlappings by processing the signal with the same elaboration and comparing the results. At the same time, even the choice of the preferable channel used to acquire the EEG signal isn't uniform in literature:

- channels $P3 - T3$ and $P4 - T4$ in [19];

- channels $P4 - T4$ in [22];
- channels $F3 - C3$ $(F4 - C4)$ $P3 - O1$ $(P4 - O2)$ $T3 - T5$ $(T4 - T6)$ in [28];
- channels $C3 - A2$ $A1$ in [16]
- channels $P3 - C3$ in [24].

We have decided to cover most of the brain and to test the following bipolar channel before making a choice:

- F3-C3 (F4-C4);
- P3-C3 (P4-C4);
- P3-T3 (P4-T4).

3.1 Initial division in 2 and 4 second epochs

The first tests have been led by splitting the EEG signal in 2 second epochs with no overlapping. Then with 4 second epochs with 50% overlapping.
For this initial analysis, we have chosen the P3-C3 channel because it was the most commonly used in literature.
The signal has been computed with the MATLAB command pwelch, obtaining the valuation of the power spectral density (PSD) of the input signal, using a Welch average estimator. Every computed signal segment has been divided in epochs with a desired lenght and overlapping using an Hamming window [1]. This method is summarized in Figure3.1.

The power spectral density of our signals can display information that is hard to identify otherwise and it reveals how the power of a signal varies with frequency [30]. The PSD $G_x(f)$ of a signal $x_T(t)$ is defined as:

$$G_x(f) = lim_{T\to\infty} G_{xT}(f) = lim_{T\to\infty} \frac{|X_T(f)|^2}{T}$$

where

$$X_T(f) = \int_{-T/2}^{T/2} x(t) e^{-j2\pi ft} dt.$$

[29]

In Figure3.2, you can see the PSD trend for one of the 19 subjects. The PSD has a decreasing trend and we can often notice a peak value in the alpha band. It seems there are not many differences between the two window lengths at first sight, except for the amplitude of the peak values.

After the PSD computation, we have calculated the mean value of the spectral density in each traditional frequency band for all subjects in the glycaemic states. Then, we have statically compared the mean values in each glycaemic state:

[1] Hamming window is one of the most popular window shapes: $w(n) = 0.54 - 0.46cos(\frac{2\pi n}{N-1})$, $0 \leq n \leq N$. [29]

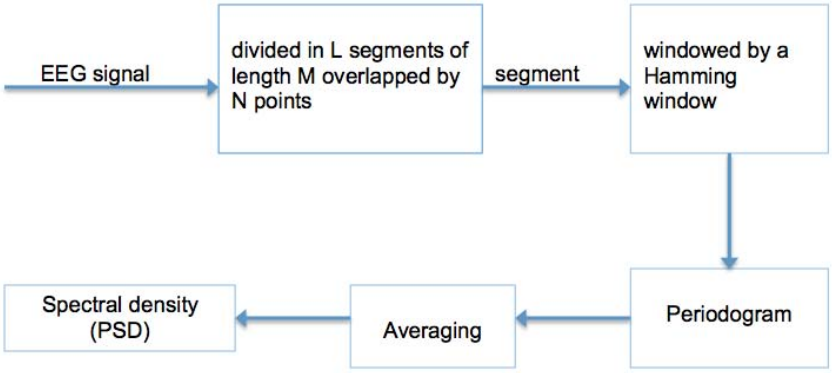

Figure 3.1: The Welch's method is one technique for signal frequency analysis. The EEG signal is divided in short time series by applying a window function. Then, the spectral analysis is applied to each interval, assumed to be stationary and regular.

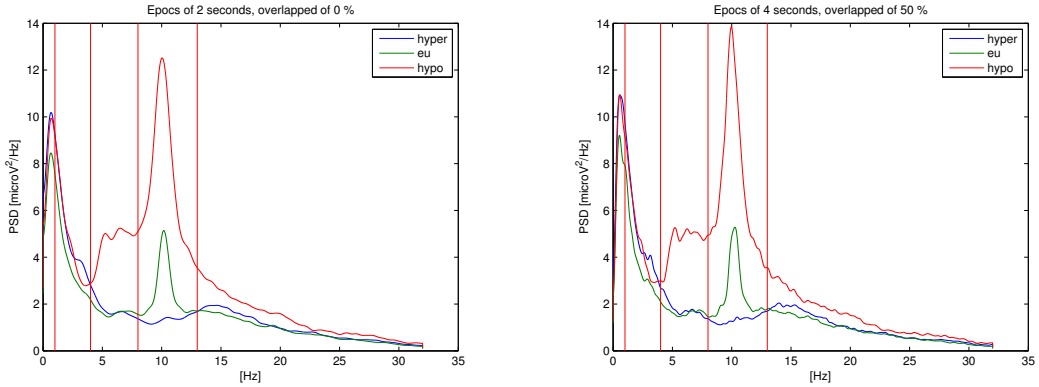

(a) ETW13: 2 second epochs with no overlap **(b)** ETW13: 4 second epochs with 50% overlap

Figure 3.2: P3-C3: PSD

- euglycaemic values vs hypoglycaemic ones.

. We have compared the results performing a t-test (if the data had a standard normal distribution) or a sign-test (if the data did not verify the t-test assumptions).[2]

We have plotted our results in Figure3.3 and in Figure3.4. We have summarized the results of the statistic test in Table3.1 and in Table3.2.

Observing Figure3.3, we can notice that the mean PSD value increases passing from euglycaemia to hyperglycaemia.
This increase is statically relevant in theta and alpha bands, while the results are not significant in delta band.

[2]These statistic tests declare if the means of two groups are statistically different from each other. The test returns a test decision (0) for the null hypothesis if there are no differences between means of two groups, it rejects the null hypothesis (1) at the 5% significance level, if the difference between the population distributions do not have a mean equal to zero.

2 second length	Delta	Theta	Alpha
Eu vs Hypo	0	1	1
4 second length	Delta	Theta	Alpha
Eu vs Hypo	0	1	1

Table 3.1: Statistic results. 1 stands for statically significant difference, 0 stands for no significant difference.

2 second length	Delta	Theta	Alpha
Eu vs Hypo	0.6474	$7.2 * 10^{-5}$	0.0044
4 second length	Delta	Theta	Alpha
Eu vs Hypo	0.6476	$5.9 * 10^{-5}$	0.0044

Table 3.2: P-values. The p-value indicates the probability that the two population are not statistically different.

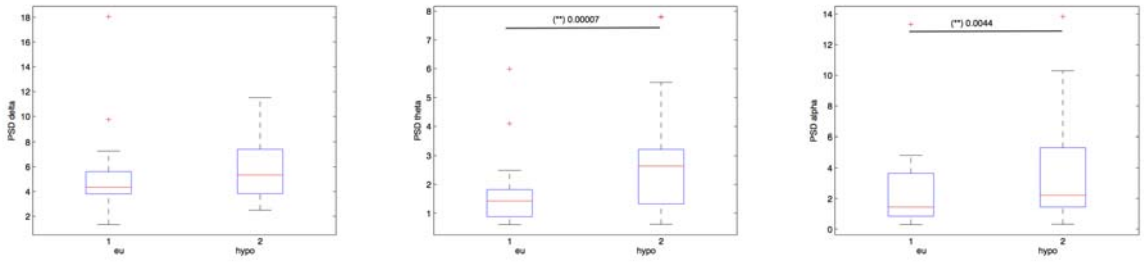

(a) PSD in delta band **(b)** PSD in theta band **(c)** PSD in alpha band

Figure 3.3: 2s epoch. Boxplots of PSD mean value in the two glycaemic states from all subjects. The red line is the median value, the edges of the box are the 75th and 25th percentiles, the red crosses are the outliers. Double stars (**) indicate statically significant difference, the number near to the double stars is the p-value.

There are no differences between the 2 second length windowing (Figure3.3) and the 4 second length windowing (Figure3.4). The results are very similar.
This first study suggests that insulin-induced hypoglycaemia results in an increase in the power spectral density of the theta and alpha band. Probably, this effect is due to a reduced brain metabolism, indeed theta and alpha bands indicate relaxing states. This measure of the PSD seems to be a good tool to detect hypoglycaemic state.

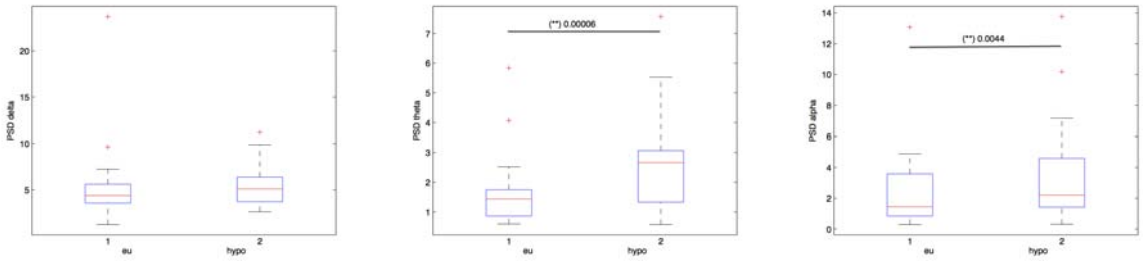

(a) PSD in delta band **(b)** PSD in theta band **(c)** PSD in alpha band

Figure 3.4: 4s epoch. Boxplots of PSD mean value in the two glycaemic states from all subjects. The red line is the median value, the edges of the box are the 75th and 25th percentiles, the red crosses are the outliers. Double stars (**) indicate statically significant difference, the number near to the double stars is the p-value.

3.2 Choice of epoch length

Taking the previous results into account and the window length in the majority of the papers, we have chosen to use windows of 4 second length. We have decided to test different overlappings: 0% 50% and 75% for every chosen bipolar channel (F3-C3, F4-C4; P3-C3, P4-C4; P3-T3, P4-T4).
We have repeated the same frequency analysis of paragraph 3.1:

- computation of the PSD with Welch's method;
- computation of mean value of the PSD
- statistical analysis and comparison between the euglycaemic state and the hypoglycaemic one.

In Table3.3 and in Table3.4, we have documented the results from statistics. We have compared the hypoglyceamic and euglycaemis state in each chosen channel for all subjects with different overlapping in the EEG windowing. The results about the channels in the brain left side are in Table3.3, and the ones about the brain right side are in Table3.4.

We can notice that the channels in the left side are a rich source of information in alpha and theta band. The worst results in the left side are about F3-C3 channel. We expected this behaviour because F3-C3 is a frontal channel, so its EEG measure can be corrupted by the electrooculogram [3].
The channels outcomes of the right side are less informative. The channel F4-C4 results are surely corrupted by noise, the other channels results highlight a significant difference only in theta band.
Thus, the most revealing channels seem to be P3-T3 and P3-C3 channels in this kind of analysis. We can observe P3-T3 PSD mean values in Figure3.5 and P3-C3 PSD mean values in Figure3.6 with the three different overlappings.

[3]Electro-oculography is a technique for measuring the action potential of the human eye to record eye-movements.

Channel	% Overlapping	Delta (p-value)	Theta (p-value)	Alpha (p-value)
P3-T3	0%	0 (0.1671)	1 $(1.67 * 10^{-5})$	1(0.0192)
	50%	0 (0.0631)	1 $(3.74 * 10^{-5})$	1(0.0192)
	75%	0 (0.0636)	1 $(4.89 * 10^{-5})$	1(0.0192)
Channel	% Overlapping	Delta (p-value)	Theta (p-value)	Alpha (p-value)
P3-C3	0%	0 (0.6476)	1 $(7.56 * 10^{-5})$	1(0.0044)
	50%	0 (0.6476)	1 $(5.9 * 10^{-5})$	1(0.0044)
	75%	0 (0.06476)	1 $(1.03 * 10^{-4})$	1(0.0044)
Channel	% Overlapping	Delta (p-value)	Theta (p-value)	Alpha (p-value)
F3-C3	0%	0 (0.5464)	0 (0.3435)	1(0.0044)
	50%	0 (0.5441)	0 (0.3417)	1(0.0044)
	75%	0 (0.5509)	0 (0.3451)	1(0.0044)

Table 3.3: Statistical results for brain left side. In each table, we have reported the results of the statistics for each channel with three different overlappings. 1 stands for statically significant difference, 0 stands for no significant difference between euglycaemic and hypoglycaemic state. The p-value (likelihood of no difference between glycaemic states) is in brakets.

Channel	% Overlapping	Delta (p-value)	Theta (p-value)	Alpha (p-value)
P4-T4	0%	0 (0.3593)	1 (0.0044)	0(0.1671)
	50%	0 (0.3593)	1 (0.0044)	0(0.1671)
	75%	0 (0.3593)	1 (0.0044)	0(0.1671)
Channel	% Overlapping	Delta (p-value)	Theta (p-value)	Alpha (p-value)
P4-C4	0%	0 (1)	1 $(7.28 * 10^{-4})$	0(0.0636)
	50%	0 (1)	1 $(7.28 * 10^{-4})$	0(0.0636)
	75%	0 (1)	1 $(7.28 * 10^{-4})$	0(0.1671)
Channel	% Overlapping	Delta (p-value)	Theta (p-value)	Alpha (p-value)
F4-C4	0%	0 (1)	0 (1)	0(0.1671)
	50%	0 (1)	0 (1)	0(0.1671)
	75%	0 (1)	0 (1)	0(0.1671)

Table 3.4: Statistic results for brain right side. In each table, we have reported the results of the statistics for each channel with three different overlappings. 1 stands for statically significant difference, 0 stands for no significant difference between euglycaemic and hypoglycaemic state. The p-value (likelihood of no difference between glycaemic states) is in brakets.

We have obtained significant results with all three overlappings. Thus, we have decided to go on using a EEG windowing of 4 second length epochs with 50% overlapping, moreover this percentage is the default choise in the MATLAB

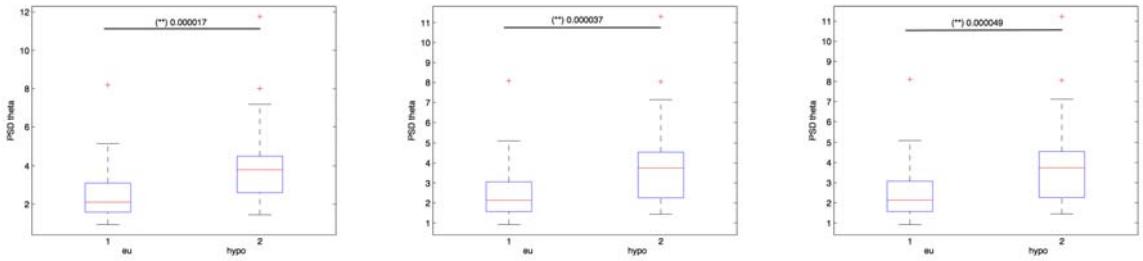

(a) Theta band: 0% overlapping **(b)** Theta band: 50% overlapping **(c)** Theta band: 75% overlapping

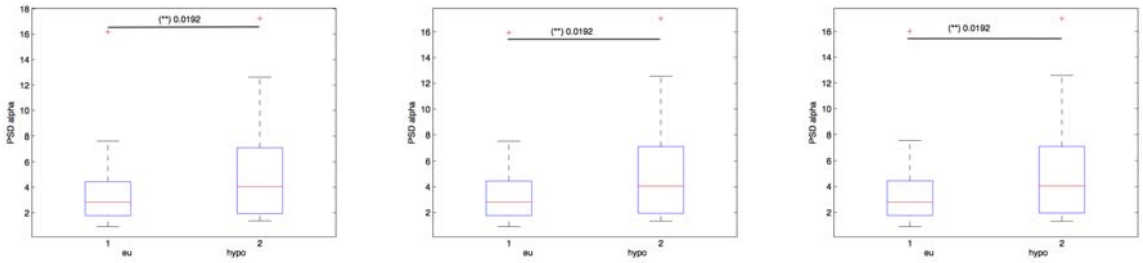

(d) Alpha band: 0% overlapping **(e)** Alpha band: 50% overlapping **(f)** Alpha band: 75% overlapping

Figure 3.5: P3-T3 channel. Boxplots of PSD mean value in the two glycaemic states from all subjects. The red line is the median value, the edges of the box are the 75th and 25th percentiles, the red crosses are the outliers. Double stars (**) indicate statically significant difference, the number near to the double stars is the p-value.

methods that we use.

We are satisfied by our outcomes in the brain left side, the value of the PSD increases passing from euglycaemia to hypoglycaemia and this outcome confirms the papers results.
The computation of the power spectrum density for the EEG signal can be considered a standard analysis, because a lot of papers base their dissection on it. So, we have decided to find different indexes and methods and to test them as hypoglycaemia indicators.

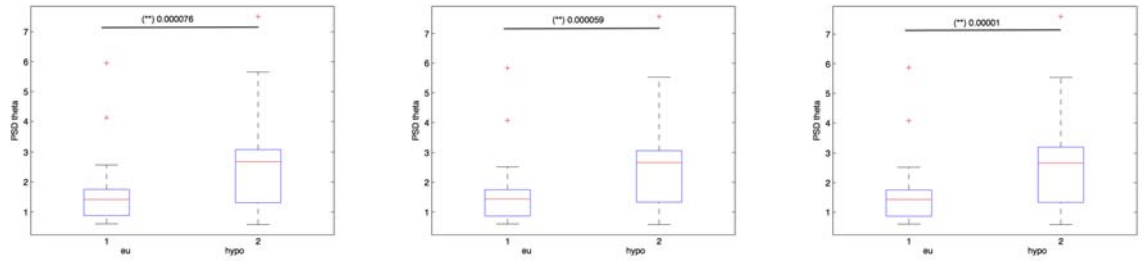

(a) Theta band: 0% overlapping **(b)** Theta band: 50% overlapping **(c)** Theta band: 75% overlapping

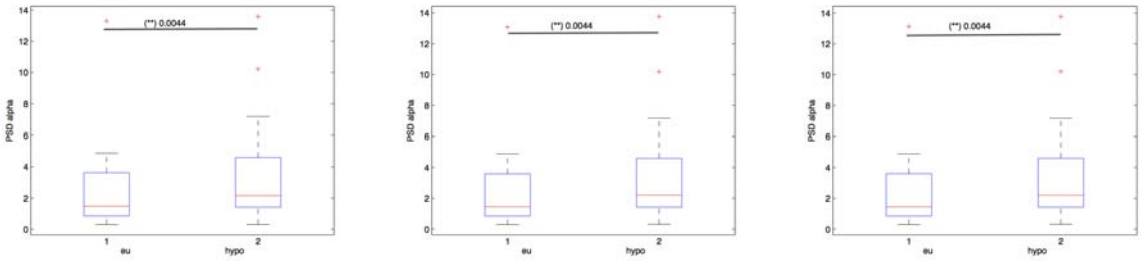

(d) Alpha band: 0% overlapping **(e)** Alpha band: 50% overlapping **(f)** Alpha band: 75% overlapping

Figure 3.6: P3-C3 channel. Boxplots of PSD mean value in the two glycaemic states from all subjects. The red line is the median value, the edges of the box are the 75th and 25th percentiles, the red crosses are the outliers. Double stars (**) indicate statically significant difference, the number near to the double stars is the p-value.

3.3 Other Hypoglycaemia indicators

In addition to the conventional frequency analysis in delta $(1-4$ Hz), theta $(4-8$ Hz), and alpha $(8-13$ Hz) bands, we have found other useful indexes to highlight differences among EEG signal in euglycaemia and hypoglycaemia.

The EEG signal of each subject has been divided in epochs of 4 second length, filtered by a Hamming window with a 50% overlapping as suggested in the paper [22].
In the publication above, the EEGraphic activity was recorded by subcutaneous electrodes, placed in P4-T4 position, in awake patients during the daylight.
We chose to reproduce these results and to deepen the analysis by using not only the P4-T4 position as a source, but also P4-C4, F4-C4 in the right-brain and the specular bipolar left-brain channels P3-T3, P3-C3, F3-C3.

The studied hypoglycaemia indicators are:

1. peak frequency in the unified theta-alpha $(4-13$ Hz) band;

2. centroid in each of the three conventional bands (delta $(1-4$ Hz), theta $(4-8$ Hz) e alpha $(8-13$ Hz));

3. integral of the spectral density and of the logarithm of the squared spectral density (power spectral density computed with Welch method as in the previous analysis).

3.3.1 Peak frequency

Observing the subjects' EEG track in each band, in most cases we have noticed a peak in the PSD (spectral density) in the unified theta-alpha ($4-13$ Hz) band as you can see in Figure3.2 for the subject ETW13. This peak also seems to change in magnitude when the patient is in hypoglycaemia.
We have computed the frequency and the amplitude of the peak in the unified theta-alpha band for each subject in every chosen channel as you can see (for the left-brain) in Figure3.7 for channel P3-T3, in Figure3.8 for channel P3-C3, in Figure3.9 for channel F3-C3 and (for the right-brain) in Figure3.10 for channel P4-T4, in Figure3.11 for channel P4-C4 and in Figure3.12 for channel F4-C4.
We have performed t-test, as usual, to compare the results of all subjects and to discover significant differences between euglycaemic and hypoglycaemic state. T-test results are reported in Table3.5

Channel	Frequency	Amplitude
P3-T3	0 (0.1596)	0 (0.0963)
P3-C3	0 (0.0963)	0 (0.2379)
F3-C3	1 (0.0309)	0 (0.8145)

Channel	Frequency	Amplitude
P4-T4	1 (0.0309)	1 (0.0309)
P4-C4	0 (0.0963)	0 (0.0963)
F4-C4	0 (0.8145)	0 (0.8145)

Table 3.5: Statistic results for Peak Value. In each table, we have reported the results of the statistics for each channel for the frequency and amplitude of the peak value in theta-alpha band. 1 stands for statically significant difference, 0 stands for no significant difference between euglycaemic and hypoglycaemic state. The p-value (likelihood of no difference between glycaemic states) is in brakets.

We have noticed that the peak value frequency increases passing from euglycaemia to hypoglycaemia (FigureA.1a, FigureA.2a, FigureA.4a, FigureA.3a, Figure3.11a, Figure3.12a) while the amplitude behaviour is not uniform in all channels.
The most significant channel (as you can see in Table3.5) is P4-T4. There's statically significant difference between euglycaemia and hypoglycaemia in both frequency and amplitude of the peak value.
The measure of the peak frequency seems to be a good indicator only in P4-T4 channel.

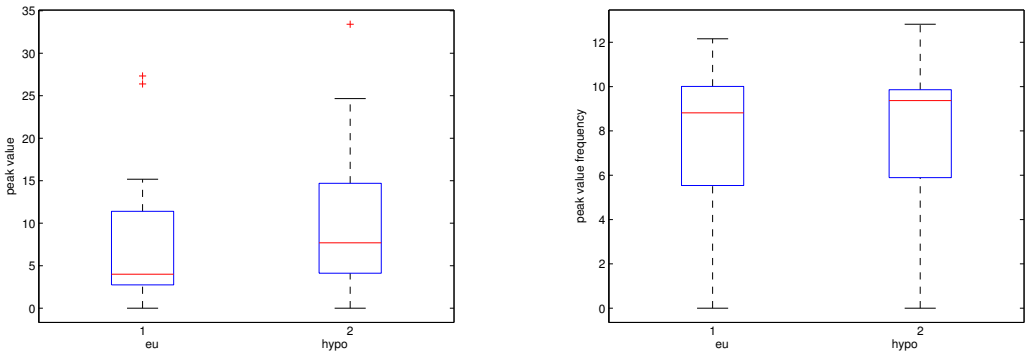

(a) Frequency **(b)** Amplitude

Figure 3.7: P3-T3: Peak Value. The red line is the median value, the edges of the box are the 75th and 25th percentiles, the red crosses are the outliers. Double stars (**) indicate statically significant difference, the number near to the double stars is the p-value.

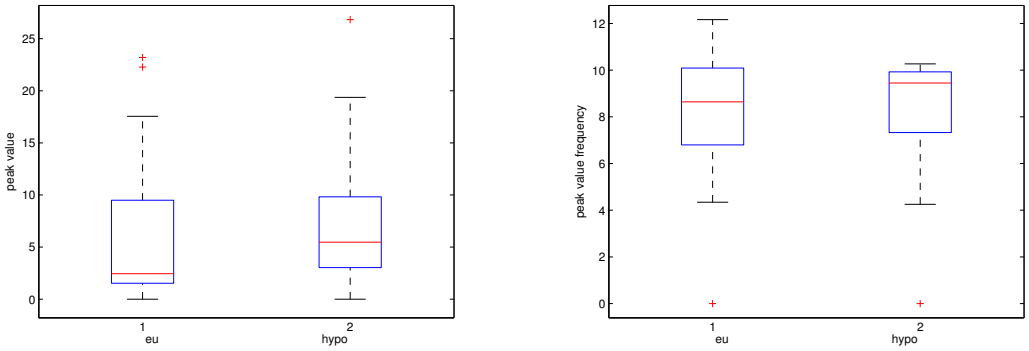

(a) Frequency **(b)** Amplitude

Figure 3.8: P3-C3: Peak Value. The red line is the median value, the edges of the box are the 75th and 25th percentiles, the red crosses are the outliers. Double stars (**) indicate statically significant difference, the number near to the double stars is the p-value.

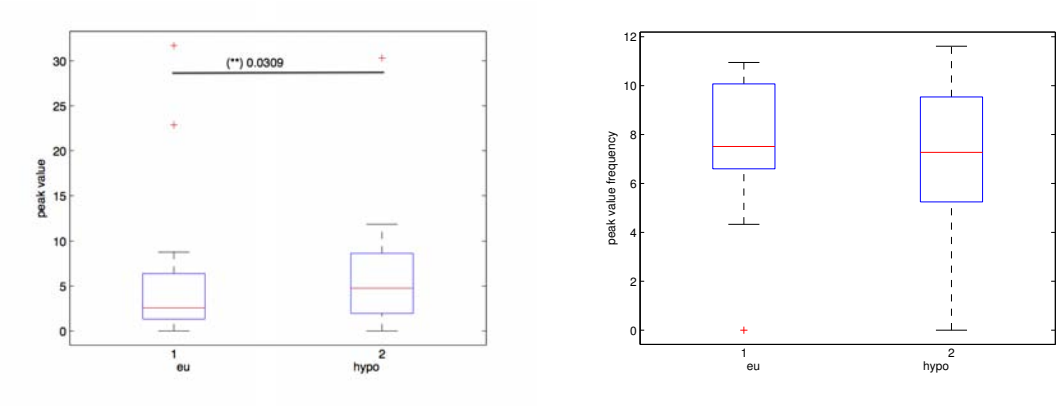

(a) Frequency **(b)** Amplitude

Figure 3.9: F3-C3: Peak Value. The red line is the median value, the edges of the box are the 75th and 25th percentiles, the red crosses are the outliers. Double stars (**) indicate statically significant difference, the number near to the double stars is the p-value.

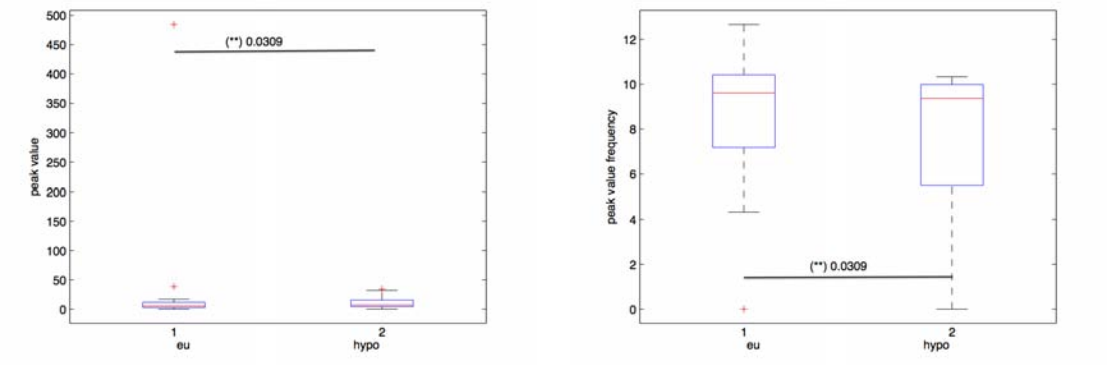

(a) Frequency **(b)** Amplitude

Figure 3.10: P4-T4: Peak Value. The red line is the median value, the edges of the box are the 75th and 25th percentiles, the red crosses are the outliers. Double stars (**) indicate statically significant difference, the number near to the double stars is the p-value.

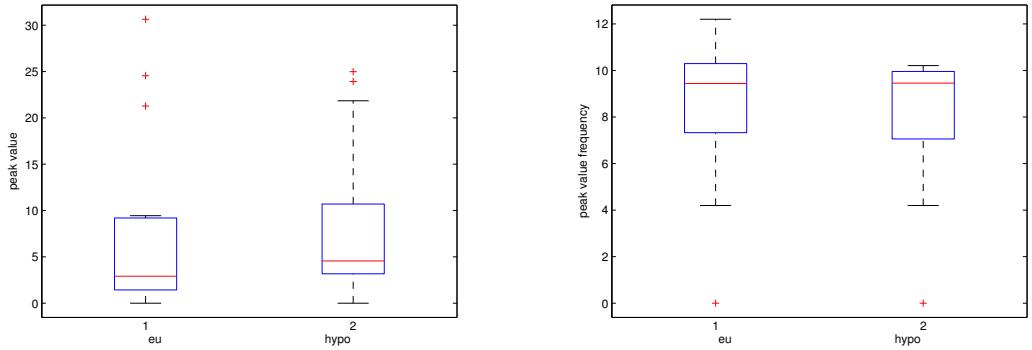

(a) Frequency **(b)** Amplitude

Figure 3.11: P4-C4: Peak Value. The red line is the median value, the edges of the box are the 75th and 25th percentiles, the red crosses are the outliers. Double stars (**) indicate statically significant difference, the number near to the double stars is the p-value.

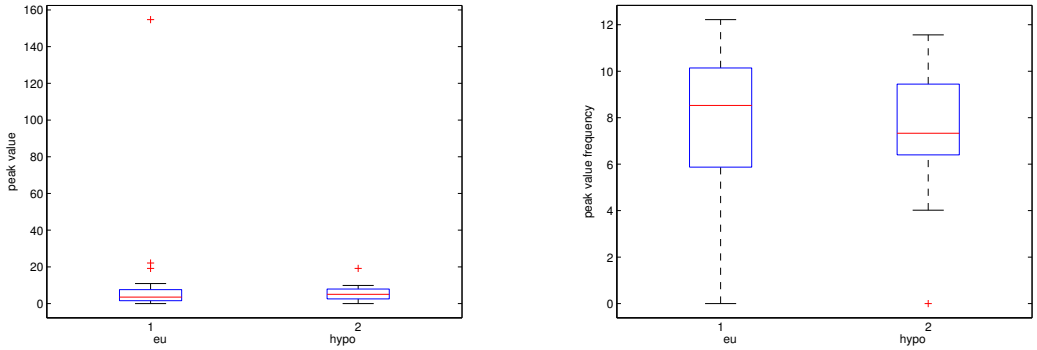

(a) Frequency **(b)** Amplitude

Figure 3.12: F4-C4: Peak Value. The red line is the median value, the edges of the box are the 75th and 25th percentiles, the red crosses are the outliers. Double stars (**) indicate statically significant difference, the number near to the double stars is the p-value.

3.3.2 Centroid

In the paper [22], the centroid frequency is described as the center of gravity of each frequency band that subdivides the area under the spectral curve into two of equal size.
The centroid is also described (for example in [31]) as the spectral baricenter where the frequencies $f(x)$ are weighted by their likelihood defined as: $p(x) = \frac{PSD(x)}{\sum_{x=1}^{N} PSD(x)}$.

$$centroid\_frequency = \frac{\sum(PSD(x)f(x))}{\sum(PSD(x))}$$

We have chosen to use both definitions to test which one would highlight the most the differences between eu- and hypoglycaemia. Results are exposed in Figure3.13, Figure3.14, Figure3.15, Figure3.16, Figure3.17, Figure3.18.
Then, we have performed t-test to compare the results of all subjects and to discover significant differences between euglycaemic and hypoglycaemic state (results in Table3.6).

Channel	Delta (*)	Theta (*)	Alpha (*)	Delta (**)	Theta (**)	Alpha (**)
P3-T3	0 (0.1284)	0 (0.2588)	0 (0.1664)	0 (0.1110)	0 (0.2036)	1 (0.0388)
P3-C3	0 (0.1064)	1 (0.0370)	0 (0.2786)	0 (0.1470)	1 (0.0391)	1 (0.0633)
F3-C3	0 (0.0963)	0 (0.0891)	0 (0.2564)	0 (0.3739)	0 (0.0911)	0 (0.3586)
Channel	Delta (*)	Theta (*)	Alpha (*)	Delta (**)	Theta (**)	Alpha (**)
P4-T4	0 (0.8050)	1 (0.0075)	1 (0.0208)	0 (0.4807)	1 (0.0075)	1 (0.0054)
P4-C4	0 (0.8912)	1 (0.0139)	0 (0.1495)	0 (0.7932)	1 (0.0158)	1 (0.0280)
F4-C4	0 (0.2741)	0 (0.0862)	0 (0.5900)	0 (0.3449)	0 (0.1078)	0 (0.8915)

Table 3.6: Statistic results for centroid frequency. In the table, we have reported the results of the statistics for each channel for the centroid frequency using the general definition(*) and the paper definition as spectrum median(**). 1 stands for statically significant difference, 0 stands for no significant difference between euglycaemic and hypoglycaemic state. The p-value (likelihood of no difference between glycaemic states) is in brakets.

The centroid frequency value seems to decrease in alpha band and to increase in delta and theta bands as we have summarized in Table3.7.

As you can see in Table3.7, the paper definition (**) is more effective than the general definition (*) of centroid frequency in discrimination between eu- and hypo-glycaemia. We can also observe that the centroid frequency could be a hypo-detector in theta and alpha band because we have obtained statically significant results in these two bands and a similar behaviour in all channels. Using the definition of spectrum median (**), the centroid frequency seems to increase in theta band passing from eu- to hypo-glycaemia and to decrease in alpha band. Using the general definition (*), we obtain the same result for the centroid frequency trend.

Channel	Delta (*)	Theta (*)	Alpha (*)	Delta (**)	Theta (**)	Alpha (**)
P3-T3	↑	↑	↓	↑	↑	↓ •
P3-C3	↑	↑ •	↓	↑	↑ •	↓ •
P4-T4	↑	↑ •	↓ •	↑	↑ •	↓ •
P4-C4	↑	↑ •	↓	↑	↑ •	↓ •
F3-C3	↓	↑	↑	↓	↑	↓
F4-C4	↓	↑	↑	↓	↑	-

Table 3.7: Centroid frequency trend. We have reported the results for the centroid frequency using the general definition(*) and the paper definition as spectrum median(**). Up-arrow (↑) stands for a general increase passing from eu- to hypo-glycaemia, down-arrow (↓) for a general decrease, bullet (•) for statically significant difference.

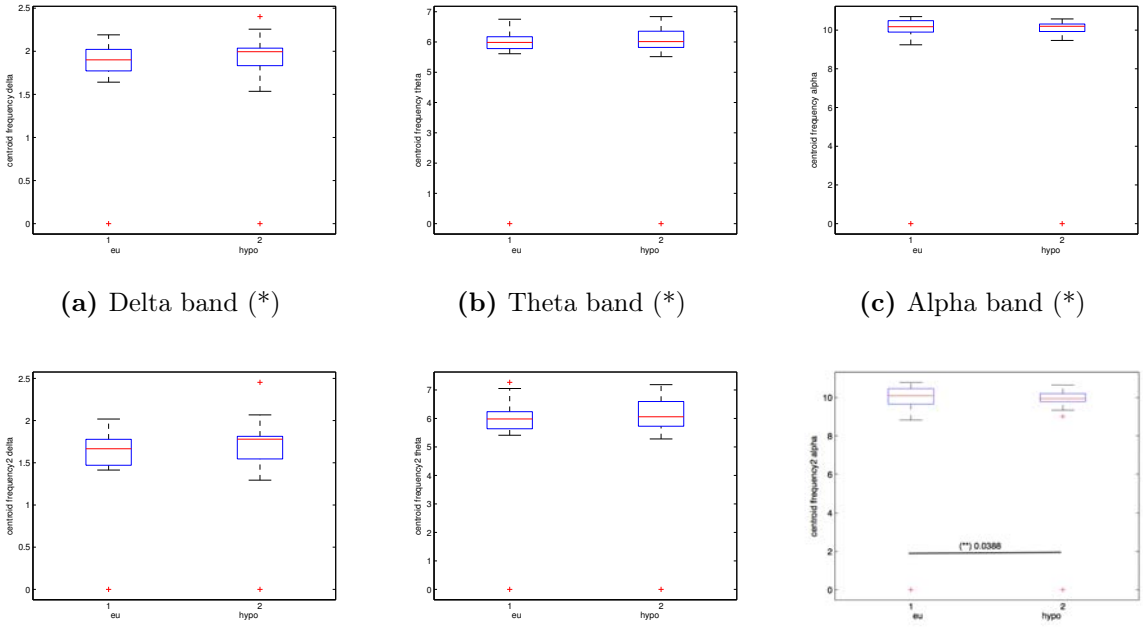

(a) Delta band (*) **(b)** Theta band (*) **(c)** Alpha band (*)

(d) Delta band (***) **(e)** Theta band (***) **(f)** Alpha band (***)

Figure 3.13: P3-T3: Centroid Frequency. We have reported the results for the centroid frequency using the general definition(*) and the paper definition as spectrum median(***). The red line is the median value, the edges of the box are the 75th and 25th percentiles, the red crosses are the outliers. Double stars (**) indicate statically significant difference, the number near to the double stars is the p-value.

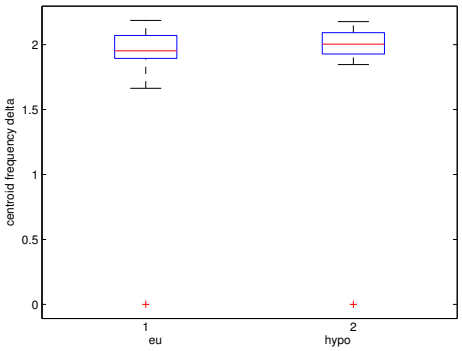

(a) Delta band (*)

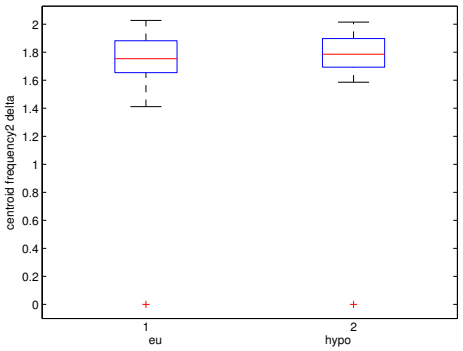

(b) Delta band (***)

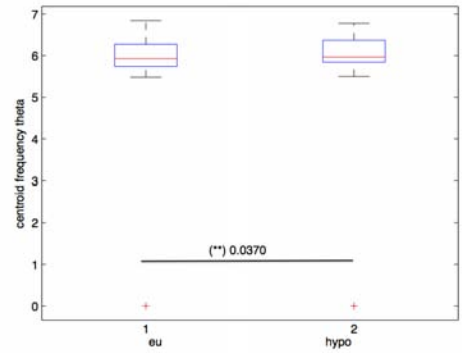

(c) Theta band (*)

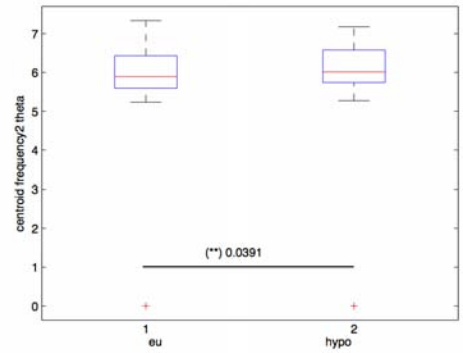

(d) Theta band (***)

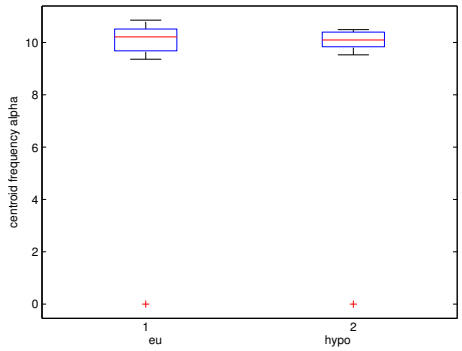

(e) Alpha band (*)

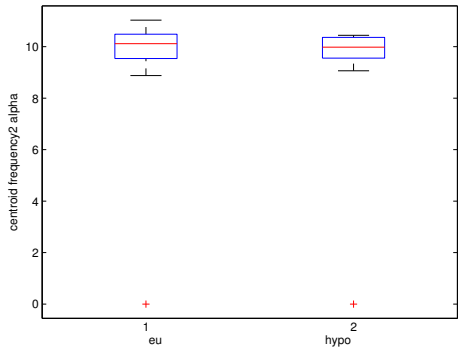

(f) Alpha band (***)

Figure 3.14: P3-C3: Centroid Frequency. We have reported the results for the centroid frequency using the general definition(*) and the paper definition as spectrum median(***). The red line is the median value, the edges of the box are the 75th and 25th percentiles, the red crosses are the outliers. Double stars (**) indicate statically significant difference, the number near to the double stars is the p-value.

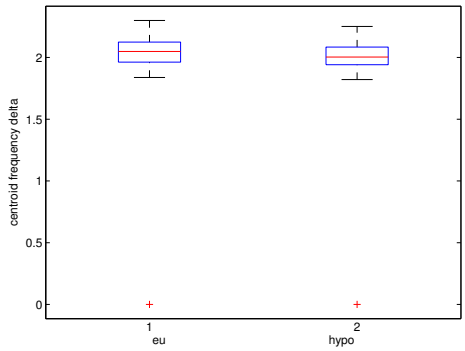

(a) Delta band (*)

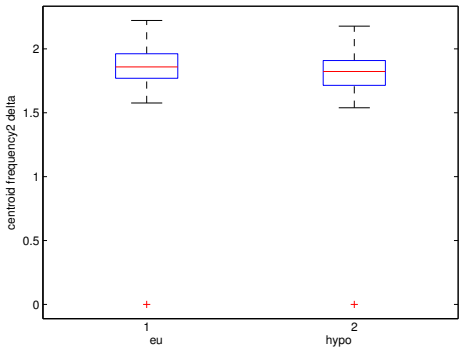

(b) Delta band (***)

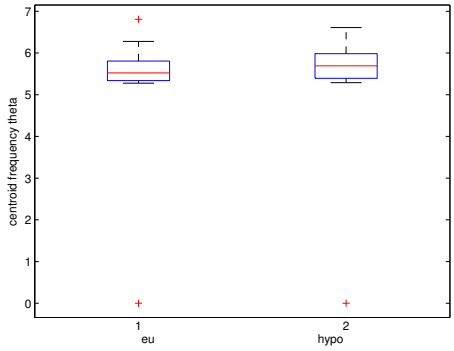

(c) Theta band (*)

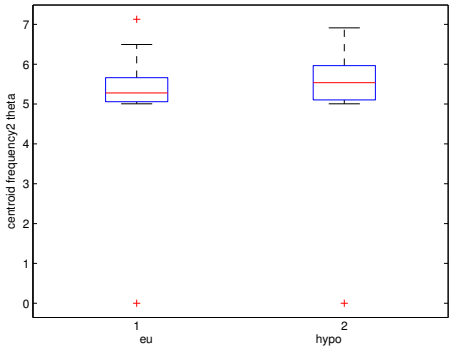

(d) Theta band (***)

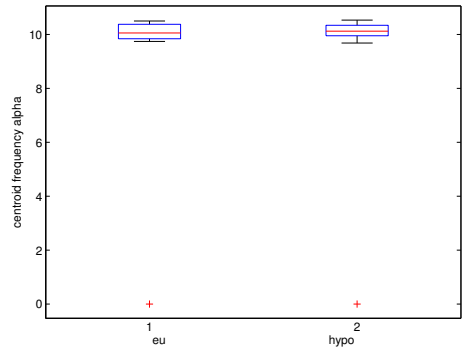

(e) Alpha band (*)

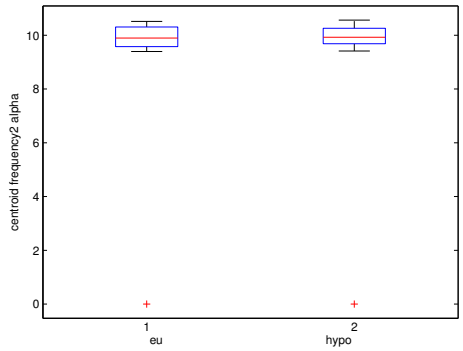

(f) Alpha band (***)

Figure 3.15: F3-C3: Centroid Frequency. We have reported the results for the centroid frequency using the general definition(*) and the paper definition as spectrum median(***). The red line is the median value, the edges of the box are the 75th and 25th percentiles, the red crosses are the outliers. Double stars (**) indicate statically significant difference, the number near to the double stars is the p-value.

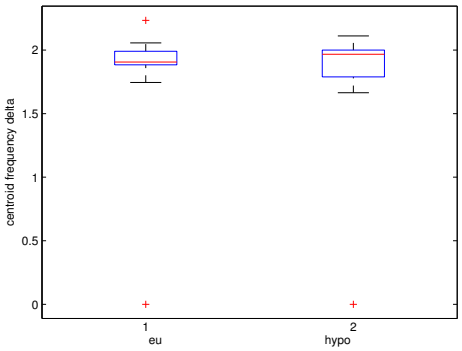

(a) Delta band (*)

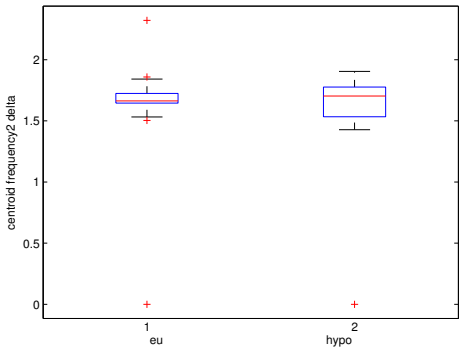

(b) Delta band (***)

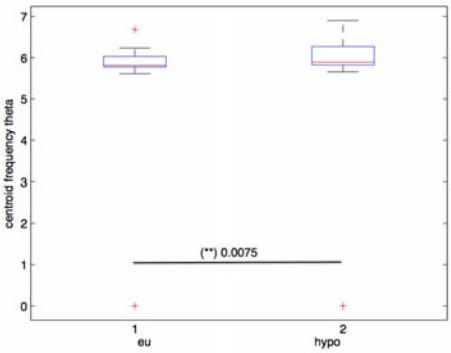

(c) Theta band (*)

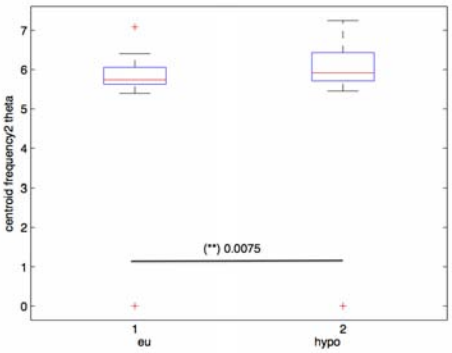

(d) Theta band (***)

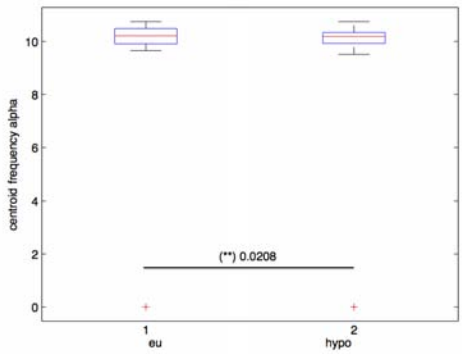

(e) Alpha band (*)

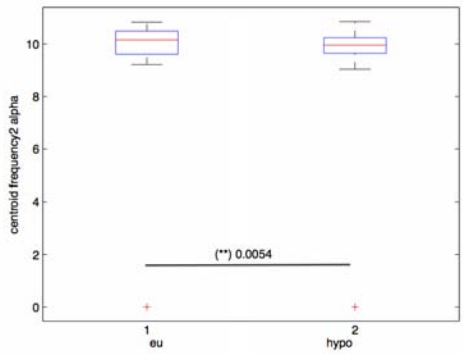

(f) Alpha band (***)

Figure 3.16: P4-T4: Centroid Frequency. We have reported the results for the centroid frequency using the general definition(*) and the paper definition as spectrum median(***). The red line is the median value, the edges of the box are the 75th and 25th percentiles, the red crosses are the outliers. Double stars (**) indicate statically significant difference, the number near to the double stars is the p-value.

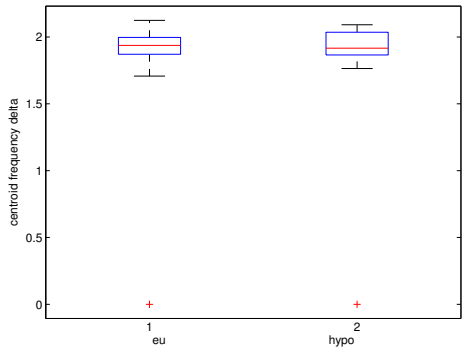

(a) Delta band (*)

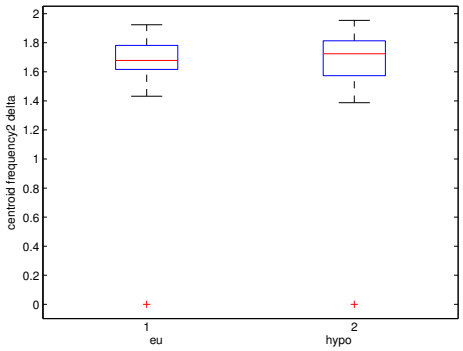

(b) Delta band (***)

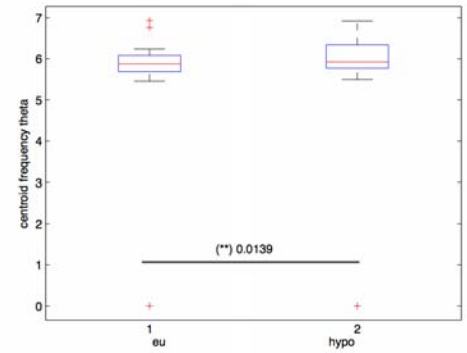

(c) Theta band (*)

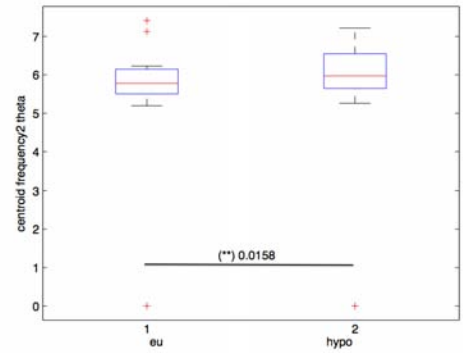

(d) Theta band (***)

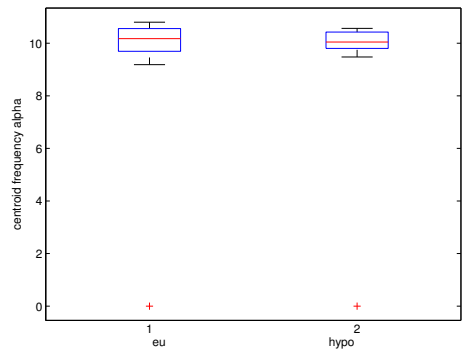

(e) Alpha band (*)

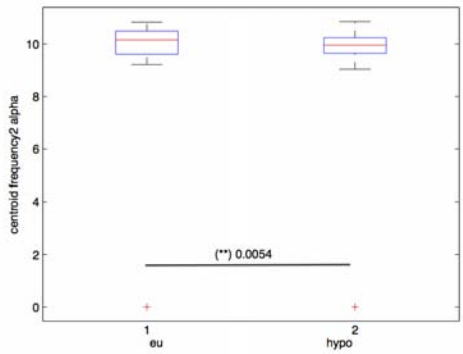

(f) Alpha band (***)

Figure 3.17: P4-C4: Centroid Frequency. We have reported the results for the centroid frequency using the general definition(*) and the paper definition as spectrum median(***). The red line is the median value, the edges of the box are the 75th and 25th percentiles, the red crosses are the outliers. Double stars (**) indicate statically significant difference, the number near to the double stars is the p-value.

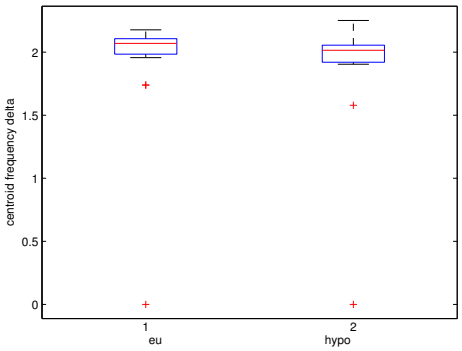

(a) Delta band (*)

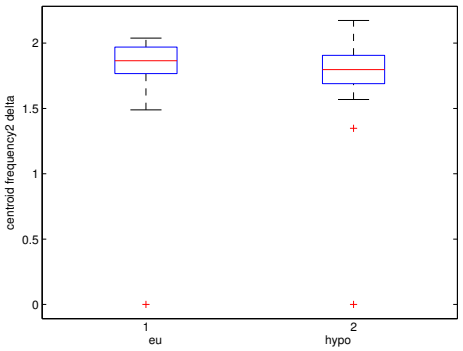

(b) Delta band (***)

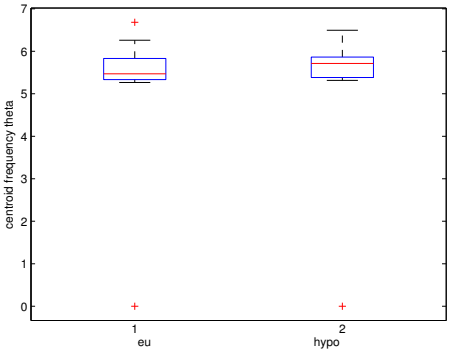

(c) Theta band (*)

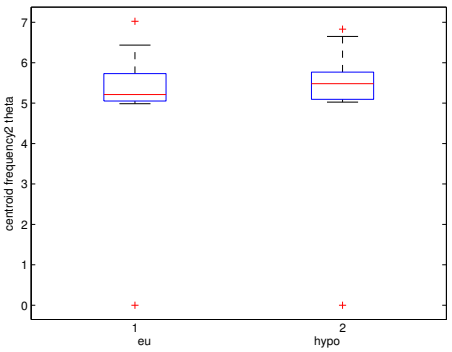

(d) Theta band (***)

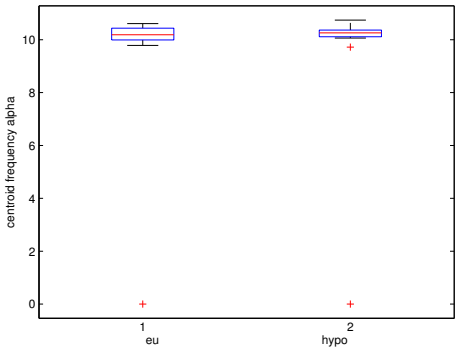

(e) Alpha band (*)

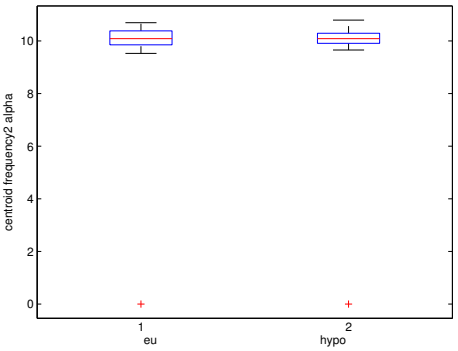

(f) Alpha band (***)

Figure 3.18: F4-C4: Centroid Frequency. We have reported the results for the centroid frequency using the general definition(*) and the paper definition as spectrum median(***). The red line is the median value, the edges of the box are the 75th and 25th percentiles, the red crosses are the outliers. Double stars (**) indicate statically significant difference, the number near to the double stars is the p-value.

3.3.3 Power spectrum

We have examined the spectral density trend in the conventional band in the previous analysis (3.2). We have taken this choice to see if the EEG signal, without further manipulation, would highlight different behaviors in the selected periods of euglycemia and hypoglycemia.
In some papers, the EEG signal was further processed studying the integral of the squared and log transformed PSD, to ensure that the EEG features were normally distributed [19].
In other publications, it's studied the integral of the power spectral density to derive the power of the signal in each bandwith ($[f_L, f_H]$):

$$Power = \int_{f_L}^{f_H} PSD(f)df.$$

We have repeated a similar frequency analysis of paragraph 3.2:

- computation of the PSD with Welch's method;
- computation of the PSD integral and of the squared and log transformed PSD integral;
- computation of mean value of the previous results;
- statistic analysis and comparison between the euglycaemic state and the hypoglycaemic one.

Eventually, we have chosen to compare the data from the PSD (and $logPSD^2$) integral trend with the only PSD trend to see if EEG signal is enough informative without further manipulation.

The statistics results are presented in Table3.8.

Channel	Delta (*)	Theta (*)	Alpha (*)	Delta (**)	Theta (**)	Alpha (**)
P3-T3	0 (0.0963)	1 ($5.05 * 10^{-5}$)	1 (0.0309)	1 (0.0219)	1 ($5.47 * 10^{-8}$)	1 (0.0075)
P3-C3	0 (0.8145)	1 ($7.52 * 10^{-5}$)	1 (0.0075)	0 (0.4807)	1 ($7.10 * 10^{-5}$)	1 (0.0024)
F3-C3	0 (0.5170)	0 (0.3328)	1 (0.0075)	0 (1)	0 (0.1047)	1 ($8.97 * 10^{-4}$)
Channel	Delta (*)	Theta (*)	Alpha (*)	Delta (**)	Theta (**)	Alpha (**)
P4-T4	0 (0.4807)	1 (0.0013)	0 (0.0963)	0 (0.4907)	1 (0.0075)	0 (0.2379)
P4-C4	0 (1)	1 (0.0013)	0 (0.0963)	0 (0.7999)	1 (0.0033)	1 (0.0057)
F4-C4	0 (1)	0 (1)	0 (0.2379)	0 (0.8145)	0 (0.8145)	0 (0.4496)

Table 3.8: Statistic results for PSD and $logPSD^2$ integral. In the table, we have reported the results of the statistics for each channel for the PSD integral (*) and the $logPSD^2$ integral (**). 1 stands for statically significant difference, 0 stands for no significant difference between euglycaemic and hypoglycaemic state. The p-value (likelihood of no difference between glycaemic states) is in brakets.

We can note that the results in Table3.8 for the two methods of integral computation are very similar. The $logPSD^2$ integral gains statically difference

between eu- and hypoglycaemic state in delta band in P3-T3 channel and in alpha band in P4-C4 channel.

In Table3.9, we have compared the best statistics results of the above analysis with the results obtained by the testing of the PSD in paragraph 3.2.

Channel	Delta ($\int logPSD^2$ vs PSD)	Theta ($\int logPSD^2$ vs PSD)	Alpha ($\int logPSD^2$ vs PSD)
P3-T3	1 vs 0	1 vs 1	1 vs 1
P3-C3	0 vs 0	1 vs 1	1 vs 1
F3-C3	0 vs 0	0 vs 0	1 vs 0
P4-T4	0 vs 0	1 vs 1	0 vs 0
P4-C4	0 vs 0	1 vs 1	1 vs 0
F4-C4	0 vs 0	0 vs 0	0 vs 0

Table 3.9: PSD: comparison of statistics results. In the table, we have reported the comparison of the statistics results for each channel for the $logPSD^2$ integral (**) and for the PSD. 1 stands for statically significant difference, 0 stands for no significant difference between euglycaemic and hypoglycaemic state.

The $logPSD^2$ integral gains statically difference between eu- and hypoglycaemic state in alpha band in F3-C3 channel and in P4-C4 channel.

The PSD and the $logPSD^2$ integral (from Figure3.19 to Figure3.24) tendency is summed up in Table3.10. Their values increases passing from euglycaemia to hypoglycaemia in all three bands. Thus, the increase in the power spectrum can be considered another possible indicator of hypoglycaemia, in particular in theta band, where the statically difference between eu- and hypo-glycaemia is present in most of the channels (P3-T3, P3-C3, P4-T4, P4-C4). The results in F3-C3 and F4-C4 are not notable as usual.
To sum up, PSD, PSD integral and $logPSD^2$ integral appear to emphasize the difference between eu- and hypo-glycaemia with similar results. They especially highlight an increase in the theta power spectrum.

Channel	Delta (*)	Theta (*)	Alpha (*)	Delta (**)	Theta (**)	Alpha (**)
P3-T3	↑	↑ •	↑ •	↑ •	↑ •	↑ •
P3-C3	↑	↑ •	↑ •	↑	↑ •	↑ •
P4-T4	↑	↑ •	↑	↑	↑ •	↑
P4-C4	↑	↑ •	↑	↑	↑ •	↑ •
F3-C3	-	↑	↑ •	↑	↑	↑ •
F4-C4	↓	-	↑	↓	-	↑

Table 3.10: PSD and $logPSD^2$ integral trend. We have reported the results for the PSD integral (*) and the $logPSD^2$ integral(**). Up-arrow (↑) stands for a general increase passing from eu- to hypo-glycaemia, down-arrow (↓) for a general decrease, bullet (•) for statically significant difference.

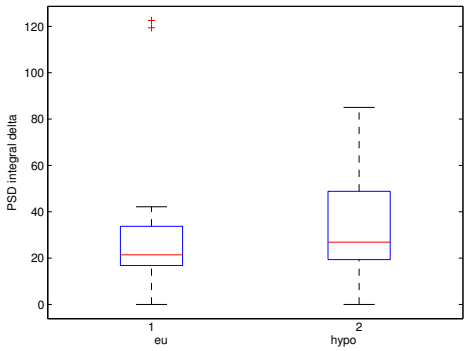

(a) Delta band (*)

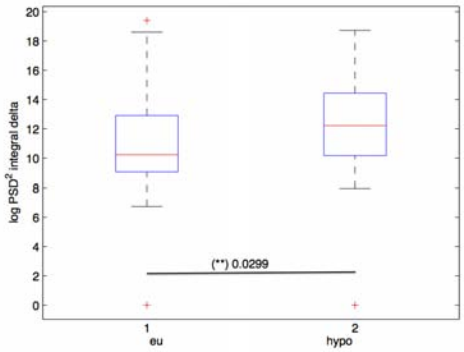

(b) Delta band (***)

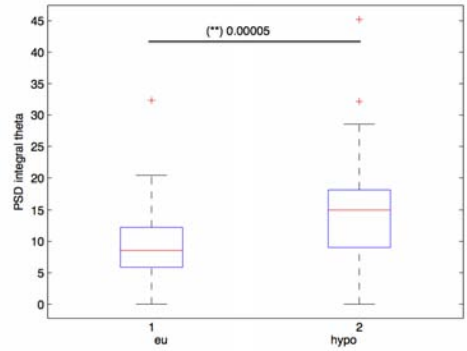

(c) Theta band (*)

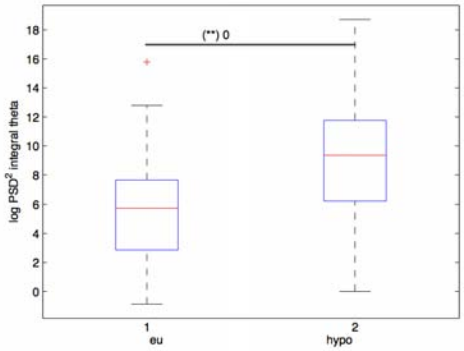

(d) Theta band (***)

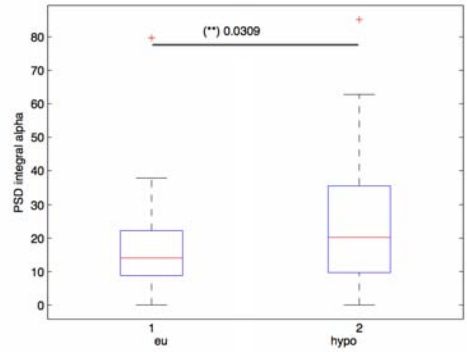

(e) Alpha band (*)

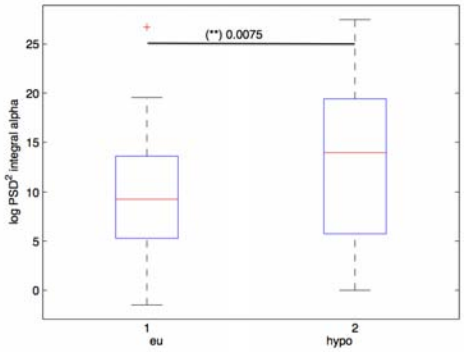

(f) Alpha band (***)

Figure 3.19: P3-T3: PSD and $logPSD^2$ integral. We have reported the results for the PSD integral (*) and the $logPSD^2$ integral(***). The red line is the median value, the edges of the box are the 75th and 25th percentiles, the red crosses are the outliers. Double stars (**) indicate statically significant difference, the number near to the double stars is the p-value.

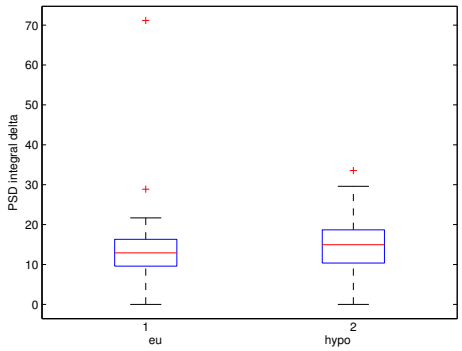

(a) Delta band (*)

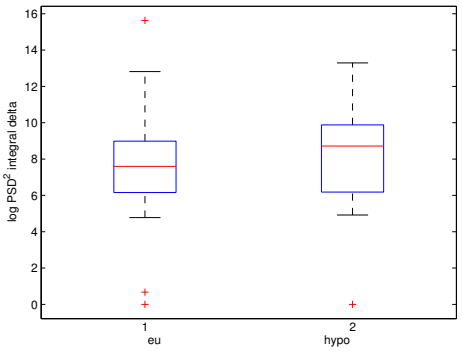

(b) Delta band (***)

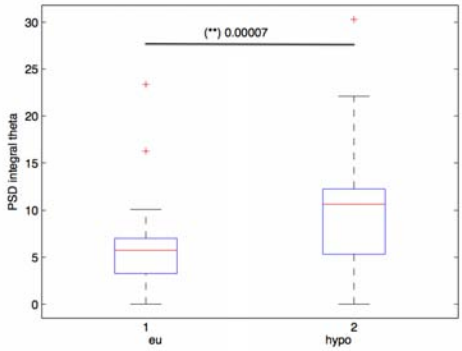

(c) Theta band (*)

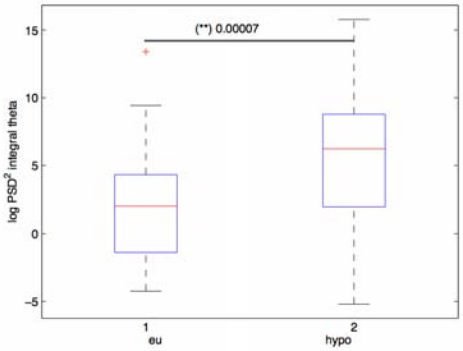

(d) Theta band (***)

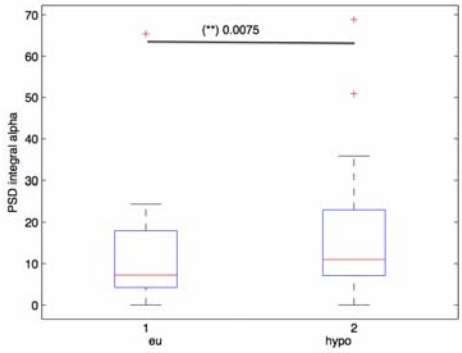

(e) Alpha band (*)

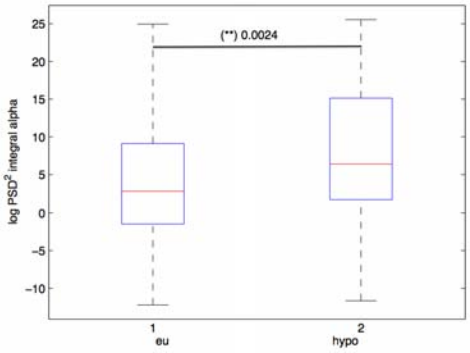

(f) Alpha band (***)

Figure 3.20: P3-C3: PSD and $logPSD^2$ integral. We have reported the results for the PSD integral (*) and the $logPSD^2$ integral(***). The red line is the median value, the edges of the box are the 75th and 25th percentiles, the red crosses are the outliers. Double stars (**) indicate statically significant difference, the number near to the double stars is the p-value.

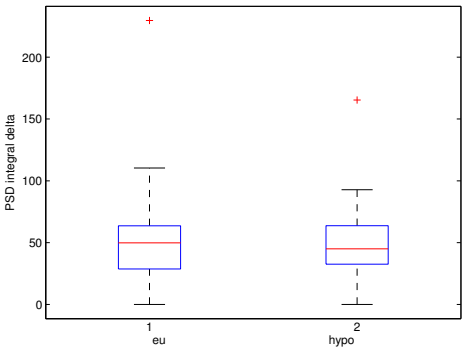

(a) Delta band (*)

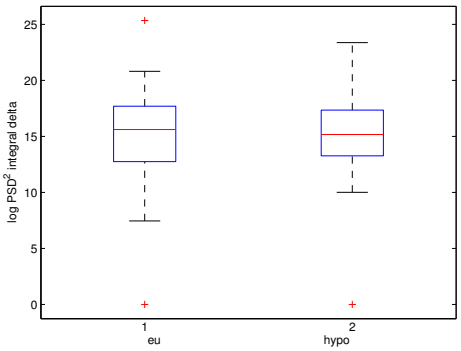

(b) Delta band (***)

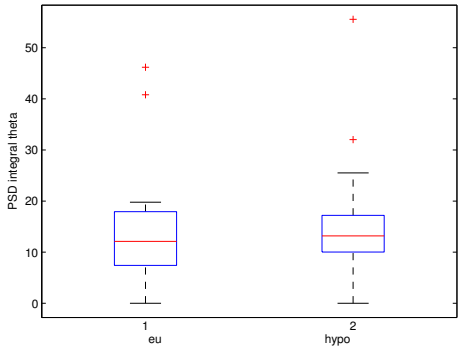

(c) Theta band (*)

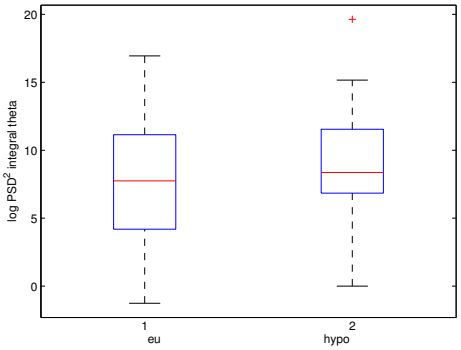

(d) Theta band (***)

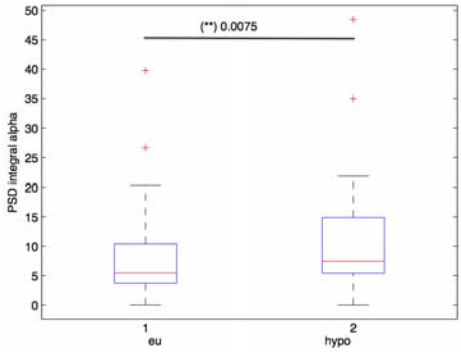

(e) Alpha band (*)

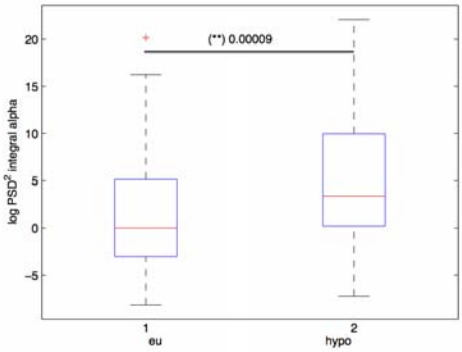

(f) Alpha band (***)

Figure 3.21: F3-C3: PSD and $logPSD^2$ integral. We have reported the results for the PSD integral (*) and the $logPSD^2$ integral(***). The red line is the median value, the edges of the box are the 75th and 25th percentiles, the red crosses are the outliers. Double stars (**) indicate statically significant difference, the number near to the double stars is the p-value.

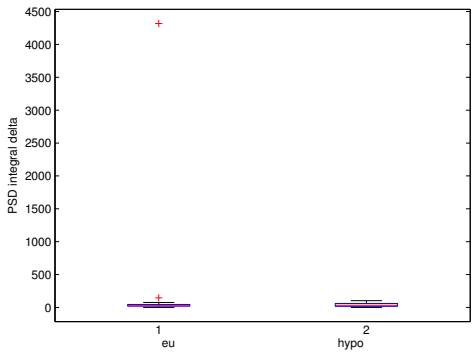

(a) Delta band (*)

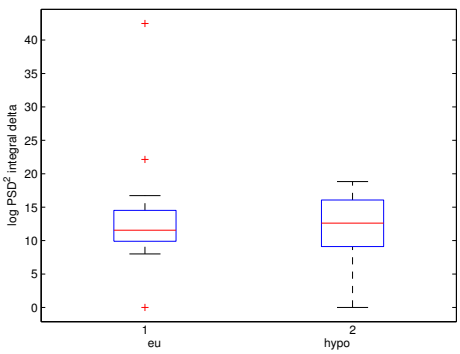

(b) Delta band (***)

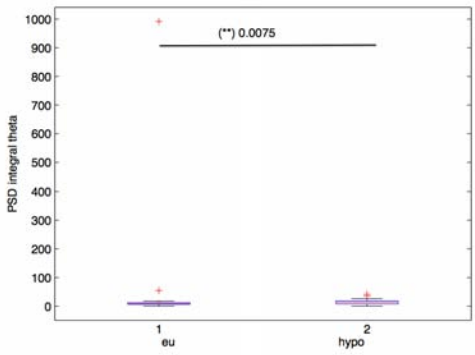

(c) Theta band (*)

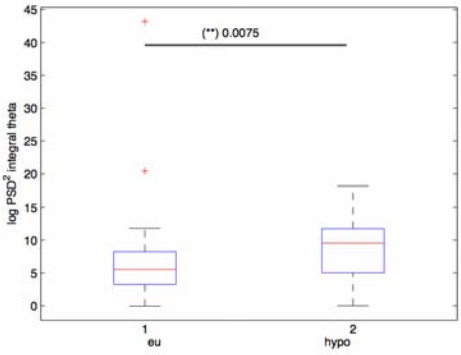

(d) Theta band (***)

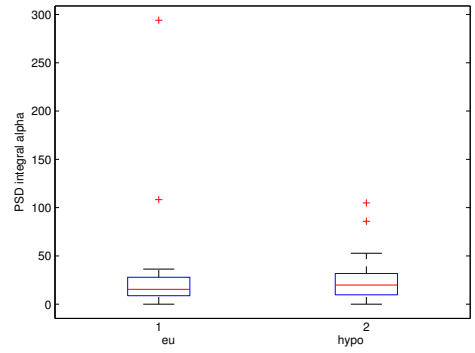

(e) Alpha band (*)

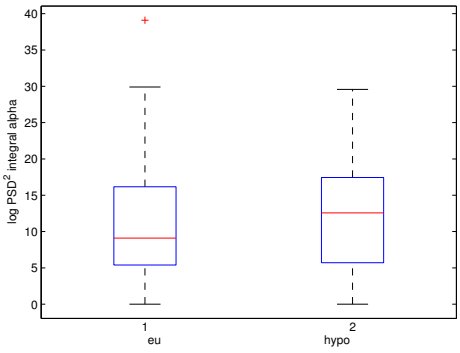

(f) Alpha band (***)

Figure 3.22: P4-T4: PSD and $logPSD^2$ integral. We have reported the results for the PSD integral (*) and the $logPSD^2$ integral(***). The red line is the median value, the edges of the box are the 75th and 25th percentiles, the red crosses are the outliers. Double stars (**) indicate statically significant difference, the number near to the double stars is the p-value.

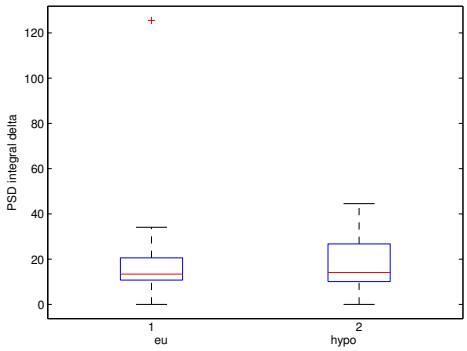

(a) Delta band (*)

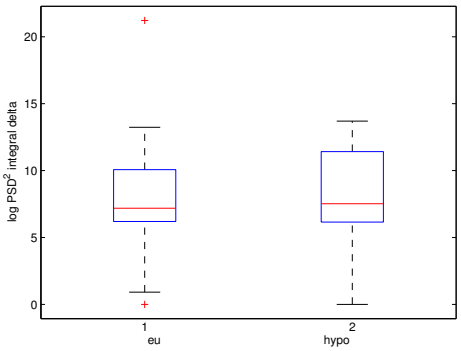

(b) Delta band (***)

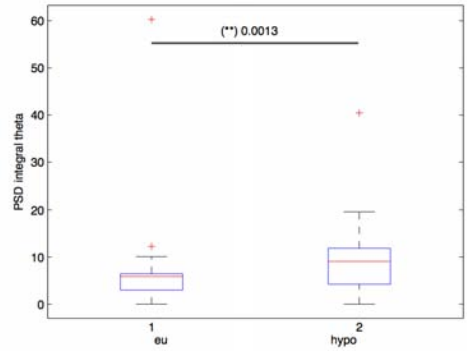

(c) Theta band (*)

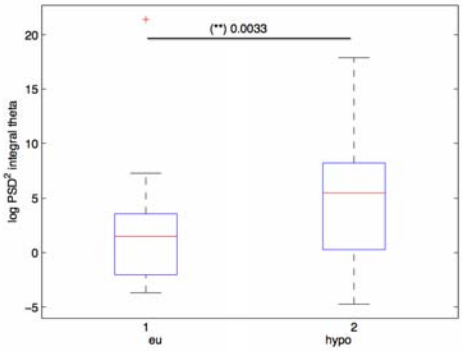

(d) Theta band (***)

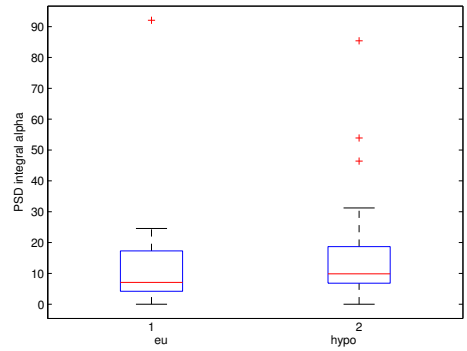

(e) Alpha band (*)

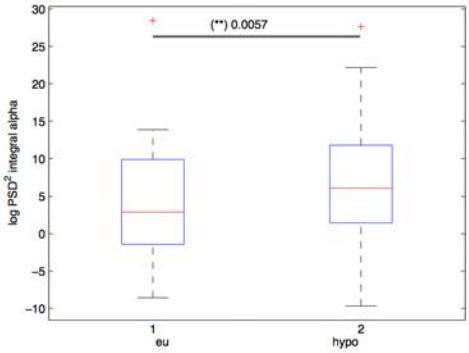

(f) Alpha band (***)

Figure 3.23: P4-C4: PSD and $logPSD^2$ integral. We have reported the results for the PSD integral (*) and the $logPSD^2$ integral(***). The red line is the median value, the edges of the box are the 75th and 25th percentiles, the red crosses are the outliers. Double stars (**) indicate statically significant difference, the number near to the double stars is the p-value.

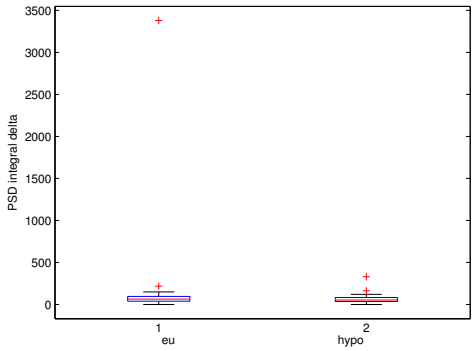

(a) Delta band (*)

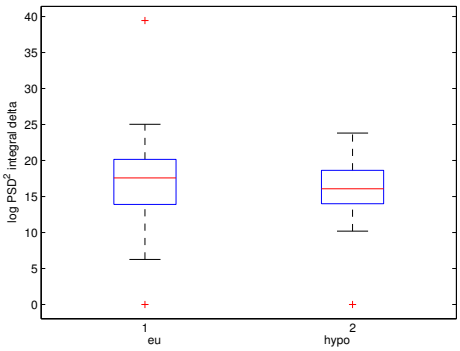

(b) Delta band (***)

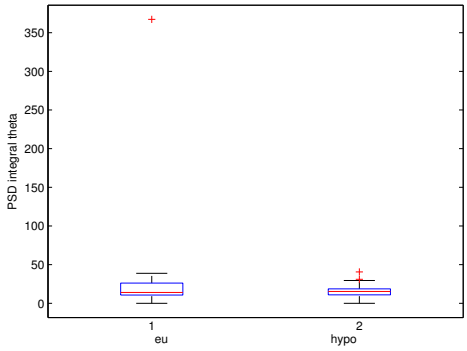

(c) Theta band (*)

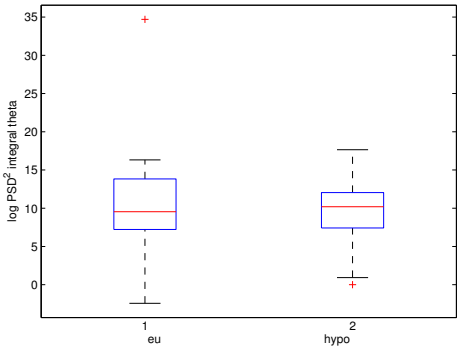

(d) Theta band (***)

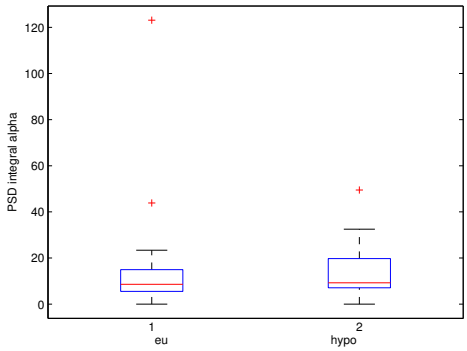

(e) Alpha band (*)

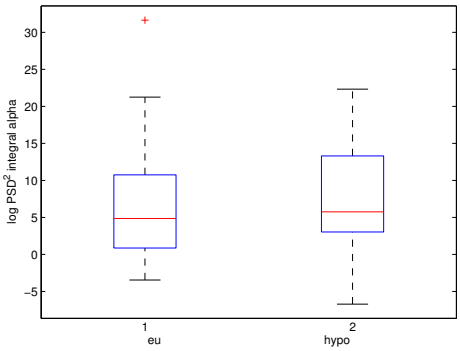

(f) Alpha band (***)

Figure 3.24: F4-C4: PSD and $logPSD^2$ integral. We have reported the results for the PSD integral (*) and the $logPSD^2$ integral(***). The red line is the median value, the edges of the box are the 75th and 25th percentiles, the red crosses are the outliers. Double stars (**) indicate statically significant difference, the number near to the double stars is the p-value.

3.4 Possible margins of improvement

Observing the whole results, the F3-C3 and F4-C4 channels do not show significant outcomes. Taking their brain position in consideration, these channels would probably interfere with the EOG, so these signals need a pre-elaboration to be used in the hypoglycaemia detection.
We have decided to discard the use of F3-C3 and F4-C4 channels to avoid a pre-elaboration of the signal and because of the informative results that can be estimated by the other channels.
Our frequency analysis is founded on the comparison between euglycaemia and hypoglycaemia, so it would be of interest to involve the 15/30 minute period before the hypoglycaemic one to try to give a warning to the patient.
Moreover, it would be interesting to see if the EEG signal is also informative in the time domain.
Eventually, the frequency analysis could be improved by computing subjective boundaries for the three frequency bands (delta, theta and alpha) for each patient and by basing the study on utilizing these new bands.
So, in Chapter 4, we have decided to focus on personalizing the alpha band, because of the significant results obtained in this EEG frequency range, and then on computing again all the hypoglycaemic indicators in the new alpha band limitations.

Chapter 4

Spectral analysis with EEG alpha band individualization

We used the conventional bands (delta ($1-4$ Hz), theta ($4-8$ Hz) e alpha ($8-13$ Hz)) to compute the spectral density and the other hypoglycaemia indicators.
We wondered if the limitations of these bands could be customized for each subject and if the same indicators, in the personalized bands, could improve by being more effective.
In the paper [32], it's discussed the well-known approaches to compute the individual alpha frequency (the peak frequency in the alpha band).
The first step to investigate the alpha frequency is to detect the personalized alpha band for each subject.
We have decided to exploit this approach to detect the personalized alpha band for each subject and to compute again all the hypoglycaemic indicators with these new limitations.
We present this simple pilot-study to evaluate if it's worth undertaking this task.

4.1 The extended band (EB) method

The extended band (EB) method was proposed by *Klimesh et al.* in the 1990 [33]. It's based on visual inspecting, thus it results subjective, and it's applied to a resting spectrum. In our study, we have chosen the PSD during euglycemia as resting spectrum.
EB method consists of a few steps:

1. EEG spectra without detectable alpha peak are discarded by visually inspecting;
2. the starting point of the ascending edge is considered as f_1 by visually inspecting;
3. the ending point of the descendind edge is considered as f_2 by visually inspecting;
4. the extended alpha band (from f_1 to f_2) is detected by averaging the boundaries obtained by each channel.

The first step is to discard EEG resting spectra without a detecable alpha peak. We found three subjects to be discarded in our database: PET03, KIP12 and OLR08 (in Figure4.1).

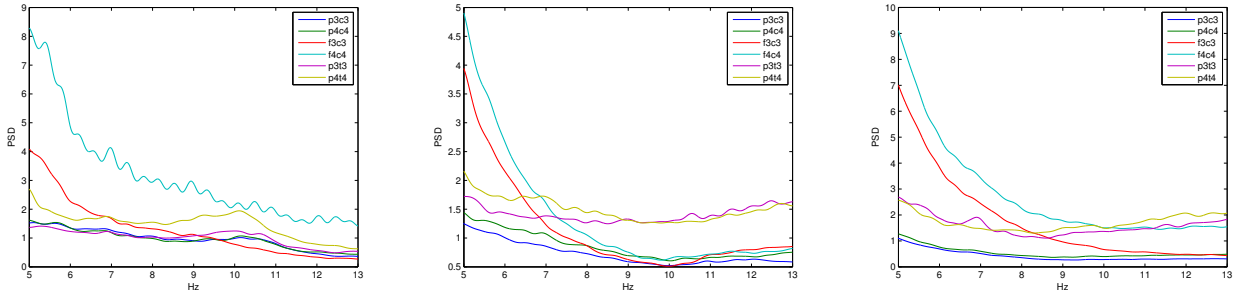

(a) PET03 **(b)** KIP12 **(c)** OLR08

Figure 4.1: EB method: PSD discarded

Then, we have computed the boundaries for each subject, obtaining the values in Figure4.2.

	P3-C3		P4-C4		F3-C3		F4-C4		P3-T3		P4-T4			
	f1	f2	f1	f2	f1	f2	f1	f2	f1	f2	f1	f2	mean(f1)	mean(f2)
ANT	7,231	10,41	7,166	9,833	8,165	9,842			7,513	10,2	7,248	11,62	7,4646	10,381
ANB	7	9,249	7	9,249	7	9,084	7	9,084	7,076	9,386			7,0152	9,2104
BOE	6,263	13	8,497	13	5,351	9,204	5,611	9,48	8,497	13	6,458	13	6,7795	11,7806667
CAJ	5,498	8,083	5,682	7,932	5,988	7,886	6,012	8,078					5,795	7,99475
ERN									7,7	13	7,7	13	7,7	13
ETW	8,664	11,81	8,021	12,01			9,528	11,16	9,489	11,96	9,15	11,84	8,9704	11,756
FLP	7	13	7	13	8,577	13			6,098	13	6,098	13	6,9546	13
GIM	8,094	11,57	8,117	11,25	9,584	11,75	8,539	11,79	8,231	11,54	8	11,22	8,4275	11,52
KIH	7,849	10,72	7,849	10,72	8,488	10,27	8,488	10,27	7,849	10,52	7,849	10,52	8,062	10,5033333
KIP														
LAB	8,939	11	8,86	10,73					8,754	11,33	8,871	11	8,856	11,015
LOH	7	13	7,58	13	9,658	12,14	9,611	13	6,399	12,81	6,399	12,64	7,7745	12,765
MAA	9,04	10,98	9,04	11,34			9	11,32	8,374	13	8,374	13	8,7656	11,928
OLR														
PEH					7,431	10,53							7,431	10,53
PEL	6,03	10,42	7,044	10,48	5	10	5	9	7,642	11	7,48	10,02	6,366	10,1533333
PEN	6,8	9,617	6,851	9,448					6,894	9,143			6,84833333	9,40266667
PET														
SOP	7,706	13,55	7,689	13,55									7,6975	13,55
													7,55673333	11,1556344

Figure 4.2: EB method: application to all subjects

For instance, in Figure4.3, we have reported the resting spectrum (euglycaemic PSD) in each channel and the boundaries (red vertical lines) computed for subject ETW13.

4.2 Implementation

We have calculated the same hypoglycaemia indicators in the personalized alpha band to compare them with the results in the conventional band.
We have computed the centroid frequency and the integral of both the spectral density and the logarithm of the squared spectral density in the new alpha band for each of the following channel:

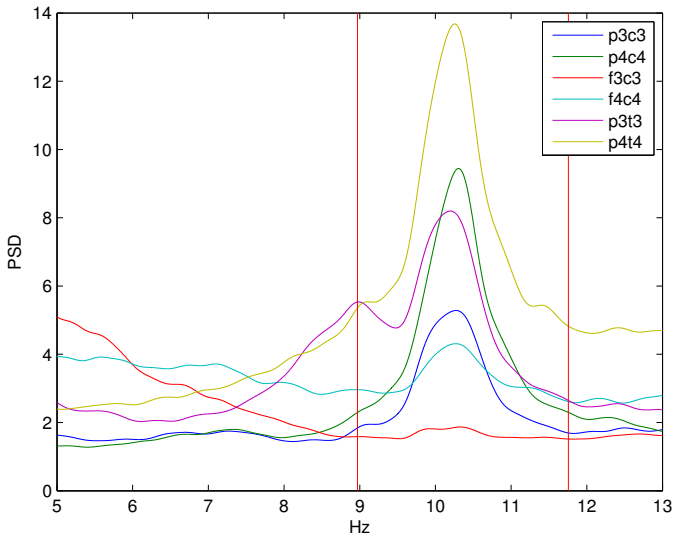

Figure 4.3: EB method: subject ETW13. We can see euglycaemic PSD in all selected channels in different colours. The vertical red lines stand for the boundaries of the personalized alpha band.

- P3-T3 (P4-T4)
- P3-C3 (P4-C4).

We have omitted the channels F3-C3 and F4-C4 from this analysis, because they did not display good results in the above paragraphs.
We show the results divided for each channel from Figure4.4 to Figure4.7.

4.3 Results

We have performed the usual statistical comparison between eu- and hypoglycaemia results to emphasize the significant difference. The results are summed up in Table4.1.

The outcomes are very satisfactory, in particular if we compare them with the ones obtained by the previous analysis, (as you can see in Table4.2).

We have earned statically difference in the centroid frequency for channels P3-T3, P3-C3 and P4-C4, and in the power spectrum for channel P4-T4, thanks to the alpha band personalization.

Channel	Centroid frequency (*)	Centroid frequency (**)	$\int PSD$	$\int logPSD^2$
P3-T3	1 (0.0011)	$1(8.44 * 10^{-5})$	1 (0.0059)	1 (0.0023)
P3-C3	1 $(3.5 * 10^{-4})$	$1(1.65 * 10-4)$	1 (0.0245)	1 (0.0075)
P4-T4	1 (0.0370)	1(0.0213)	1 (0.0213)	0 (0.0914)
P4-C4	1 $(9.95 * 10^{-5})$	$1(5.79 * 10-5)$	0 (0.1013)	1 (0.0073)

Table 4.1: Statistic results for the alpha band personalization. We have reported the results of the statistics for each channel. 1 stands for statically significant difference, 0 stands for no significant difference between euglycaemic and hypoglycaemic state. The p-value (likelihood of no difference between glycaemic states) is in brakets. (*) stands for the centroid frequency computed as $\frac{\sum(PSD(x)f(x))}{\sum(PSD(x))}$, (**) stands for the centroid frequency computed as spectrum median.

Channel	Centroid frequency (*)	Centroid frequency (**)	$\int PSD$	$\int logPSD^2$
P3-T3	1 (0)	1(1)	1 (1)	1 (1)
P3-C3	1 (0)	1(0)	1 (1)	1 (1)
P4-T4	1 (1)	1(1)	1 (0)	0 (0)
P4-C4	1 (0)	1(1)	0 (1)	1 (1)

Table 4.2: Comparison between the analysis based on the alpha band personalized and the conventional analysis based on the standard alpha band (results in brakets). 1 stands for statically significant difference, 0 stands for no significant difference between euglycaemic and hypoglycaemic state. (*) stands for the centroid frequency computed as $\frac{\sum(PSD(x)f(x))}{\sum(PSD(x))}$, (**) stands for the centroid frequency computed as spectrum median.

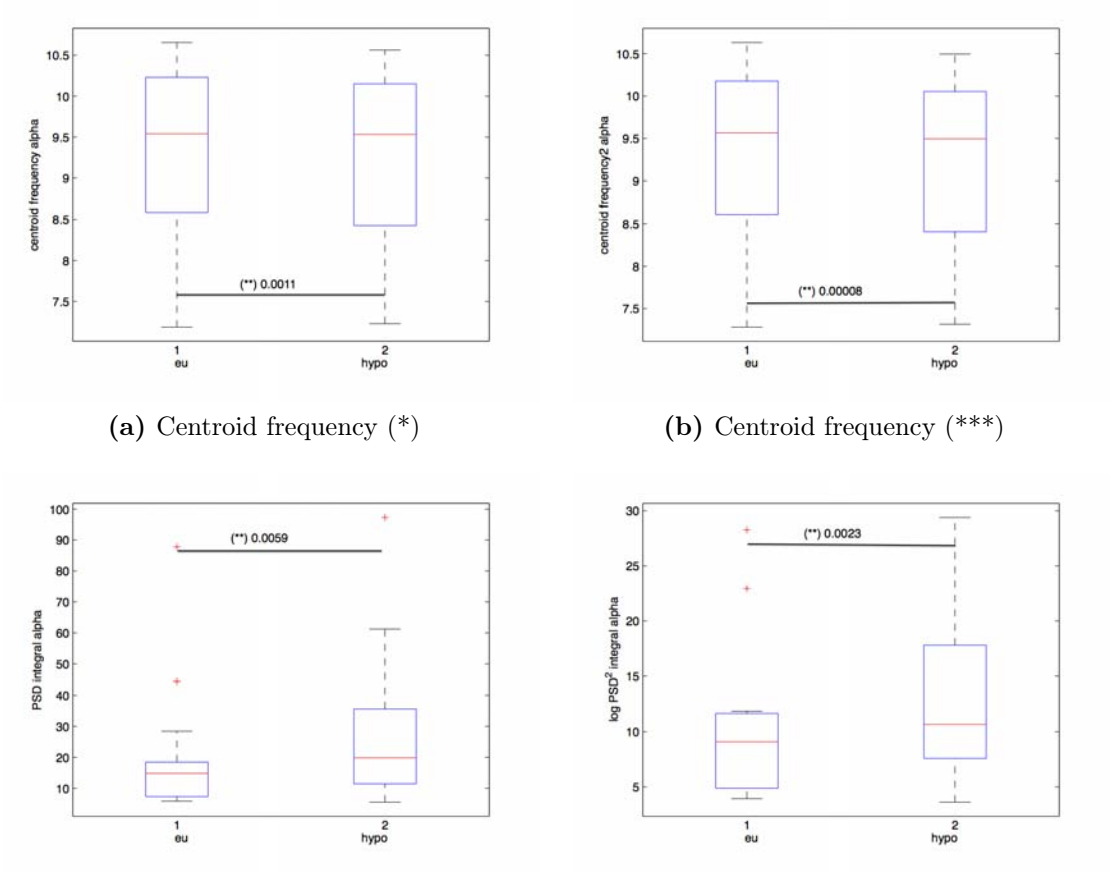

(a) Centroid frequency (*)

(b) Centroid frequency (***)

(c) $\int PSD$

(d) $\int logPSD^2$

Figure 4.4: P3-T3: alpha band personalization. (*) stands for the centroid frequency computed as $\frac{\sum(PSD(x)f(x))}{\sum(PSD(x))}$, (***) stands for the centroid frequency computed as spectrum median. The red line is the median value, the edges of the box are the 75th and 25th percentiles, the red crosses are the outliers. Double stars (**) indicate statically significant difference, the number near to the double stars is the p-value.

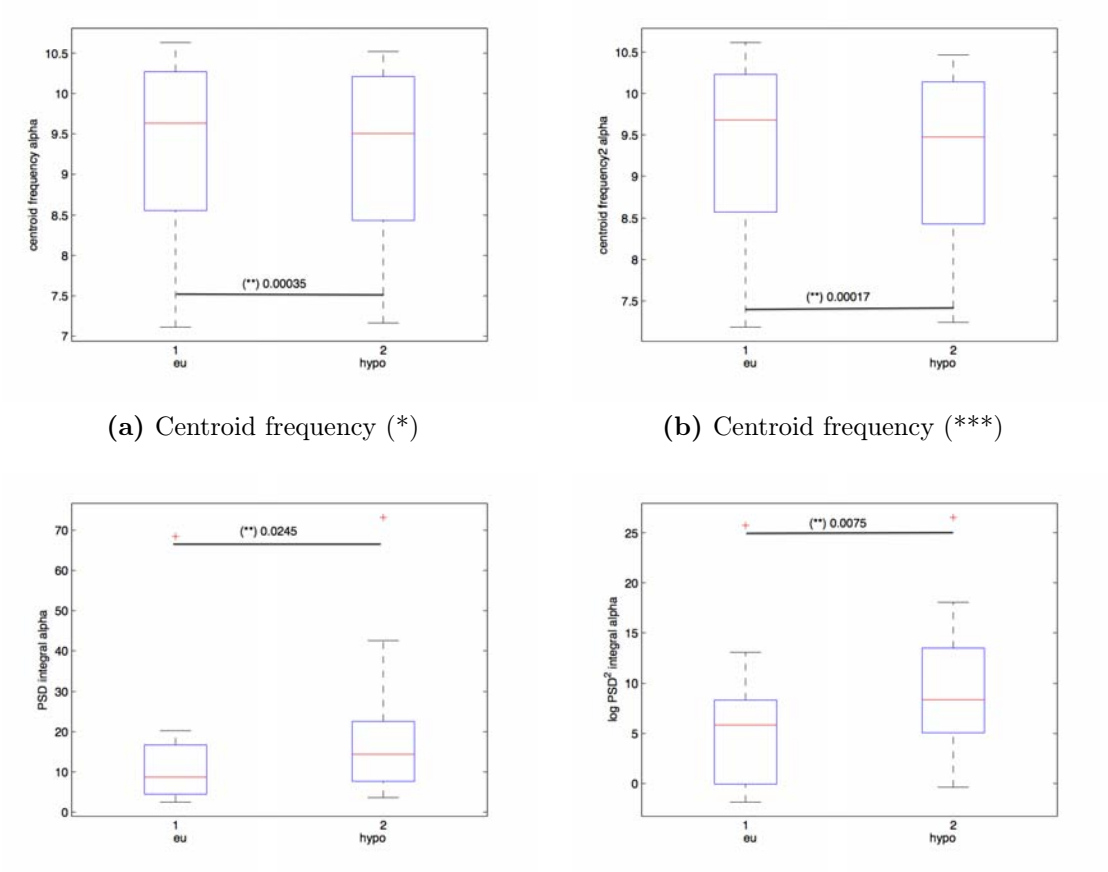

(a) Centroid frequency (*)

(b) Centroid frequency (***)

(c) $\int PSD$

(d) $\int logPSD^2$

Figure 4.5: P3-C3: alpha band personalization. (*) stands for the centroid frequency computed as $\frac{\sum(PSD(x)f(x))}{\sum(PSD(x))}$, (***) stands for the centroid frequency computed as spectrum median. The red line is the median value, the edges of the box are the 75th and 25th percentiles, the red crosses are the outliers. Double stars (**) indicate statically significant difference, the number near to the double stars is the p-value.

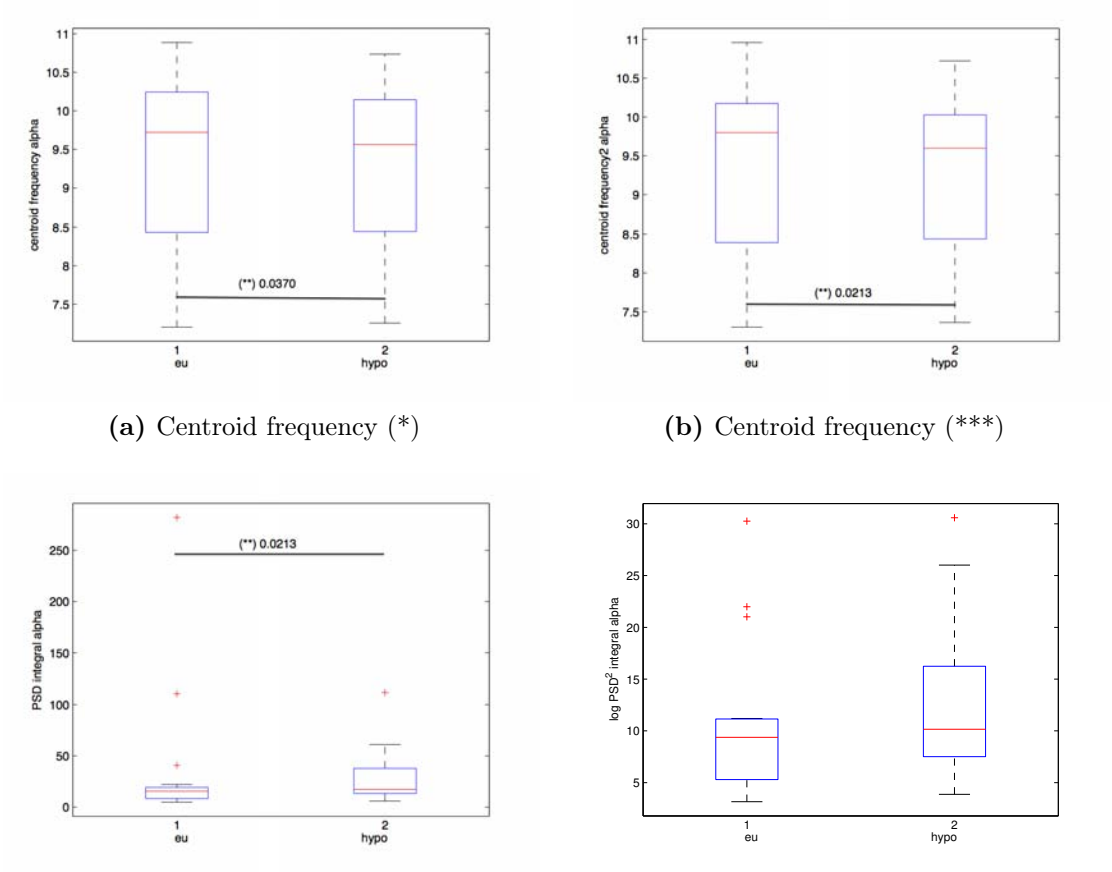

(a) Centroid frequency (*)

(b) Centroid frequency (***)

(c) $\int PSD$

(d) $\int logPSD^2$

Figure 4.6: P4-T4: alpha band personalization. (*) stands for the centroid frequency computed as $\frac{\sum(PSD(x)f(x))}{\sum(PSD(x))}$, (***) stands for the centroid frequency computed as spectrum median. The red line is the median value, the edges of the box are the 75th and 25th percentiles, the red crosses are the outliers. Double stars (**) indicate statically significant difference, the number near to the double stars is the p-value.

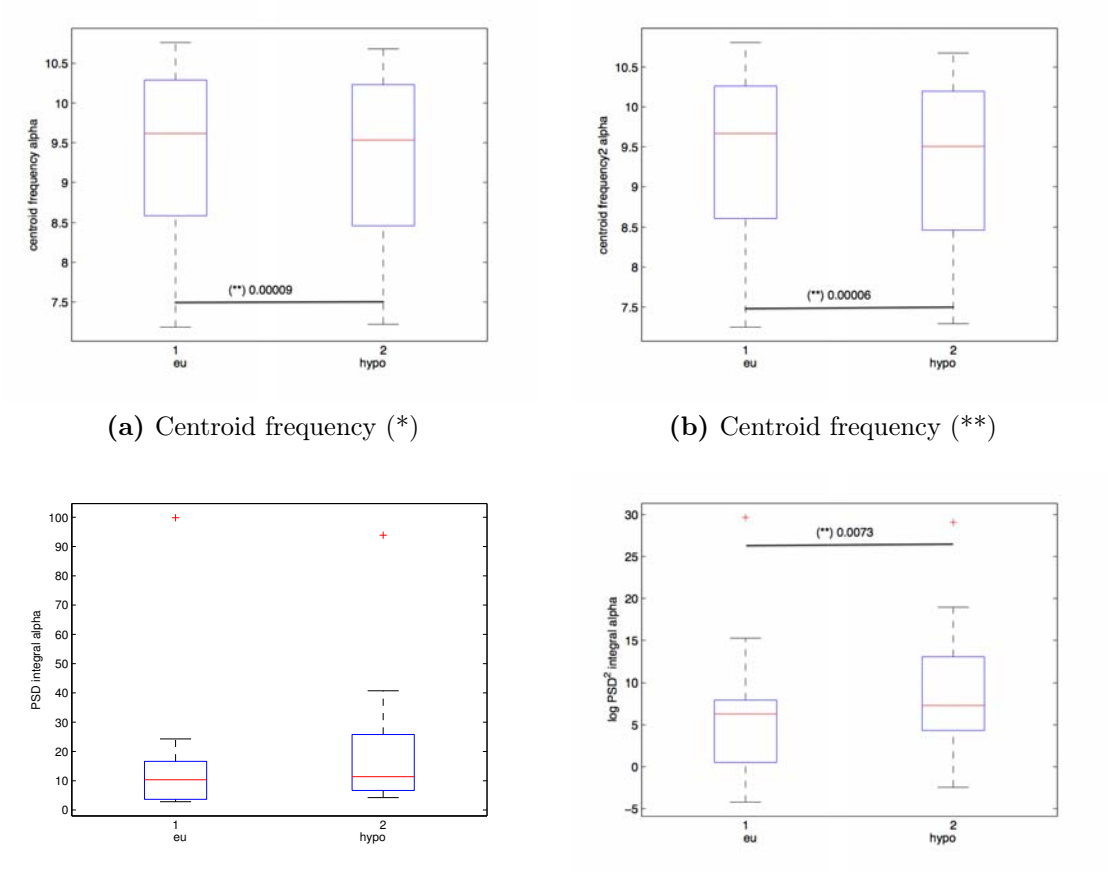

(a) Centroid frequency (*) **(b)** Centroid frequency (**)

(c) $\int PSD$ **(d)** $\int logPSD^2$

Figure 4.7: P4-C4: alpha band personalization. (*) stands for the centroid frequency computed as $\frac{\sum(PSD(x)f(x))}{\sum(PSD(x))}$, (***) stands for the centroid frequency computed as spectrum median. The red line is the median value, the edges of the box are the 75th and 25th percentiles, the red crosses are the outliers. Double stars (**) indicate statically significant difference, the number near to the double stars is the p-value.

4.4 Possible margins of improvement

This pilot-study has stressed that the band personalization can improve the results. It suggests that it could be useful pre-processing the EEG signal to compute the personalized bands. The research of the subjective boundaries could be considered as a device-calibration in the system to detect hypoglycaemia.
Unfortunately, the method used to customize the alpha band is a subjective method, so this analysis could be further enhanced for instance, by the Channel Reactivity Based (CRB) method recently presented in [32].

Chapter 5

Use of a new reactivity index measure to detect hypoglycaemia

5.1 The reactivity index

This chapter is based on the idea of the paper [23], which investigated if and how levels of glucose concentrations affect the time course of EEG power modulations in the conventional theta, alpha and beta bands. This was done by studying the variability of the EEG signal exploiting the reactivity index ρ.
The reactivity index was introduced in the paper [32]. It quantifies the EEG power decrease between a reference and a test interval.
Briefly, we choose a reference $r(t)$ and a test $t(t)$ interval from a time series. Then, we compute the power spectrum of the test $T(f)$ and the reference $R(f)$ interval in the chosen frequency band $[f_a, f_b]$. Now, we can calculate the reactivity index as:

$$\rho = \frac{\int_{f_a}^{f_b} R(f) - T(f)}{f_b - f_a} \quad [\frac{\mu V^2}{Hz}].$$

$\int_{f_a}^{f_b} R(f) - T(f)$ represents the area delimited by the resting and test spectra in the frequency interval $[f_a, f_b]$. So, a positive value of ρ stands for a power decrease and a negative value for a power increase.

5.2 Implementation

We have decided to follow the procedure of the paper [23] for dealing with the EEG variability computation.
It consists of a few passages:

- selection of EEG signal in time domain;
- selection of a series of couples: reference and test time intervals ($r_i(t)$, $t_i(t)$) (they last 2 minutes and they distance 10 minutes. The successive couple ($r_2(t)$, $t_2(t)$) is obtained by shifting $r_1(t)$ and $t_2(t)$ by 0.5 minutes);

- computation of the power spectral density of each couple $((r_i(t), t_i(t)) \rightarrow (R_i(f), T_i(f)))$;
- computation of the reactivity index for each couple $\rho_i = \frac{\int_{fa}^{fb} R_i(f) - T_i(f)}{fb - fa}$.
- selection of ρ belonging to 1 hour EEG time interval;

These steps were repeated for each subject and for the alpha, theta and beta bands. For each patient, the 1 hour EEG time intervals were selected from the hypoglycaemia and then from the euglycaemia period.
The PSD of the couple ($r_i(t)$, $t_i(t)$) is obtained by applying the Welch method in EEG 2 second length epoch with no overlapping.
Moreover, the EEG signal was pre-elaborated for this analysis, thus we have excluded EEG values with amplitude greater than 100, because they were surely artifacts.
The above steps are summarized in Figure5.1.

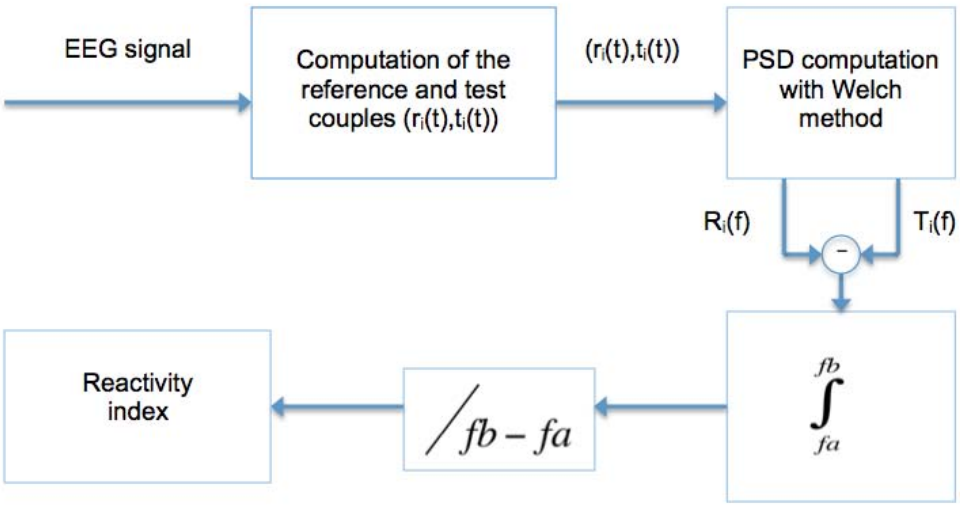

Figure 5.1: Reactivity Index computation.

At the end of this elaboration, we have obtained 30 ρ values for the hypoglycaemic period and 30 ρ values for the euglycaemic period. Then, we have computed their standard deviation and performed a statistic test with all the results from all subjects.

5.3 Results

We have reported our statistic outcomes in Table 5.1 on the facing page.

As you can see in Table5.1, the EEG variability is significant in theta band, where the EEG variability seems to increase passing from euglycaemia to hypoglycaemia, as you can notice from Figure5.2 to Figure5.5.

Channel	Alpha	Theta	Beta
P3-T3	0 (0.8978)	1 (0.0044)	0 (0.9570)
P3-C3	0 (0.1671)	1 $(4.29 * 10^{-4})$	0 (0.0636)
P4-T4	0 (0.3595)	1 (0.0096)	0 (0.2771)
P4-C4	0 (0.3593)	1 (0.0014)	0 (0.3593)

Table 5.1: Statistic results for ρ computation. We have reported the results of the statistics for each channel. 1 stands for statically significant difference, 0 stands for no significant difference between euglycaemic and hypoglycaemic state. The p-value (likelihood of no difference between glycaemic states) is in brakets.

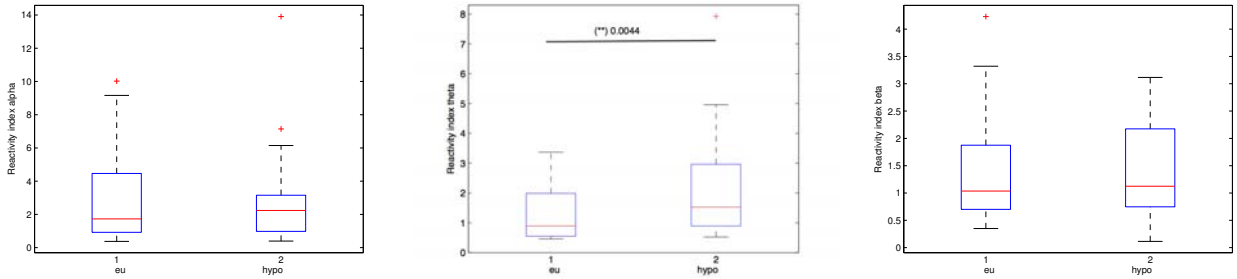

(a) Variability in alpha band **(b)** Variability in theta band **(c)** Variability in beta band

Figure 5.2: P3-T3: standard deviation of reactivity index. The red line is the median value, the edges of the box are the 75th and 25th percentiles, the red crosses are the outliers. Double stars (**) indicate statically significant difference, the number near to the double stars is the p-value.

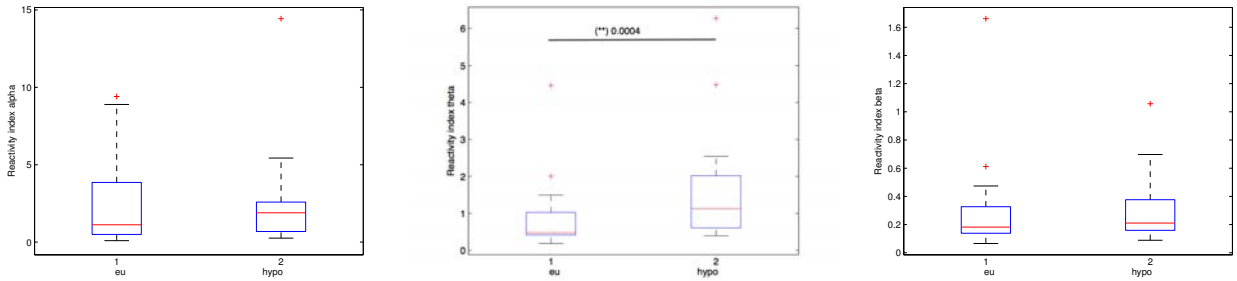

(a) Variability in alpha band **(b)** Variability in theta band **(c)** Variability in beta band

Figure 5.3: P3-C3: standard deviation of reactivity index. The red line is the median value, the edges of the box are the 75th and 25th percentiles, the red crosses are the outliers. Double stars (**) indicate statically significant difference, the number near to the double stars is the p-value.

The overall results are satisfying. The reactivity index highlight that its application in theta band can be a good indicator for hypoglycaemia detection. In Table5.2, we have reported, from statistics, the median and the 75th and the 25th

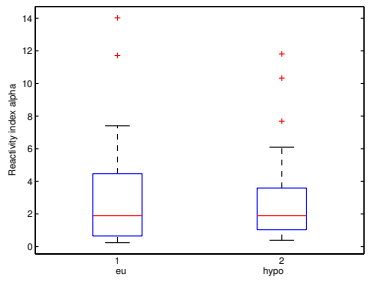

(a) Variability in alpha band

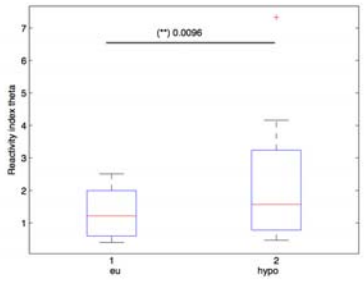

(b) Variability in theta band

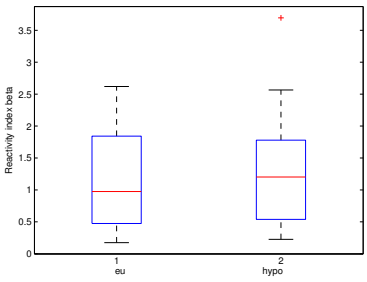

(c) Variability in beta band

Figure 5.4: P4-T4: standard deviation of reactivity index. The red line is the median value, the edges of the box are the 75th and 25th percentiles, the red crosses are the outliers. Double stars (**) indicate statically significant difference, the number near to the double stars is the p-value.

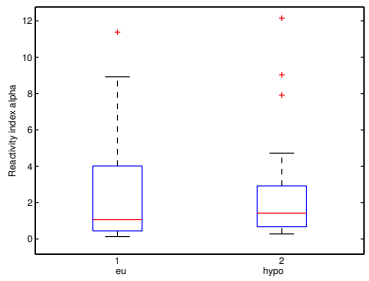

(a) Variability in alpha band

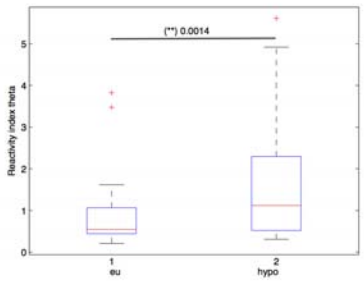

(b) Variability in theta band

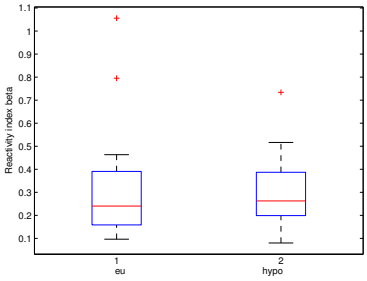

(c) Variability in beta band

Figure 5.5: P4-C4: standard deviation of reactivity index. The red line is the median value, the edges of the box are the 75th and 25th percentiles, the red crosses are the outliers. Double stars (**) indicate statically significant difference, the number near to the double stars is the p-value.

percentile of the values in theta band for each channel to highlight the comparison between eu- and -hypoglycaemia and to confirm the increase in variability.

5.4 Possible margins of improvement

This measurement of the reactivity index variability has led to good results. Probably, they can be refined with a different choice of reference and test intervals. We have decided to use reference/test intervals of 2 minute length and a 0.5 minutes distance from each other. Moreover, the distance between the reference interval and its test was of 10 minutes. Maybe, we can improve the outcomes changing the value of these three parameters and comparing the results.
Furthermore, the reactivity index variability could be an adequate instrument to test the difference between euglycaemic and pre-hypoglycaemic period (circa 30 minutes before).
The reactivity index study could be amplified and improved in this way.

	P3-T3:	Eu	Hypo	P3-C3:	Eu	Hypo
median		0.8923	1.5242		0.47689	1.1314
75^{th} percentile		1.9841	2.963		1.026	2.0228
25^{th} percentile		0.54673	0.88784		0.41861	0.60675
	P4-T4:	Eu	Hypo	P4-C4:	Eu	Hypo
median		1.2158	1.571		0.54828	1.207
75^{th} percentile		1.9947	3.238		1.0638	2.297
25^{th} percentile		0.60016	0.78108		0.44324	0.52156

Table 5.2: Reactivity index variability passing from euglycaemia to hypoglycaemia. The 25^{th} percentile, the median value and the 75^{th} percentile are presented to emphasize the increase in variability in hypoglycaemia.

Chapter 6

Conclusions and future challanges

6.1 Summary of the overall results

People with type 1 diabetes require insulin therapy and other treaments to live long and healthy. In particular, they need to avoid hypoglycaemic events. The use of the brain as biosensor has been recently proposed along with the Hyposafe device in order to further investigate its potential to detect hypoglycaemia and to try to improve patients condition.
In the present thesis, we have studied some refinements as well as some new techniques to process the EEG to detect hypoglycaemia.
We have managed data from 19 subjects exposed to insulin-induced hypoglycaemia. We have tested and applied different methods to the following bipolar channel: F3-C3, F4-C4, P3-C3, P4-C4, P3-T3, P4-T4 (we have soon left out F3-C3 and F4-C4 channels from our analysis because they do not show significant outcome since they probably interfere with the EOG).
The outcomes of the initial analysis (the spectral measures in the conventional bands) reveal an increase in the power spectral density (PSD) in theta and alpha band. In particular, the left brain channels (P3-T3, P3-C3) show a statistical notable increase in both theta and alpha band passing from euglycaemia to hypoglycaemia, while the right brain channels (P4-T4, P4-C4) exhibit a significant increase only in theta band. We can deduce that the left brain seems to be a preferable brain side to apply this kind of analysis.
Observing the subjects' PSD track in each band, in most cases we have noticed a peak in the unified theta-alpha (4-13 Hz) band, but only the P4-T4 channel shows a statistically significant difference in both magnitude and frequency of this peak passing from eu- to hypo-glycaemia.
About the centroid frequency, P3-C3, P3-T3 and P4-T4 channels reveal a statistical significant increase in theta band and a significant statistical decrease in alpha band, passing from euglycaemia to hypoglycaemia, using the paper [22] definition, while only P4-T4 shows a significant statistical outcome in both bands as spectral baricenter.
Computing the integral of the squared and log transformed PSD we have found best results in the left brain . To be specific, we have noted an increase in theta and alpha band passing from euglycaemia to hypoglycaemia. The results were statically

significant in P3-T3, P3-C3 and P4-C4 channels in both alpha and theta bands.
But, we were interested in comparing the data from the PSD (and $logPSD^2$) integral trend with the PSD trend to see if EEG signal without further manipulation was enough informative. We have noticed that we have gained statistical difference only in alpha band in P4-C4 channel using the $logPSD^2$ integral.
Thus, if we were interested only in analysing the EEG changes in theta band, we could simply exploit the PSD trend.
Exploiting the personalized alpha band for each subject to compute again all the hypoglycaemic indicators with these new limitations, we have obtained outstanding outcomes. We have earned in statistical difference between euglycaemia and hypoglycaemia in both centroid frequency definitions in P3-T3, P3-C3 and P4-C4 channels. We have also gained statistical difference in P4-T4 channel in PSD integral and in squared and log transformed PSD integral.
We have once again obtained best results in the left side of the brain.
Eventually, we have tested that the EEG variability changes passing from euglycaemia to hypoglycaemia exploiting the reactivity index. We have reached important results in theta band in all channels (P3-T3, P3-C3, P4-T4, P4-C4): ρ variability increases passing from euglycaemia to hypoglycaemia.

To sum up, the increase in PSD value in theta band, the increase in the centroid frequency and the reactivity index variability have demonstrated that there are remarkable EEG changes passing from euglycaemia to hypoglycaemia. These parameters could be integrated with the hyposafe device to detect hypoglycaemic events, but these techniques can and still need to be improved.

6.2 Possible further developments

For istance, we have proved that the use of subjective boundaries for the alpha band has enhanced the results. So, it could be useful to compute personalized limits for both alpha and theta band, utilizing this passage as a device calibration before its daily use. But, we need to use a more powerful and more objective method to personalize the frequency band such as the Channel Reactivity Based Method proposed in [32].
Maybe, the reactivity index variability could be more perceptive using personalized frequency bands and changing its basic parameters.
Moreover, we should try to apply all the presented methods in the 15-30 minute period before the hypoglycaemic state to give a warning to the patient. Thus, we demand a detailed analysis comparing the pre-hypoglycaemic state with the euglycaemic one in order to discover if these techniques continue to be robust in the glycaemic states comparison.
In the end, this study was mainly based on the frequency domain, it would be intersting to deepen the time domain analysis to research hypoglycaemic peculiarities.

Appendix A

Hyperglycaemia vs hypoglycaemia

The main goal of this study was to show the presence of changes in the EEG signal passing from euglycaemia to hypoglycaemia.
The above analysis has also been led comparing:

- hyperglycaemia to euglycaemia;
- hyperglycaemia to hypoglycaemia.

In this appendix, we present a brief excursus of all previous methods, highlighting the comparison between hyperglycaemia to euglycaemia and hyperglycaemia to hypoglycaemia.
We have decided to propose directly the analysis in the following channels:

- P3-C3 (P4-C4);
- P3-T3 (P4-T4).

A.1 Hypoglycaemia indicators

The EEG signal of each subject has been divided in epochs of 4 second length, filtered by a Hamming window with a 50% overlapping.
Then, we have studied:

1. peak frequency in the unified theta-alpha (4-13 Hz) band;
2. centroid in each of the three conventional bands (delta (1-4 Hz), theta (4-8 Hz) e alpha (8-13 Hz));
3. integral of the spectral density and of the logarithm of the squared spectral density.

A.1.1 Peak frequency

We have computed the frequency and the amplitude of the peak in the unified theta-alpha band for each subject in every chosen channel. We have performed t-test, as usual, to compare the results of all subjects and to discover significant

Channel	Glycaemic states difference	Frequency	Amplitude
P3-T3	hyper-eu	0 (0.1893)	1 (0.0309)
P3-T3	hyper-hypo	0 (0.0427)	1 (0.0013)
P3-C3	hyper-eu	0 (0.4807)	1 (0.0013)
P3-C3	hyper-hypo	0 (0.4807)	1 (0.0189)
Channel	Glycaemic states difference	Frequency	Amplitude
P4-T4	hyper-eu	0 (0.1893)	1 (0.0075)
P4-T4	hyper-hypo	1 (0.0427)	1 (0.0013)
P4-C4	hyper-eu	0 (0.2379)	1 (0.0075)
P4-C4	hyper-hypo	0 (0.4807)	1 $(1.45 * 10^{-4})$)

Table A.1: Statistic results for Peak Value. In each table, we have reported the results of the statistics for each channel for the frequency and amplitude of the peak value in theta-alpha band. 1 stands for statically significant difference, 0 stands for no significant difference between euglycaemic and hypoglycaemic state. The p-value (likelihood of no difference between glycaemic states) is in brakets.

differences between hyperglycaemic and hypoglycaemic state and hyperglycaemic and euglycaemic state. The results are in TableA.1.

As you can notice in TableA.1, the amplitude of the peak changes its value passing from hyperglycaemia to hypo- or eu-glycaemia.
As you can see from FigureA.1 to FigureA.4 , it seems to increases passing from hyperglycaemia to euglycaemia and from euglycaemia to hypoglycaemia.

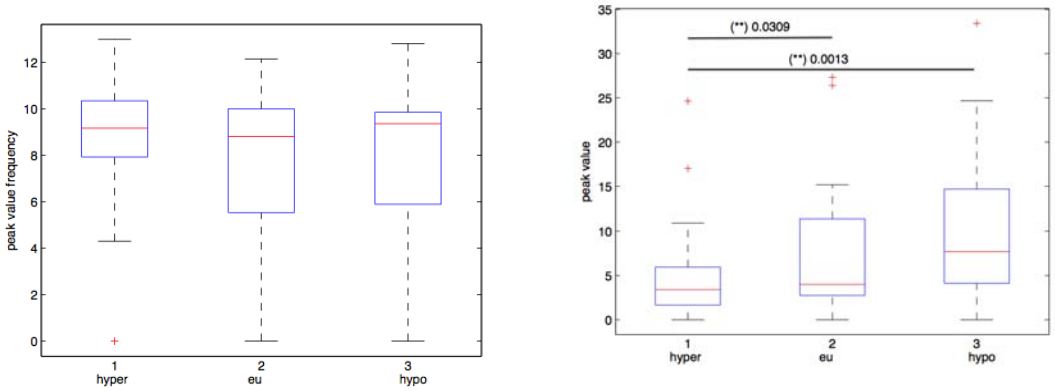

(a) Frequency **(b)** Amplitude

Figure A.1: P3-T3: Peak Value. The red line is the median value, the edges of the box are the 75th and 25th percentiles, the red crosses are the outliers. Double stars (**) indicate statically significant difference, the number near to the double stars is the p-value.

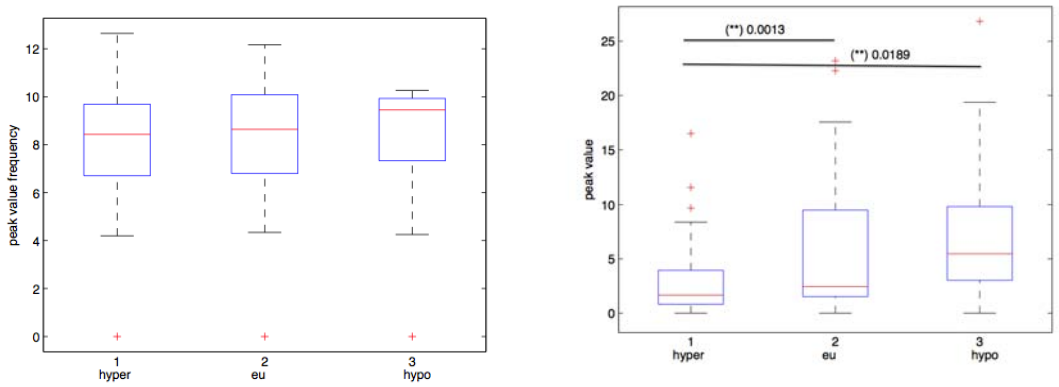

(a) Frequency **(b)** Amplitude

Figure A.2: P3-C3: Peak Value. The red line is the median value, the edges of the box are the 75th and 25th percentiles, the red crosses are the outliers. Double stars (**) indicate statically significant difference, the number near to the double stars is the p-value.

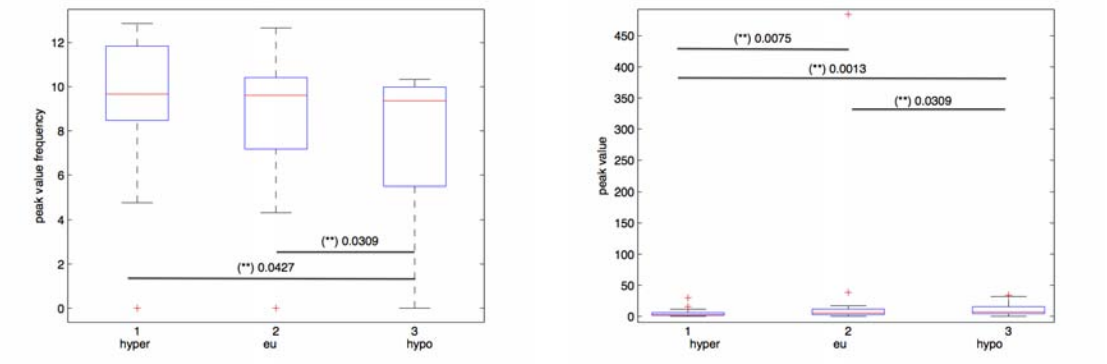

(a) Frequency **(b)** Amplitude

Figure A.3: P4-T4: Peak Value. The red line is the median value, the edges of the box are the 75th and 25th percentiles, the red crosses are the outliers. Double stars (**) indicate statically significant difference, the number near to the double stars is the p-value.

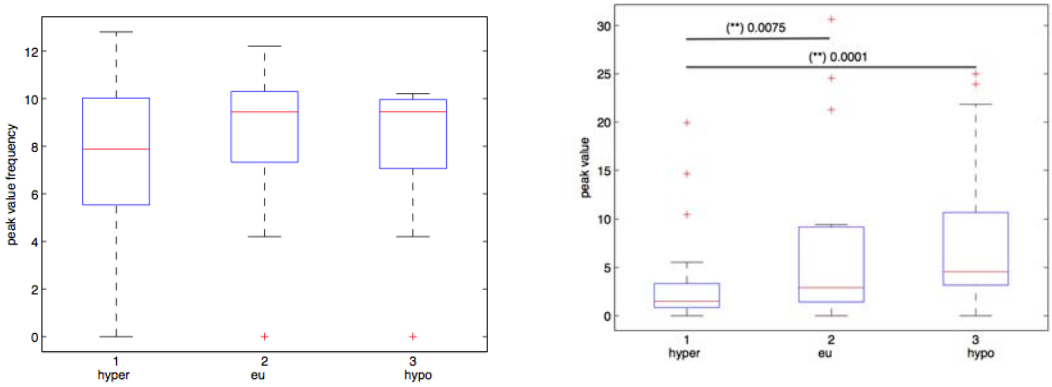

(a) Frequency **(b)** Amplitude

Figure A.4: P4-C4: Peak Value. The red line is the median value, the edges of the box are the 75th and 25th percentiles, the red crosses are the outliers. Double stars (**) indicate statically significant difference, the number near to the double stars is the p-value.

A.1.2 Centroid

The centroid frequency has been described:

- as the spectral baricenter where the frequencies f(x) are weighted by their likelihood PSD(x);
- as "the center of gravity of each frequency band that subdivides the area under the spectral curve into two of equal size".

We have chosen to use both definitions to test which one would highlight the most the differences between the different glycaemic states.
Then, we have performed t-test to compare the results of all subjects (TableA.2).

Channel	Glycaemic states difference	Delta (*)	Theta (*)	Alpha (*)	Delta (**)	Theta (**)	Alpha (**)
P3-T3	hyper-eu	0 (0.4505)	0 (0.5247)	1 (0.0075)	0 (0.5011)	0 (0.0963)	1 (0.0075)
P3-T3	hyper-hypo	1 (0.0411)	0 (0.2649)	1 (0.0011)	0 (0.0658)	1 (0.0075)	1 (0.0309)
P3-C3	hyper-eu	0 (1)	0 (0.0185)	1 (0.2379)	0 (0.8145)	0 (0.1435)	1 (0.0055)
P3-C3	hyper-hypo	0 (0.3635)	0 (0.0089)	1 (0.0132)	0 (0.4089)	1 (0.0390)	1 (0.0185)
Channel	Glycaemic states difference	Delta (*)	Theta (*)	Alpha (*)	Delta (**)	Theta (**)	Alpha (**)
P4-T4	hyper-eu	0 (0.7710)	0 (0.4807)	0 (0.1959)	0 (0.8145)	1 (0.0075)	1 (0.0015)
P4-T4	hyper-hypo	0 (0.9369)	0 (0.0748)	1 ($7.56 * 10^{-4}$)	0 (0.8615)	1 (0.0093)	1 (0.0182)
P4-C4	hyper-eu	0 (0.2379)	1 (0.0309)	0 (0.8145)	1 (0.0272)	0 (0.0963)	1 (0.0021)
P4-C4	hyper-hypo	0 (0.1350)	1 (0.0041)	1 (0.0105)	0 (0.1069)	0 (0.0932)	0 (0.0963)

Table A.2: Statistic results for centroid frequency. In the table, we have reported the results of the statistics for each channel for the centroid frequency using the general definition(*) and the paper definition as spectrum median(**). 1 stands for statically significant difference, 0 stands for no significant difference between euglycaemic and hypoglycaemic state. The p-value (likelihood of no difference between glycaemic states) is in brakets.

You can see the trend of the centroid in delta, theta and alpha band from FigureA.5 to FigureA.8 in all channels. It seems to decrease in alpha band using the centroid definition and it seems to increase in theta band using both definitions. The statistic results (TableA.2) suggest us that the more relevant outcomes are in alpha and theta band with the paper definition (centroid computed as spectrum median).

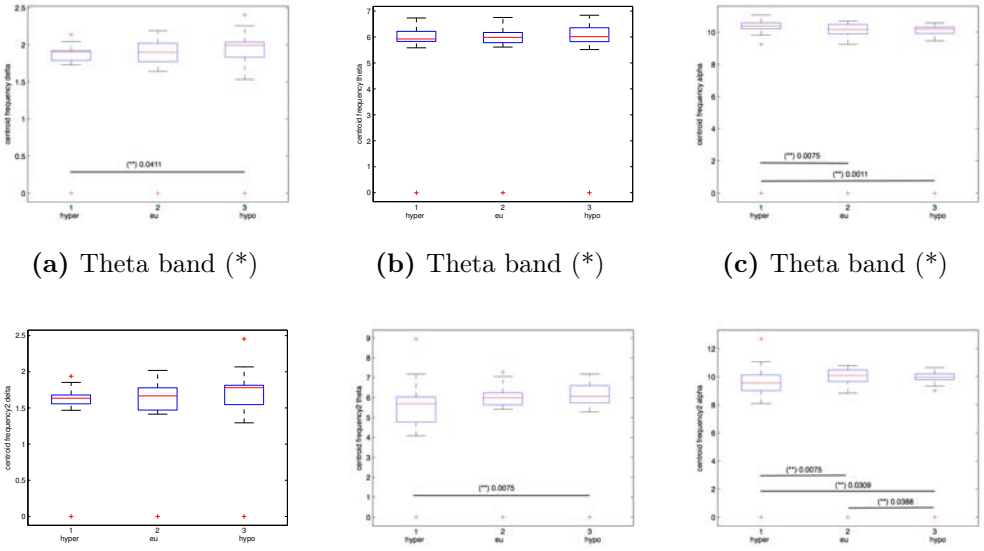

(a) Theta band (*) **(b)** Theta band (*) **(c)** Theta band (*)

(d) Alpha band (***) **(e)** Alpha band (***) **(f)** Alpha band (***)

Figure A.5: P3-T3: Centroid Frequency. We have reported the results for the centroid frequency using the general definition(*) and the paper definition as spectrum median (***). The red line is the median value, the edges of the box are the 75th and 25th percentiles, the red crosses are the outliers. Double stars (**) indicate statically significant difference, the number near to the double stars is the p-value.

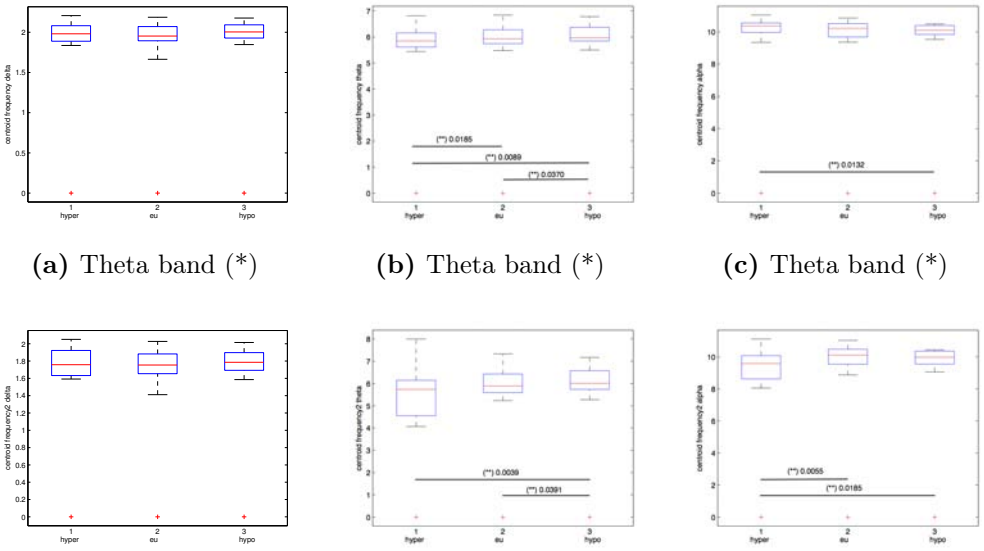

(a) Theta band (*) **(b)** Theta band (*) **(c)** Theta band (*)

(d) Alpha band (***) **(e)** Alpha band (***) **(f)** Alpha band (***)

Figure A.6: P3-C3: Centroid Frequency. We have reported the results for the centroid frequency using the general definition (*) and the paper definition as spectrum median(***). The red line is the median value, the edges of the box are the 75th and 25th percentiles, the red crosses are the outliers. Double stars (**) indicate statically significant difference, the number near to the double stars is the p-value.

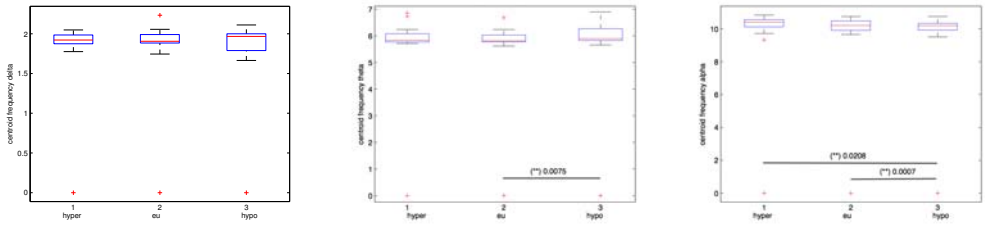

(a) Theta band (*) **(b)** Theta band (*) **(c)** Theta band (*)

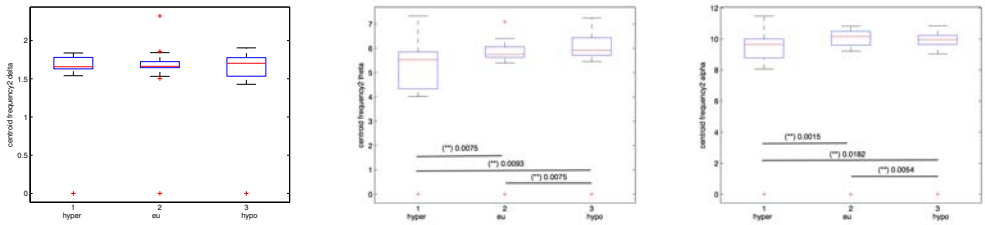

(d) Alpha band (***) **(e)** Alpha band (***) **(f)** Alpha band (***)

Figure A.7: P4-T4: Centroid Frequency. We have reported the results for the centroid frequency using the general definition (*) and the paper definition as spectrum median(***). The red line is the median value, the edges of the box are the 75th and 25th percentiles, the red crosses are the outliers. Double stars (**) indicate statically significant difference, the number near to the double stars is the p-value.

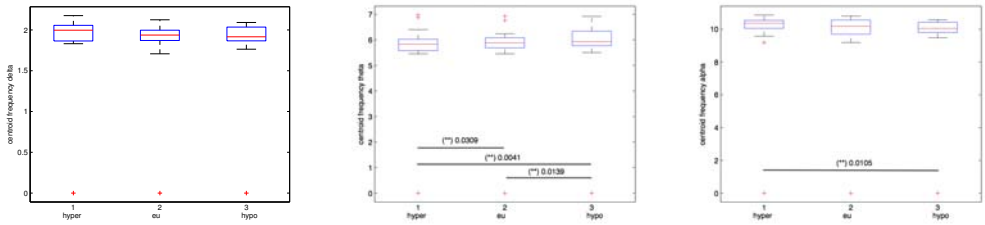

(a) Theta band (*) **(b)** Theta band (*) **(c)** Theta band (*)

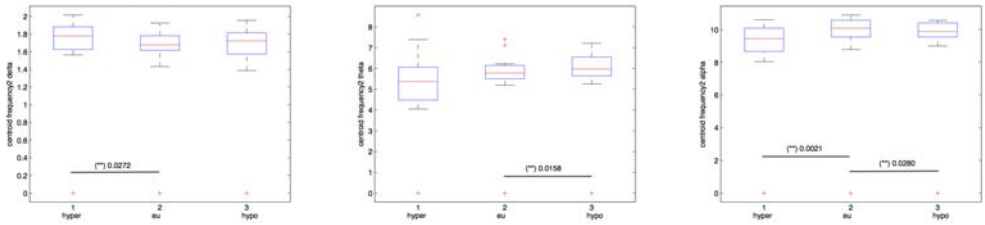

(d) Alpha band (***) **(e)** Alpha band (***) **(f)** Alpha band (***)

Figure A.8: P4-C4: Centroid Frequency. We have reported the results for the centroid frequency using the general definition (*) and the paper definition as spectrum median (***). The red line is the median value, the edges of the box are the 75th and 25th percentiles, the red crosses are the outliers. Double stars (**) indicate statically significant difference, the number near to the double stars is the p-value.

A.1.3 Power spectrum

We have also studied the integral of the power spectral density to derive the power of the signal in each bandwith ($[f_L, f_H]$).
In short, we have:

- computed the PSD with Welch's method;
- computed the PSD integral and of the squared and log transformed PSD integral;
- computed the mean value of the previous results;
- made the statistic analysis and compared hyperglycaemic state and hypoglycaemic one.

We report the results for the four channels (TableA.3, from FigureA.9 to FigureA.12).

Channel	Glycaemic states difference	Delta (*)	Theta (*)	Alpha (*)	Delta (**)	Theta (**)	Alpha (**)
P3-T3	hyper-eu	0 (0.4307)	0 (0.0963)	1 (0.0075)	0 (0.4807)	1 (0.0309)	1 (0.0079)
P3-T3	hyper-hypo	1 (0.0309)	1 $(1.45 * 10^{-4})$	0 (0.0963)	1 (0.0075)	1 $(1.45 * 10^{-4})$	1 (0.0012)
P3-C3	hyper-eu	0 (0.4807)	1 (0.0357)	1 (0.0013)	0 (0.4807)	1 (0.0309)	1 $(1.45 * 10^{-4})$
P3-C3	hyper-hypo	1 (0.0100)	1 $(7.26 * 10^{-6})$	1 (0.0075)	0 (0.0963)	1 $(7.62 * 10^{-6})$	1 $(2.18 * 10^{-4})$
Channel	Glycaemic states difference	Delta (*)	Theta (*)	Alpha (*)	Delta (**)	Theta (**)	Alpha (**)
P4-T4	hyper-eu	1 (0.0309)	1 (0.0075)	1 (0.0013)	1 (0.0309)	1 (0.0013)	1 (0.0013)
P4-T4	hyper-hypo	1 (0.0013)	1 $(1.45 * 10^{-4})$	1 (0.0013)	1 (0.0013)	1 $(1.45 * 10^{-4})$	1 (0.0017)
P4-C4	hyper-eu	0 (0.0963)	0 (0.0963)	1 (0.0075)	0 (0.2379)	0 (0.0963)	1 $(1.45 * 10^{-4})$
P4-C4	hyper-hypo	1 (0.0127)	1 $(1.45 * 10^{-4})$	1 (0.0013)	0 (0.0963)	1 $(1.45 * 10^{-4})$	1 $(6.35 * 10^{-4})$

Table A.3: Statistic results for PSD and $logPSD^2$ integral. In the table, we have reported the results of the statistics for each channel for the PSD integral (*) and the $logPSD^2$ integral (**). 1 stands for statically significant difference, 0 stands for no significant difference between euglycaemic and hypoglycaemic state. The p-value (likelihood of no difference between glycaemic states) is in brakets.

We can notice a general increase in the power spectrum in all subjects passing from hyper- to eu-glycaemia and from eu- to hypo-glycaemia.

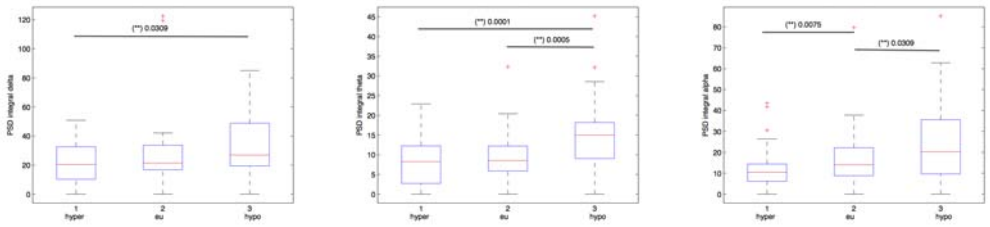

(a) Theta band (*) **(b)** Theta band (*) **(c)** Theta band (*)

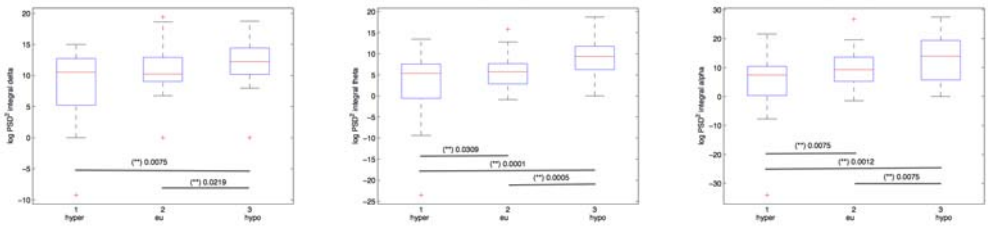

(d) Alpha band (***) **(e)** Alpha band (***) **(f)** Alpha band (***)

Figure A.9: P3-T3: PSD integral (*) and $logPSD^2$ integral (***). We have reported the results for the PSD integral and the $logPSD^2$ integral. The red line is the median value, the edges of the box are the 75th and 25th percentiles, the red crosses are the outliers. Double stars (**) indicate statically significant difference, the number near to the double stars is the p-value.

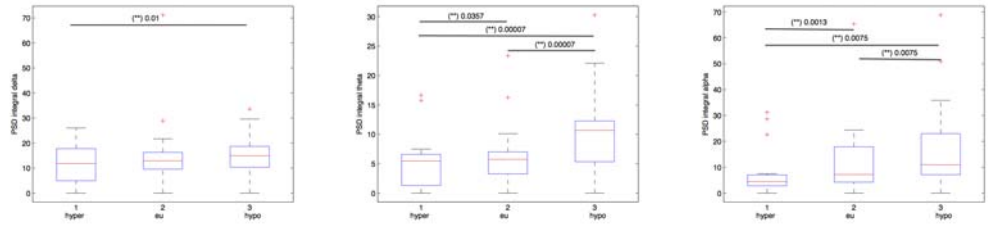

(a) Theta band (*) **(b)** Theta band (*) **(c)** Theta band (*)

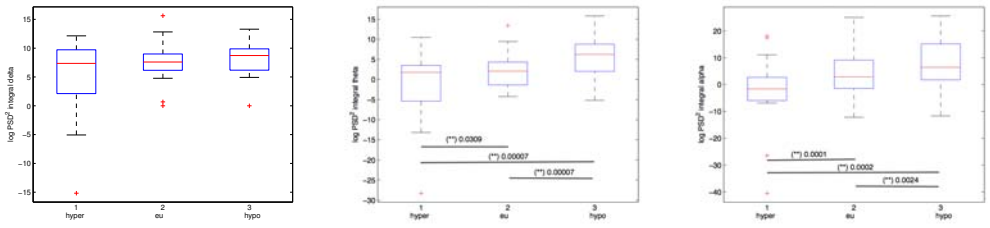

(d) Alpha band (***) **(e)** Alpha band (***) **(f)** Alpha band (***)

Figure A.10: P3-C3: PSD integral (*) and $logPSD^2$ integral(***). We have reported the results for the PSD integral and the $logPSD^2$ integral. The red line is the median value, the edges of the box are the 75th and 25th percentiles, the red crosses are the outliers. Double stars (**) indicate statically significant difference, the number near to the double stars is the p-value.

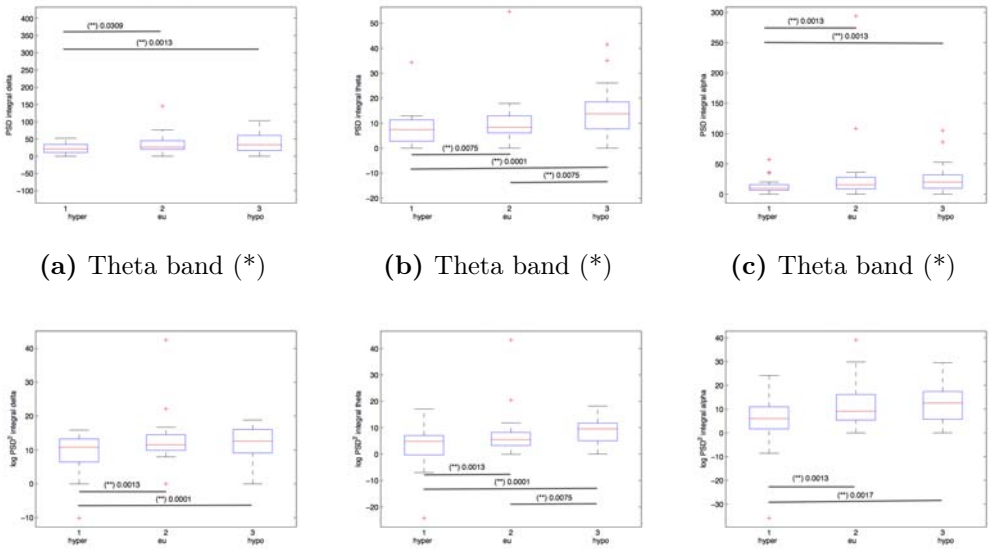

(a) Theta band (*) **(b)** Theta band (*) **(c)** Theta band (*)

(d) Alpha band (***) **(e)** Alpha band (***) **(f)** Alpha band (***)

Figure A.11: P4-T4: PSD integral (*) and $logPSD^2$ integral (***). We have reported the results for the PSD integral and the $logPSD^2$ integral. The red line is the median value, the edges of the box are the 75th and 25th percentiles, the red crosses are the outliers. Double stars (**) indicate statically significant difference, the number near to the double stars is the p-value.

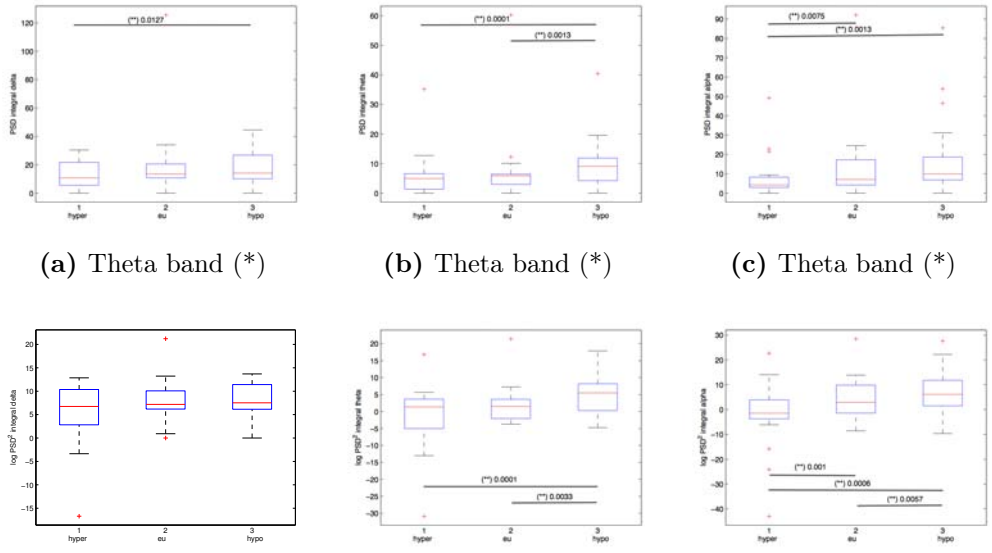

(a) Theta band (*) **(b)** Theta band (*) **(c)** Theta band (*)

(d) Alpha band (***) **(e)** Alpha band (***) **(f)** Alpha band (***)

Figure A.12: P4-C4: PSD integral (*) and $logPSD^2$ integral (***). We have reported the results for the PSD integral and the $logPSD^2$ integral. The red line is the median value, the edges of the box are the 75th and 25th percentiles, the red crosses are the outliers. Double stars (**) indicate statically significant difference, the number near to the double stars is the p-value.

A.2 EB method

We have computed the personalized alpha band for each subject with the EB method.
Next, we have calculated the same hypoglycaemia indicators in the personalized alpha band to compare them with the results in the conventional band.

Channel	Glycaemic states difference	Centroid frequency (*)	Centroid frequency (**)	$\int PSD$	$\int logPSD^2$
P3-T3	hyper-eu	0 (0)	0 (1)	1 (1)	1 (1)
P3-T3	hyper-hypo	1 (1)	1 (1)	1 (0)	1 (1)
P3-C3	hyper-eu	0 (0)	0 (1)	1 (1)	1 (1)
P3-C3	hyper-hypo	1 (1)	0 (1)	1 (1)	1 (1)
P4-T4	hyper-eu	0 (0)	0 (1)	1 (1)	1 (1)
P4-T4	hyper-hypo	1 (1)	1 (1)	1 (1)	1 (1)
P4-C4	hyper-eu	0 (0)	0 (1)	1 (1)	1 (1)
P4-C4	hyper-hypo	0 (1)	0 (0)	1 (1)	1 (1)

Table A.4: Statistic results for the alpha band personalization. We have reported the results of the statistics for each channel. 1 stands for statically significant difference, 0 stands for no significant difference between euglycaemic and hypoglycaemic state. The statistic result with the conventional band is in brakets. (*) stands for the centroid frequency computed as $\frac{\sum(PSD(x)f(x))}{\sum(PSD(x))}$, (**) stands for the centroid frequency computed as spectrum median.

Observing the outcomes in TableA.4, the results are not good for the centroid frequency. We have lost in statistical significance in all channels in the hyper- and eu-glycaemia comparison, computing the centroid frequency as $\frac{\sum(PSD(x)f(x))}{\sum(PSD(x))}$.
We have also lost in statistical significance in P4-C4 channel in hyper- and hypoglycaemia comparison.
There are no difference for the $\int logPSD^2$.
We have gained in statistical significance in P3-T3 channel in hyper- and hypoglycaemia comparison for the PSD integral.
To sum up, the alpha band personalization appears to be not necessary in the comparison between hyperglycaemia and eu/hypoglycaemia.

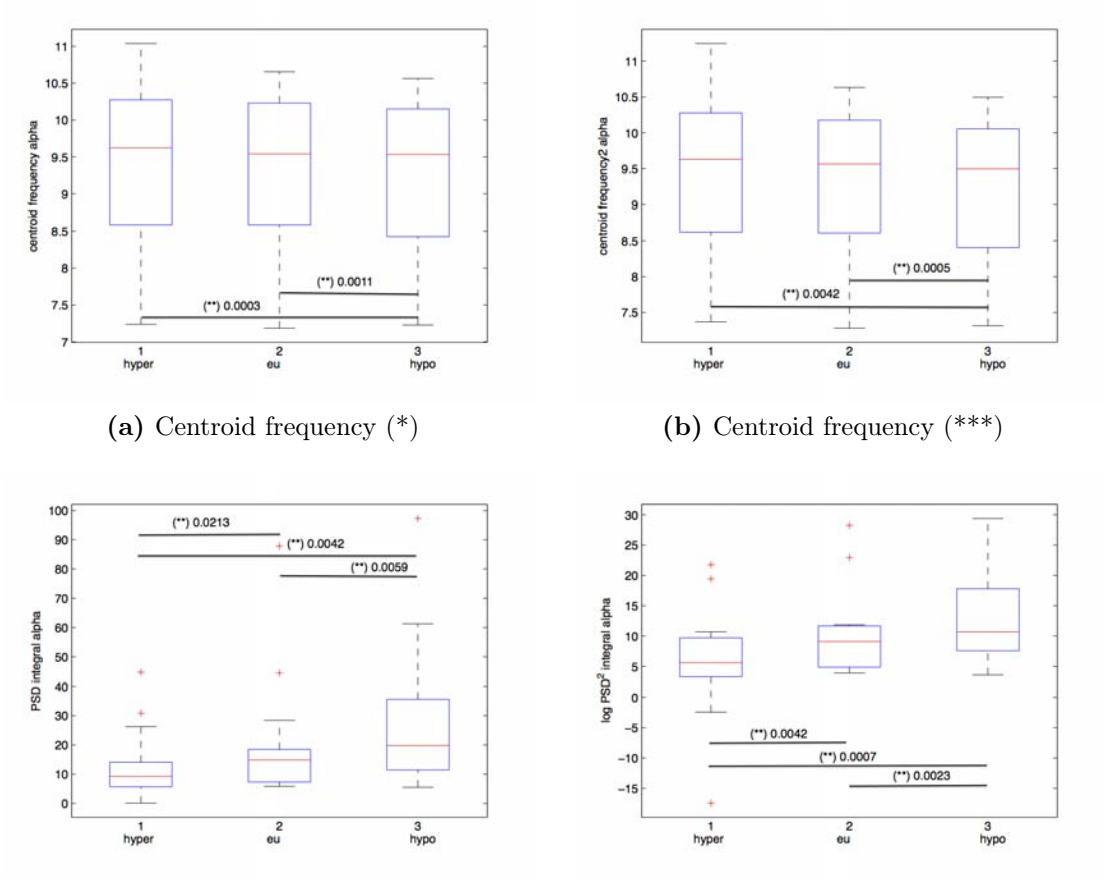

(a) Centroid frequency (*)

(b) Centroid frequency (***)

(c) $\int PSD$

(d) $\int logPSD^2$

Figure A.13: P3-T3: alpha band personalization. (*) stands for the centroid frequency computed as $\frac{\sum(PSD(x)f(x))}{\sum(PSD(x))}$, (***) stands for the centroid frequency computed as spectrum median. The red line is the median value, the edges of the box are the 75th and 25th percentiles, the red crosses are the outliers. Double stars (**) indicate statically significant difference, the number near to the double stars is the p-value.

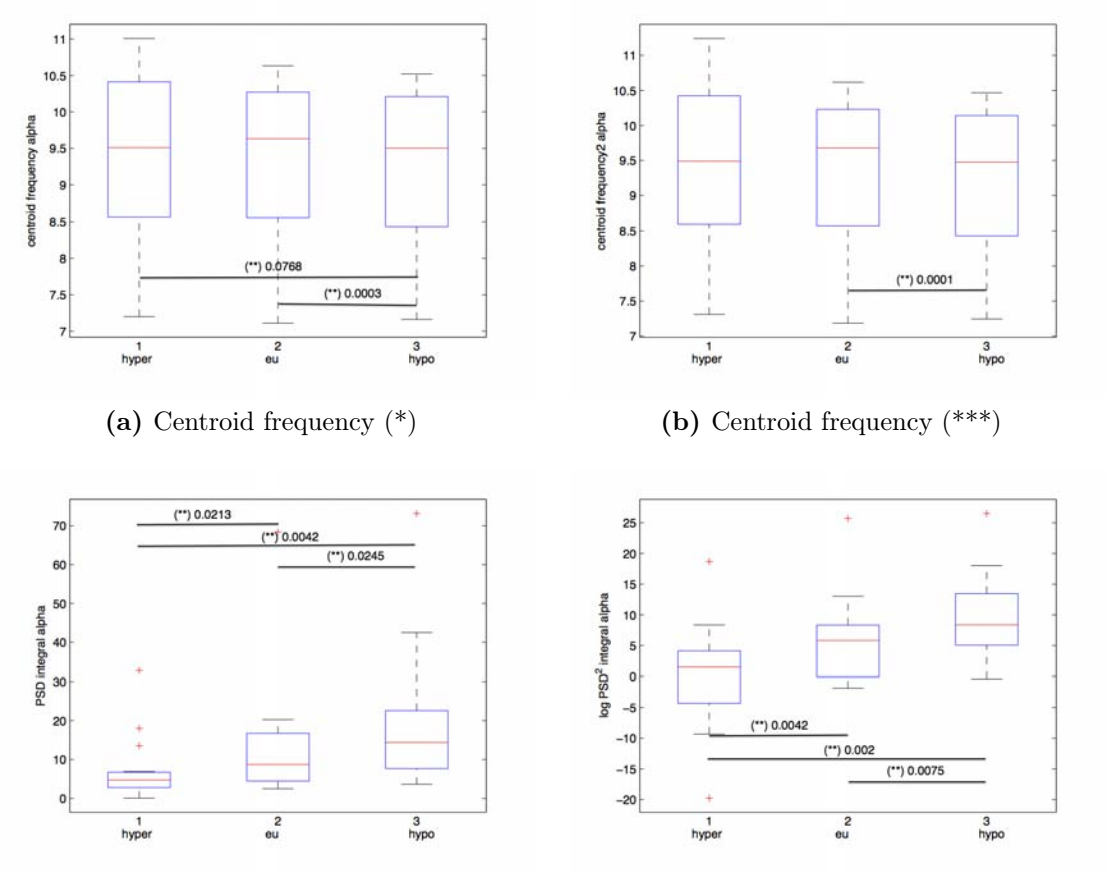

(a) Centroid frequency (*)

(b) Centroid frequency (***)

(c) $\int PSD$

(d) $\int logPSD^2$

Figure A.14: P3-C3: alpha band personalization. (*) stands for the centroid frequency computed as $\frac{\sum(PSD(x)f(x))}{\sum(PSD(x))}$, (***) stands for the centroid frequency computed as spectrum median. The red line is the median value, the edges of the box are the 75th and 25th percentiles, the red crosses are the outliers. Double stars (**) indicate statically significant difference, the number near to the double stars is the p-value.

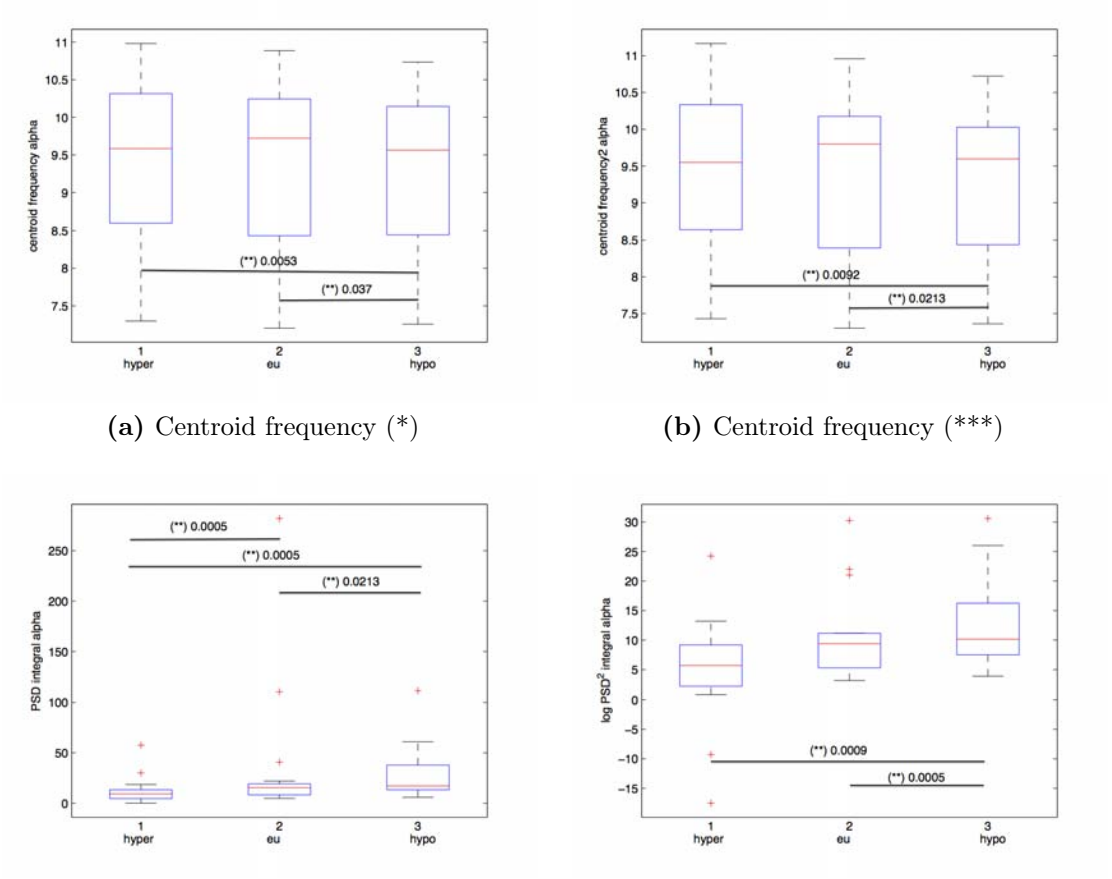

(a) Centroid frequency (*)

(b) Centroid frequency (***)

(c) $\int PSD$

(d) $\int logPSD^2$

Figure A.15: P4-T4: alpha band personalization. (*) stands for the centroid frequency computed as $\frac{\sum(PSD(x)f(x))}{\sum(PSD(x))}$, (***) stands for the centroid frequency computed as spectrum median. The red line is the median value, the edges of the box are the 75th and 25th percentiles, the red crosses are the outliers. Double stars (**) indicate statically significant difference, the number near to the double stars is the p-value.

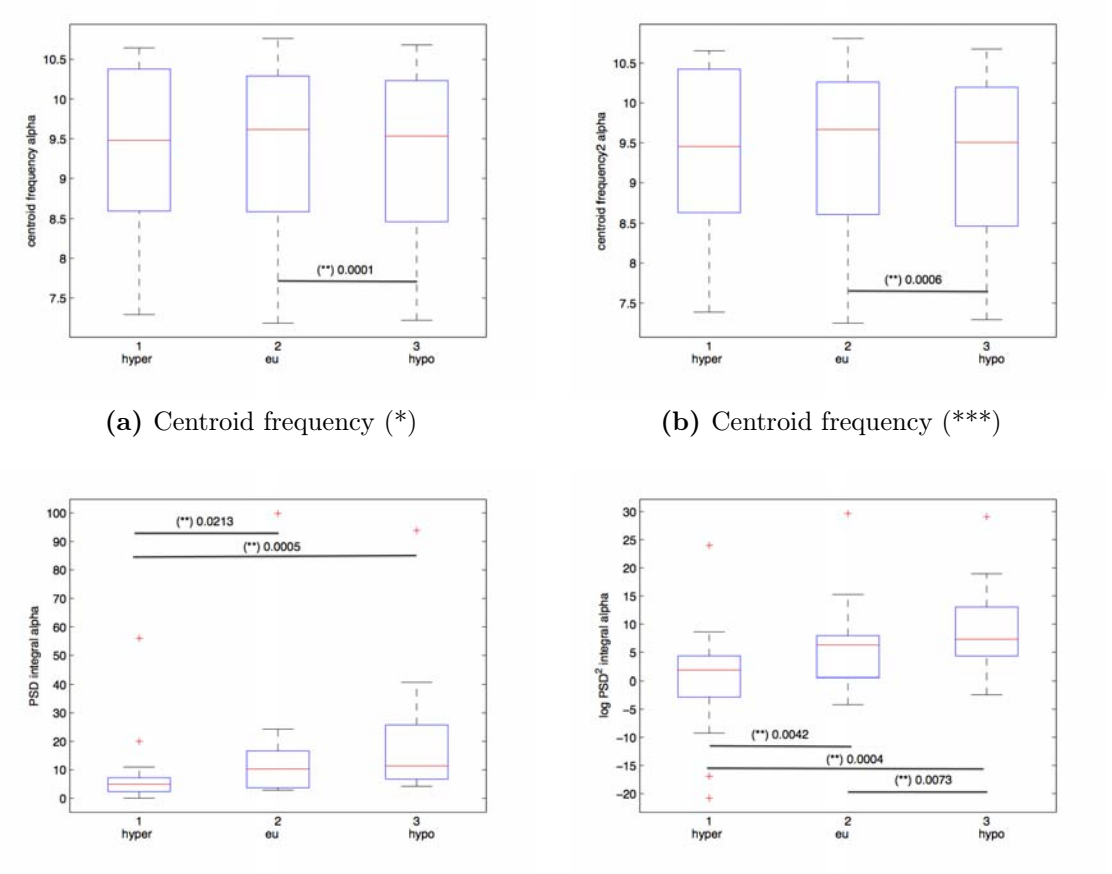

(a) Centroid frequency (*) **(b)** Centroid frequency (***)

(c) $\int PSD$ **(d)** $\int logPSD^2$

Figure A.16: P4-C4: alpha band personalization. (*) stands for the centroid frequency computed as $\frac{\sum(PSD(x)f(x))}{\sum(PSD(x))}$, (***) stands for the centroid frequency computed as spectrum median. The red line is the median value, the edges of the box are the 75th and 25th percentiles, the red crosses are the outliers. Double stars (**) indicate statically significant difference, the number near to the double stars is the p-value.

A.3 Reactivity index

Eventually, we have computed the variability of the reactivity index and we have tested if its variability (standard deviation) increases passing from hyper or eu-glycaemic state to hypoglycaemic one.
We have used the same procedure of chapter 5:

- selection of EEG signal in time domain;
- selection of a series of couples: reference and test time intervals ($r_i(t)$, $t_i(t)$) (they last 2 minutes and they distance 10 minutes. The successive couple ($r_2(t)$, $t_2(t)$) is obtained by shifting $r_1(t)$ and $t_2(t)$ by 0.5 minutes);
- computation of the power spectral density of each couple ($(r_i(t), t_i(t)) \rightarrow (R_i(f), T_i(f))$);
- computation of the reactivity index for each couple $\rho_i = \frac{\int_{fa}^{fb} R_i(f) - T_i(f)}{f_b - f_a}$.
- selection of ρ belonging to 1 hour EEG time interval;

These steps were repeated for each subject and for the alpha, theta and beta bands. For each patient, the 1 hour EEG time intervals were selected from the hypoglycaemia and then from the euglycaemia period.
The PSD of the couple ($r_i(t)$, $t_i(t)$) is obtained by applying the Welch method in EEG 2 second length epoch with no overlapping.
Moreover, the EEG signal was pre-elaborated for this analysis, we have excluded EEG values with amplitude greater than 100, because they were surely artifacts.
Then, we have computed the standard deviation of the reactivity indexes and performed a statistic test with all results from all subjects (in TableA.5).

We can observe the change in varibility of the ρ index in each band from FigureA.17 to FigureA.20.

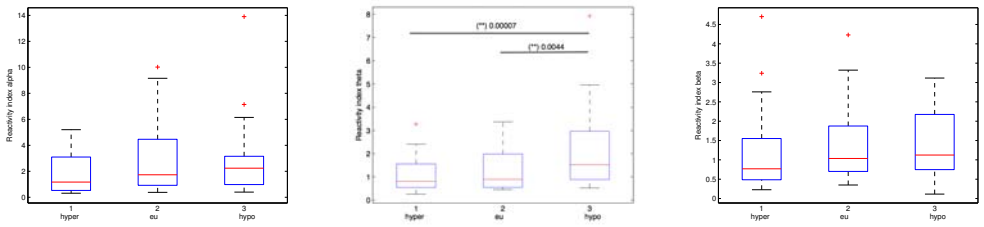

(a) Variability in alpha band **(b)** Variability in theta band **(c)** Variability in beta band

Figure A.17: P3-T3: standard deviation of reactivity index. The red line is the median value, the edges of the box are the 75th and 25th percentiles, the red crosses are the outliers. Double stars (**) indicate statically significant difference, the number near to the double stars is the p-value.

The best results are obtained in theta band: we can notice an increase in variability passing from hyperglycaemia to hypoglycaemia in all four channels.

Channel Delta (**)	Glycaemic states difference	Delta (*)	Theta (*)	Alpha (*)
P3-T3	hyper-eu	0 (0.0636)	0 (0.2728)	0 (0.636)
P3-T3	hyper-hypo	0 (0.1671)	1 $(7.63 * 10^{-5})$	0 (0.5372)
P3-C3	hyper-eu	0 (0.0636)	0 (0.2047)	0 (0.3546)
P3-C3	hyper-hypo	0 (0.0636)	1 (0.0044)	1 (0.0044)
Channel	**Glycaemic states difference**	**Delta (*)**	**Theta (*)**	**Alpha (*)**
P4-T4	hyper-eu	0 (0.0636)	1 (0.0196)	0 (0.5873)
P4-T4	hyper-hypo	0 (0.1671)	1 $(7.62 * 10^{-5})$	1 (0.0044)
P4-C4	hyper-eu	1 (0.0192)	0 (0.0809)	0 (0.1756)
P4-C4	hyper-hypo	0 (0.1671)	1 (0.0192)	0 (0.0636)

Table A.5: Statistic results for ρ variability. In the table, we have reported the results of the statistics for each channel. 1 stands for statically significant difference, 0 stands for no significant difference between euglycaemic and hypoglycaemic state. The p-value (likelihood of no difference between glycaemic states) is in brakets.

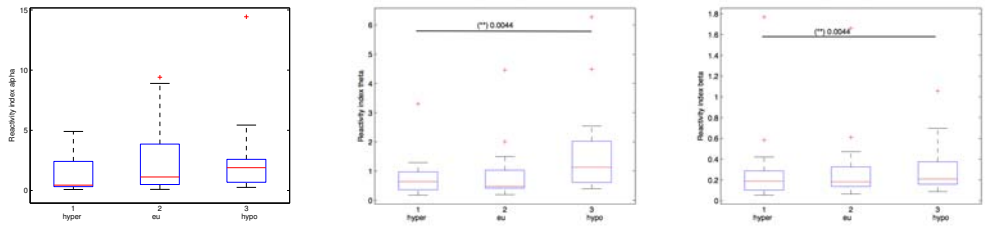

(a) Variability in alpha band **(b)** Variability in theta band **(c)** Variability in beta band

Figure A.18: P3-C3: standard deviation of reactivity index. The red line is the median value, the edges of the box are the 75th and 25th percentiles, the red crosses are the outliers. Double stars (**) indicate statically significant difference, the number near to the double stars is the p-value.

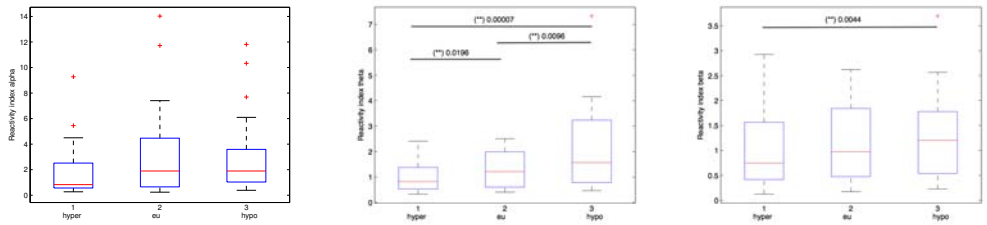

(a) Variability in alpha band **(b)** Variability in theta band **(c)** Variability in beta band

Figure A.19: P4-T4: standard deviation of reactivity index. The red line is the median value, the edges of the box are the 75th and 25th percentiles, the red crosses are the outliers. Double stars (**) indicate statically significant difference, the number near to the double stars is the p-value.

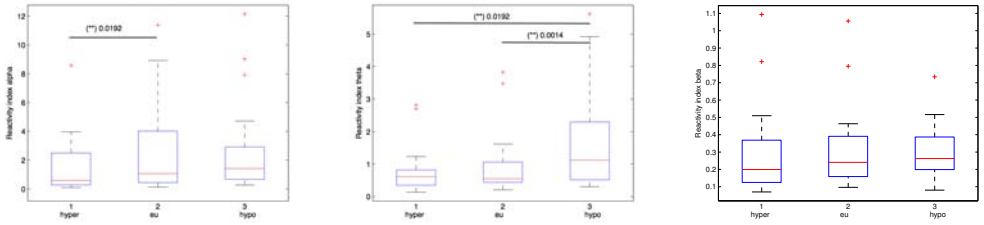

(a) Variability in alpha band **(b)** Variability in theta band **(c)** Variability in beta band

Figure A.20: P4-C4: standard deviation of reactivity index. The red line is the median value, the edges of the box are the 75th and 25th percentiles, the red crosses are the outliers. Double stars (**) indicate statically significant difference, the number near to the double stars is the p-value.

Thus, the reactivity index appears to be a good indicator to emphasize the difference between hyper- and hypoglycaemia in theta band.

Bibliography and Sitography

[1] URL: http://www.diabetes.org/. (Cit. on pp. 1, 2).

[2] World Health Organization. "Prevention of diabetes mellitus. Report of a WHO Study Group." In: Geneva 1994. (Cit. on pp. 1, 2).

[3] URL: http://www.idf.org/diabetesatlas/5e/diabetes. (Cit. on pp. 1, 2).

[4] URL: http://www.medicalnewstoday.com/info/diabetes/. (Cit. on p. 2).

[5] URL: http://diabetes.webmd.com/guide/type-1-diabetes. (Cit. on p. 2).

[6] Alberts B. Bray D. Hopkin K. Johnson A.D. Lewis J. Raff M. Roberts K. Walter P. *Essential Cell Biology*. Garland Science, 2010. (Cit. on p. 2).

[7] Barrett K.E. Barman S.M. Boitano S. Brooks H.L. *Ganong's Review of Medical Physiology, Twenty-Third Edition*. Mc Graw Hill, 2010. (Cit. on p. 2).

[8] Sparacino G. Facchinetti A. Cobelli C. ""Smart" Continuous Glucose Monitoring Sensors: On-Line Signal Processing Issues." In: *Sensors* (2010). (Cit. on p. 2).

[9] Webster J.G. *Medical Instrumentation*. John Wiley Sons, 2010. (Cit. on p. 3).

[10] URL: http://www.biomedical-engineering-online.com/content/8/1/9/figure/F7?highres=y. (Cit. on p. 4).

[11] Ross I.S. Loeser L.H. "Electroencephalographic findings in essential hypoglycemia". In: *Electroencephalography and Clinical Neurophysiology* 3 (1951), pp. 141–148. (Cit. on p. 4).

[12] Pramming S. Thorsteinsson B. Bendtson I. et al. "The relationship between symptomatic and biomechanical hypoglycaemia in insulin-dependent diabetic patients". In: *Journal of Internal Medicine* 228 (1990), pp. 641–646. (Cit. on p. 4).

[13] Hyllienmark L. Maltez J. Dandenell A. Ludvigsson J. Brismar T. "EEG abnormalities with and without relation to severe hypoglycaemia in adolescents with type 1 diabetes". In: *Diabetologia* (2005). (Cit. on pp. 4, 11).

[14] Pramming S. Thorsteinsson B. Stigsby B. Binder C. "Glycaemic threshold for changes in electroencephalograms during hypoglycaemia in patients with insulin dependent diabetes". In: *British Medical Journal* 296 (1988), pp. 665–667. (Cit. on p. 4).

[15] Elsborg R. Remvig L.S. Beck-Nielsen H. Juhl C.B. *Using the Brain as a Biosensor to Detect Hypoglycaemia*. Hypo-Safe A/S. Odense University Hospital, Sydvestjysk Sygehus Esbjerg Denmark, pp. 274–290. (Cit. on pp. 4, 5, 8).

[16] Iaione F. Marques J.L.B. "Methodology for hypoglycaemia detection based on the processing, analysis and classification of the electroencephalogram". In: *Medical Biological Engineering Computing* (2005). (Cit. on pp. 4, 12).

[17] URL: `http://hyposafe.com/info/`. (Cit. on pp. 4–6).

[18] Juhl C.B. Hoilund K. Elsborg R. Kjoer Poulsen M. Selmar P.E. Holst J.J. Christiansen C. Beck-Nielsen H. "Automated detection of hypoglycaemia-induced EEG changes recorded by subcutaneous electrodes in subjects with type 1 diabetes - The brain as a biosensor". In: *Diabetes Research and Clinical Practice* (2010). (Cit. on pp. 6, 11).

[19] Larsen A. Hojlund K. Poulsen M.K. Elsborg Madsen R. Juhl C.B. "Hypoglycemia-Associated Electrencephalogram and Electrocardiogram Changes Appear Simultaneously". In: *Journal of Diabetes Science and Technology* (2013). (Cit. on pp. 6, 11, 30).

[20] URL: `http://en.wikipedia.org/wiki/Electrocardiography`. (Cit. on p. 7).

[21] URL: `http://en.wikipedia.org/wiki/QT_interval`. (Cit. on p. 7).

[22] Remvig L.S. Elsborg R. Sejling AS. Sorensen J.A. Sonder Snogdal L. Folkestad L. Juhl C.B. "Hypoglycemia-Related Electroencephalogram Changes Are Indipendent of Gender, Age, Duration of Diabetes, and Awareness Status in Type 1 Diabetes". In: *Journal of Diabetes Science and Technology* (2012). (Cit. on pp. 7, 11, 12, 18, 23, 55).

[23] Goljahani A. Sejling A.S. Sparacino G. Fabris C. Duun-Henriksen J. Remvig LS. Cobelli C. Juhl C.B. "Variability of EEG theta power modulation in Type 1 diabetics increases during hypoglycaemia". In: (). (Cit. on pp. 8, 9, 49).

[24] Fabris C. Sejling A.S. Sparacino G. Goljahani A. Duun-Henriksen J. Remvig L.S. Cobelli C. Juhl C.B. "Hypoglycemia-related EEG changes assessed by Approximate Entropy". In: (). (Cit. on pp. 8, 9, 12).

[25] Pincus S.M. "Approximate entropy: Statistical properties and applications". In: *Proceedings of the National Academy of Sciences of the United States of America* 88 (1991), pp. 2297–2301. (Cit. on p. 8).

[26] Facchinetti A. Sparacino G. Cobelli C. "Online denoising method to handle intra-individual variability of signal-to-noise ratio in continuous glucose monitoring". In: *IEEE Transactions on Biomedical Engineering* (2011). (Cit. on p. 9).

[27] Sonder Snogdal L. Folkestad L. Elsborg R. Remvig L.S. Beck-Nielsen H. Thorsteinsson B. Jennum P. Gjerstad M. Juhl C.B. "Detection of hypoglycaemia associated EEG changes during sleep in type 1 diabates mellitus". In: *Diabetes Research and Clinical Practice* (2012). (Cit. on p. 11).

[28] Bjorgaas M. Sand T. Vik T. Jorde R. "Quantitative EEG during Controlled Hypoglycaemia in Diabetic and Non-diabetic Children". In: *Diabetic Medicine* (1998). (Cit. on p. 12).

[29] Roberts M.J. *Signals and Systems: analysis using trasform methods and MATLAB*. Mc Graw Hill, 2003. (Cit. on p. 12).

[30] Cariolaro G. Pierobon G. Calvagno G. *Segnali e Sistemi*. Mc Graw Hill, 2005. (Cit. on p. 12).

[31] Kua J.M.K. Thiruvaran T. Nosratighods M. Ambikairajah E. Epps J. "Investigation of Spectral Centroid Magnitude and Frequency for Speaker Recognition". In: *Odyssey 2010: The Speaker and Language Recognition Workshop* (2010). (Cit. on p. 23).

[32] Goljahani A. D'Avanzo C. Schiff S. Amodio P. Bisiacchi P. Sparacino G. "A novel method for the determination of EEG individual alpha frequency". In: *NeuroImage* (2011). (Cit. on pp. 39, 47, 49, 56).

[33] Klimesh W. Schimke H. Ladumer G. Pfurtscheller G. "Alpha frequency and memory performance". In: *Journal of Psychophysiology* (1990), pp. 381–390. (Cit. on p. 39).